# Hydrological Models Comparison in Simulating Streamflow in the Melka Kunture Watershed in Upper Awash Sub-basin, Ethiopia

**Abdi Guta Oljira**

**A Thesis Submitted to the Department of Water Resources Engineering, School of Civil Engineering and Architecture**
**Presented in Partial Fulfillment of the Requirements for the Degree of Master of Science in Water Resources Engineering (Specialization in Hydraulic Engineering)**

**Office of Graduate Studies**
**Adama Science and Technology University**

**September, 2023**
**Adama, Ethiopia**

# Hydrological Models Comparison in Simulating Streamflow in the Melka Kunture Watershed in Upper Awash Sub-basin, Ethiopia

**Abdi Guta Oljira**

**Advisor**
**Abdulkerim B. Serur (PhD)**

**A Thesis Submitted to the Department of Water Resources Engineering, School of Civil Engineering and Architecture**
**Presented in Partial Fulfillment of the Requirements for the Degree of Master of Science in Water Resources Engineering (Specialization in Hydraulic Engineering)**

**Office of Graduate Studies**
**Adama Science and Technology University**

**September, 2023**
**Adama, Ethiopia**

# DECLARATION

I hereby declare that this Master Thesis entitled "Hydrological Models Comparison in Simulating Streamflow in the Melka Kunture Watershed in Upper Awash Sub-basin, Ethiopia" is my original work. That is, it has not been submitted for the award of any academic degree, diploma or certificate in any other university. All sources of materials that are used for this thesis have been duly acknowledged through citation.

Abdi Guta Oljira_______ _______________ ________________

Name of Student Signature Date

## RECOMMENDATION OF THE ADVISOR

I, the advisor of this thesis, hereby certify that I have read the revised version of the thesis entitled "Hydrological Models Comparison in Simulating Streamflow in the Melka Kunture Watershed in Upper Awash Sub-basin, Ethiopia" prepared under my guidance by Abdi Guta Oljira submitted in partial fulfillment of the requirements for the degree of Master of Science in Water Resources Engineering (Specialization in Hydraulic Engineering). Therefore, I recommend the submission of the revised version of the thesis to the department following the applicable procedure.

| | | |
|---|---|---|
| Abdulkerim B. Serur (PhD) | ____________________ | ____________ |
| Advisor | Signature | Date |

# APPROVAL PAGE OF THE M.Sc. THESIS

I, the advisor of the thesis entitled "Hydrological Models Comparison in Simulating Streamflow in the Melka Kunture Watershed in Upper Awash River Basin, Ethiopia" by Abdi Guta Oljira, hereby certify that the recommendation and suggestions made by the board of examiners are appropriately incorporated into the final version of the thesis.

| | | |
|---|---|---|
| Abdulkerim B. Serur (PhD) | ____________________ | ___________ |
| Advisor | Signature | Date |

We, the undersigned, members of the Board of Examiners of the thesis by Abdi Guta Oljira have read and evaluated the thesis entitled "Hydrological Models Comparison in Simulating Streamflow in the Melka Kunture Watershed in Upper Awash Sub-basin, Ethiopia" and examined the candidate during open defense. This is, therefore, to certify that the thesis is accepted for partial fulfillment of the requirements of the degree of Master of Science in Water Resources Engineering (Specialization in Hydraulic Engineering).

| | | |
|---|---|---|
| Mesfin Benti (PhD) | ____________________ | ___________ |
| Chairperson | Signature | Date |
| Mulugeta Musie (PhD) | ____________________ | ___________ |
| Internal Examiner | Signature | Date |
| Tilahun Derib (PhD) | ____________________ | ___________ |
| External Examiner | Signature | Date |

Finally, approval and acceptance of the thesis are contingent upon the submission of its final copy to the Office of Postgraduate Studies (OPGS) through the Department Graduate Council (DGC) and School Graduate Committee (SGC).

| | | |
|---|---|---|
| ______________________ | ____________________ | ___________ |
| Department Head | Signature | Date |
| ______________________ | ____________________ | ___________ |
| School Dean | Signature | Date |
| ______________________ | ____________________ | ___________ |
| Office of Postgraduate Studies, Dean | Signature | Date |

ACKNOWLEDGEMENTS

First and foremost, I would like to express my heartfelt gratitude to the almighty God for the strength and courage bestowed upon me throughout my life. I am immensely grateful to Oda Bultum University for granting me the opportunity to pursue my M.Sc. studies and I am equally thankful to Adama science and Technology University for providing me with the opportunity to pursue my M.Sc. studies.

I extend my sincerest appreciation to my advisor, Abdulkerim B. Serur (Ph.D.), for his invaluable guidance and constructive feedback during the entire research period. I would also like to acknowledge the Ministry of Water and Energy and the Ethiopian Meteorology Institute for their cooperation in providing the hydrological and meteorological data respectively, for my study.

Furthermore, I am deeply thankful to my family and my spouse for their unwavering support and encouragement during my academic journey. Their presence has been a constant source of motivation and inspiration. I would also like to express my gratitude to all my friends for their unparalleled support and dedication.

# LIST OF ACRONYMS AND ABBREVIATIONS

| | |
|---|---|
| APEX | Agricultural Policy Environmental Extender |
| AR | Auto-Regressive |
| ARIMA | Autoregressive Integrated Moving Average |
| CRV | Central Rift Valley |
| CV | Coefficient of Variation |
| DDS | Dynamically Dimensioned Search |
| DEM | Digital Elevation Model |
| EMI | Ethiopian Meteorology Institute |
| FAO | Food and Agriculture Organization |
| FC | Field Capacity |
| FIS | Fuzzy Inference System |
| GAP | Genetic Algorithm and Powell |
| GDP | Gross Domestic Product |
| GFFS | Galway Flow Forecasting System |
| GIS | Geographic Information System |
| GUI | Graphical User Interface |
| HBV | Hydrologiska Byrans Vattenbalansevdelning |
| HEC-HMS | Hydrologic Engineering Centre - Hydrologic Modeling System |
| HRU | Hydrologic Response Unit |
| IDW | Inverse Distance Weighting |
| IPEAT+ | Integrated Parameter Estimation and Uncertainty Analysis Tool Plus |
| ITCZ | Inter-Tropical Convergence Zone |
| KW | Kinematic Wave |
| LSU | Land Scape Unit |
| LULC | Land Use Land Cover |
| MoWE | Ministry of Water and Energy |
| NR | Normal Ratio |
| NSE | Nash-Sutcliffe Efficiency |
| PBIAS | Percent Bias |
| PCI | Precipitation Concentration Index |
| PD | Probability Distribution |
| PET | Potential Evapotranspiration |
| QGIS | Quantum Geographic Information System |
| QSWAT+ | Quantum Soil and Water Assessment Tool plus |
| RMSE | Root Mean Square Error |
| RSR | Observation Standard Deviation Ratio |
| SAI | Standard Anomaly Index |
| SCFF | Snowfall Correction Factor |
| SCS | Soil Conservation Service |
| SCS-CN | Soil Conservation Service-Curve Number |
| SHE | System Hydrologique Europeen |
| SMAR | Soil Moisture Accounting and Routing |
| SUFI | Sequential Uncertainty Fitting |
| SWAT | Soil and Water Assessment Tool |
| UH | Unit Hydrograph |
| USGS | United State Geological Survey |

# TABLE OF CONTENTS

## TABLE OF CONTENTS (*Continued*)

## TABLE OF CONTENTS (*Continued*)

# LIST OF TABLES

**Tables** **Pages**

# LIST OF FIGURES

**Figures** **Pages**

## LIST OF FIGURES (*Continued*)

# LIST OF TABLE IN THE APPENDIX

**Appendix Tables** **Pages**

# LIST OF FIGURES IN THE APPENDIX

**Appendix Figures** **Pages**

# ABSTRACT

*Analysing hydro-meteorological variability and evaluating the performance of hydrological models are closely related processes in the field of hydrology. Understanding the variability of hydro-meteorological factors is crucial for accurate modeling and prediction of streamflow to overcome water-related challenges and enhance water resources management. This study aimed to identify a suitable hydrological model for simulating streamflow of Melka Kunture watershed in the Upper Awash sub-basin, in Ethiopia. The variability of historical rainfall and streamflow of the watershed was analysed using coefficient of variation, standard rainfall anomaly index, and precipitation concentration index. Three hydrological models (HEC-HMS, SWAT+, and HBV-Light) were considered, and their performances in simulating historical streamflow were evaluated using statistical model performance evaluation indices namely coefficient of determination ($R^2$), Nash-Sutcliffe efficiency (NSE), and percent bias (PBIAS). Sixteen years (2000-2015) daily rainfall and streamflow data were used for models calibration and validation at the Melka Kunture watershed outlet. The HEC-HMS model was calibrated by the optimization trial (automatic calibration); the SWAT+ Toolbox was applied to analyse sensitivity analysis (Sobol method) and calibration (Dynamically Dimensioned search method); and in the HBV-Light model, Genetic Algorithm and Powel Optimization were used to calibrate and validate the model. Based on the results obtained, the variation of rainfall within the watershed ranges from low to high seasonally and annually. The result of the annual standard rainfall anomaly index showed the precipitation within the watershed ranges from extremely wet to extremely dry, but mostly all stations get near normal rainfall annually. The annual precipitation concentration index result within watershed ranges from irregular to moderate rainfall distribution, while seasonally, the precipitation concentration index within the watershed showed strong irregularities of rainfall. The performance of HEC-HMS, SWAT+, and HBV-Light in simulating historical streamflow of the watershed were found to be ($R^2$: 0.71, NSE: 0.677, PBIAS: -0.1), ($R^2$: 0.71, NSE: 0.669, PBIAS: 9.349), and ($R^2$: 0.78, NSE: 0.8, PBIAS: 0.94), respectively during calibration. During validation, the values ($R^2$: 0.68, NSE: 0.676, PBIAS: 6.39) for HEC-HMS, ($R^2$: 0.68, NSE: 0.66, PBIAS: -0.475) for SWAT+, and ($R^2$: 0.68, NSE: 0.68, PBIAS: 0.99) for HBV-Light were obtained. Based on the statistical indices, the HBV-Light model showed good correlation between observed and simulated daily streamflow during calibration and validation periods. It outperformed the other models during calibration, while the HEC-HMS model showed better performance in simulating low streamflow conditions during both calibration and validation periods, as indicated by the Nash-Sutcliffe efficiency (NSElog) values of (HEC-HMS:0.70, SWAT+:0.19, and HBV-Light: 0.64; and HEC-HMS: 0.71, SWAT+: -2.07, and HBV-Light: 0.51) during calibration and validation, respectively. In conclusion, this study suggests that the HBV-Light model is the most suitable for simulating streamflow and HEC-HMS in simulating low streamflow conditions in the Melka Kunture watershed. Generally, the output of this study can be applied in planning, designing, and sustainable management of water resources in the Melka Kunture watershed.*



***Keywords***: *Hydro-meteorological variability, HEC-HMS, HBV-Light, SWAT+ Streamflow simulation, Melka Kunture Watershed*

# 1. INTRODUCTION

## 1.1 Background of the study

Developing the basic relationship between the diverse hydrologic systems like rainfall, runoff, soil moisture, groundwater level, and land use and land cover is crucial for effective and sustainable water resources planning and management activities with the support of hydrological models (Ayalew, 2019). The most crucial responsibilities to manage the basin's water resources are assessing hydro-meteorological variability (Alemu & Bawoke, 2019) and modeling hydrological processes such as rainfall runoff, infiltration, evapotranspiration, and groundwater discharge (M. Aliye et al., 2020). Numerous computer-based models have been created to simulate the hydrologic processes and the hydrologic effects of various watershed management challenges (Nguyen Khoi, 2015b).

The hydrological model is one of the key methods in hydrological research and management and can be divided into the physical model and the mathematical model (Gui et al., 2021). Physical models are built based on the physical background, such as the transport process of hydrological runoff (Zhang & Yang, 2018). Hydrologic Engineering Center-Hydrological Modeling System (HEC-HMS) (USACE, 2021), the Soil and Water Assessment Tool, the Soil and Water Assessment Tool Plus (SWAT+) (Bieger et al., 2017), the Hydrologiska Byråns Vattenbalansavdelning Light (HBV) model (Jan Seibert, 2005), and the MIKE-SHE model (Abbott et al., 1986), are some of the extensively used physically based models used in different regions of the world (Chathuranika et al., 2022). However, mathematical models based on machine learning generally only consider data input and output and ignore the intermediate process, so they are also called black box models, such as artificial neural networks (ANN), autoregressive integrated moving average (ARIMA), and fuzzy inference system (FIS).

Hydrological models are applied in colorful river basins worldwide for a better appreciation of hydrological procedures and water resource availability (Geyisa Namara et al., 2020a). Therefore, it is important to use the hydrological model to assess and predict the water availability of river basins and develop strategies to cope with the changing environment. Today, the need to evaluate hydrological models and assess their outcomes and capabilities has arisen as a result of their growing use to simulate processes in a basin and the differences among them (Parra et al., 2018). In this study, the performance of the Hydrological Engineering Centre-Hydrologic Modeling System (HEC-HMS) (USACE, 2021), Soil and Water Assessment Tool Plus (SWAT+) (Bieger et al., 2017), and Hydrologiska Byran's Vattenbalansavdelning (HBV) Light (Jan Seibert, 2005) in simulating streamflow were evaluated to see their level of capability to simulate streamflow of Melka Kunture watershed in the upper Awash sub-basin in Ethiopia.

The performance of these models in simulating streamflow was assessed in different areas across the world. Nguyen Khoi (2015b) evaluated the performance of HEC-HMS and SWAT models in simulating streamflow to find suitable hydrological modeling in the Srepok River catchment in the central highlands of Vietnam. The author evaluated the performance of the models using the statistical model performance evaluation criteria NSE and $R^2$ and found that the SWAT model showed satisfactory results in simulating the streamflow of the Srepok River catchment compared to the HEC-HMS model.

Al-Weshah et al. (2018) studied rainfall-runoff modeling using the Galway Flow Forecasting System (GFFS) in the upper Awash Sub-basin, Ethiopia. The author uses various GFFS models, ranging from simple linear models to soil moisture accounting and routing (SMAR), to simulate river flows in the upper Awash Sub-basin. The author used different performances to compare the model's suitability for catchment and concluded that to forecast inflows, volumes, and peak flows to Koka reservoir for better reservoir management, the SMAR model coupled with the AR updating procedure was suitable to forecast reservoir inflows (volumes) for reservoir management and peak flows for the operation of the spillway gates to avoid huge releases through the gates that might cause floods downstream.

Chathuranika et al. (2022) evaluated and compared HEC-HMS and SWAT results for the Huai Bang Sai tropical watershed in Thailand. Accordingly, the performance of both models was considered satisfactory, but the SWAT model was able to capture more satisfactory high-flow results than the HEC-HMS model. Ayalew (2019) analyzed the performance of HBV and SWAT models in simulating the rainfall-runoff process in the Geba Catchment, Upper Tekeze Basin, Ethiopia. Comparing the results of the two conceptually distributed models, the researcher found that the HBV light model result gave a promising result in simulating runoff for Geba as well as for the future study of runoff simulation for the catchment.

The performance evaluation of these hydrological models was assessed in various river basins and sub-river basins by simulating the streamflow in different river catchments and sub-catchments as some of them were raised above. Even though selecting the proper models to simulate the hydrologic processes of a specific watershed has always been a challenge, HEC-HMS, SWAT+, and HBV-light models were selected to assess the available water resource which is vital to address water related problems like flooding, drought and water scarcity within the watershed. Therefore, conducting hydrological modeling of the Melka Kunture watershed in the upper Awash sub-basin was crucial. It aimed to analyze the future variability of the hydrological regime and evaluate the water resource potential for different identified projects in the area. As a result, the comparison of hydrological models in the Melka Kunture watershed, which is influenced by human activities and subject to various impacts, can play a crucial role in the development of effective strategies for flood mitigation, drought adaptation, and overall water management. The focus of this study was to evaluate the performance of hydrological models for streamflow simulation and identify suitable hydrological model for simulating streamflow in the Melka Kunture watershed.

## 1.2 Statement of the Problem

Water-related challenges like flooding, water scarcity, and a decline in water quality have been critical problems around the globe causing massive damage to human lives, socio-economics, and the environment. Furthermore, the agricultural and industrial sectors have experienced significant growth, leading to an increased demand for domestic water supplies. This rise in demand is further amplified by population growth, resulting in higher water consumption rates. Thus, Freshwater scarcity and improper use of it are severe and growing challenges to environmental preservation and sustainable development. Unless water and land resources are managed more successfully in the current decade and beyond than they have been in the past, human health and welfare, food security, industrial development, and the ecosystems on which they depend are all in danger (International Conference on Water and the Environment, 1992).

The upper Awash sub-basin in Ethiopia, which is the target of this study, is one such region that is affected by this problem (Mitiku et al., 2020). Thus, there is a need to develop an appropriate hydrological model and sustainable management mechanisms to mitigate this problem. Several studies have been conducted on rainfall-runoff modeling in the upper Awash Sub-basin using a single model.

Zeberie (2019) conducted research on modeling rainfall-runoff relationships using SWAT in the Big Akaki Watershed, Upper Awash Basin, Ethiopia. The author reveals that the surface runoff has the same pattern as the rainfall in the watershed. Namara et al. (2020) studied rainfall-runoff modeling using HEC-HMS in the Awash Bello Catchment, Upper Awash Basin, Ethiopia. Tibebe et al. (2017) conducted research to estimate runoff at the Holetta catchment and to model rainfall-runoff relations in the area using the SWAT model in the Awash Sub-basin, Ethiopia.

In the Upper Awash sub-basin, dominantly, a single model was applied to rainfall-runoff modeling in the different watersheds. In developing a better hydrological model, a single model structure cannot adequately represent all governing processes of a watershed system’s response to hydrological processes under all conditions in the sub-basins (Thapa et al., 2017; Serur, 2023). Even if the aforementioned studies have been carried out in Upper Awash sub-basin using a single model, comparison of hydrological models in Melka Kunture watershed is yet not explored. Hence, a multi-model approach over the single model’s usage was main part of these pieces of work for capturing spatial variability of the hydrological processes within a watershed.

### 1.3 Objective of the Study

#### 1.3.1 General Objective

The general objective of this study was to identify suitable hydrological model for simulating streamflow of Melka Kunture watershed in the upper awash sub-basin in Ethiopia.

#### 1.3.2 Specific Objectives

1. To analyze the hydro-meteorological variability in the Melka Kunture watershed.
2. To assess the potential of hydrological models in simulating the streamflow of the Melka Kunture watershed.
3. To compare and select a satisfactory hydrological model or set of models for the Melka Kunture watershed.

## 1.4 Research Questions

1. What is the magnitude of hydro-meteorological variability of the Melka Kunture watershed?
2. What is the potential of HEC-HMS, SWAT+, and HBV-Light in simulating the streamflow of the Melka Kunture watershed?
3. Which hydrological model outperforms others in simulating the streamflow at the outlet of the Melka Kunture Watershed?

## 1.5 Significance of the Study

For efficiently developing and maintaining water resources in a sustainable way, hydrological models are essential tools. They provide valuable insights into the complex hydrological processes that govern the movement and availability of water. Numerous hydrological models have been developed recently, encouraging academics to examine their effectiveness in a variety of contexts (Aredo, 2020).

In the Upper Awash Sub-basin, different researchers have employed diverse hydrological models to understand the relationship between rainfall and runoff. For instance, Namara et al. (2020) utilized the HEC-HMS model to simulate rainfall runoff in the Awash Bello sub-catchment. Similarly, Tibebe et al. (2017) employed the SWAT model to analyze rainfall-runoff patterns and estimate runoff in the Holeta River. Additionally, Zeberie (2019) used SWAT to examine the rainfall-runoff relationship in the Big-Akaki watershed.

While these studies have contributed significantly to the sustainable management of water resources, it is important to note that relying solely on a single hydrological model may limit the ability to capture the spatial variability of the hydrological processes within a watershed. Therefore, conducting a comprehensive evaluation of multiple hydrological models to simulate streamflow in the Melka Kunture watershed becomes crucial. Such an assessment would provide policymakers with more accurate and realistic information for making informed decisions regarding water resource management. By comparing and selecting suitable hydrological models, policymakers can enhance their understanding of the watershed dynamics and ensure sustainable water resource management for the future.

## 1.6 Scope and Limitation of the Study

This study aimed to examine the efficiency of hydrological models in simulating streamflow in the Melka Kunture watershed and analyze the geographical and temporal variability of hydro-meteorological data. The study analyzed the spatial variability using

ArcGIS software and used statistical methods to determine the variability of the hydro-meteorological data. The streamflow of the study area was simulated and compared with the observed streamflow data at the outlet of the Melka Kunture watershed. The simulation of the streamflow was done by HEC-HMS, SWAT+, and HBV-Light hydrological models. The limitation in the hydrological modeling of the Melka Kunture watershed is the availability and quality of input data. High-quality data is essential for accurate and reliable model implementation, especially when using distributed hydrological models that require detailed information about the watershed's characteristics. The challenge lies in locating and acquiring the necessary data for model development and calibration. Without access to accurate and representative data, it becomes difficult to effectively implement the hydrological models and obtain reliable results.

### 1.7 Thesis Organization

The thesis is structured in to five chapters to systematically present the research work. The first chapter serves as a general introduction to the research work. It begins with an overview of research topic, followed by a clear research statement that outlines the specific problem or question being addressed. The chapter also presents the research objectives, outlining what the study aims to achieve. Additionally, it highlights the significance and relevance of the research, emphasizing why it is important and the potential impact it may have. The second chapter focuses on the literature review. This section provides a comprehensive review of existing works, studies, and research that is related to the research topic. The third chapter provides detailed information about the chosen study area. It includes a description of the geographic location, environmental characteristics, and any specific consideration relevant to the research. Additionally, this chapter presents the methodology employed in the study, data collection method and materials used. The fourth chapter presents the findings of the research work. It includes the results obtained from the analysis conducted. The chapter provides a comprehensive discussion and interpretation of the findings, comparing them to the existing literature and addressing any unexpected result or significant result. The fifth and final chapter concludes the thesis by summarizing the main findings of the research. Finally, recommendations may be provided for future research directions from the study.

# 2. LITERATURE REVIEW

## 2.1 Hydro-meteorological Variability

The climate is one of the most important factors that affects the spatial and temporal patterns of water resources on earth, and it can be thought of as the main support system for all other natural resources, including water (Abera et al., 2017). The inter-annual and intra-seasonal climate variability over the African continent is higher (Melat Eshetu, 2021a). Ethiopia is among the developing countries that have suffered as a result of hydro-meteorological variability (Malede et al., 2022). The spatial and temporal variability of climate in Ethiopia is due to the migration of the Inter-Tropical Convergence Zone (ITCZ) and its complex topographic and geographical features (Kidanewold et al., 2014).

## 2.2 Seasonal and Annual Variability of rainfall

Understanding the seasonal and annual variability of rainfall is crucial for water resource management, agriculture, and ecosystem functioning (Abegaz and Mekoya, 2020). It helps in predicting water availability, planning irrigation strategies, assessing drought or flood risks, and managing water resource sustainability. The river flow varies considerably from one stream to another due to seasonal rainfall variation and distinct concentration times. Therefore, assessing seasonal and annual historical climate variability is essential to providing crucial information for better practices in food production and overall economic growth. Some literature was reviewed regarding seasonal and annual hydro-meteorological variability across the world.

Melat Eshetu (2021) studied the hydro-climatic variability and trend analysis of the Mojo River watershed, Awash River Basin, Ethiopia. The author's result revealed that most of the stations showed low variation in annual rainfall (CV < 20%), while the main (Kiremt) and short (Belg) season rainfall indicated CV ranging from low to high. Also, the result of the variability analysis in maximum, minimum, and average streamflow indicates that there is high variability (CV > 30%) on both an annual and seasonal basis. The annual and Kiremt streamflow showed relatively high CV (40.1%, 63%, and 72.4%), while the Belg discharge showed very high CV (118.5%, 115.8%, and 134.7%) for maximum, minimum, and average streamflow, respectively, and this is due to the increase in temperature that causes high evapotranspiration. The author evaluated the trend analysis of the climate using Sen's slope estimator and the Man-Kendall trend test method. The annual and seasonal rainfall trend analysis of the Mojo River watershed showed no significant trend at all stations for the past 30 years. A majority of the stations in the Mojo River watershed show an increasing trend in annual daily average temperature ranging from 0.2 $^{0}C$ to 0.6 $^{0}C$ and due to an increased temperature, evapotranspiration increased, which caused a highly significant decline in streamflow.

Orke and Li (2021) studied hydro-climatic variability in the Bilate Watershed, Ethiopia. The author's result indicated that the variation in rainfall and streamflow has higher variability during the Bega (dry) and the Belg (minor rainy) seasons than in the Kiremt (main rainy) season. Regarding the variability of the temperature, a high variability of the minimum temperature over the past 30 years was observed in the Bilate watershed. Lambe & Kundapura (2021) investigated the variability analysis of meteorological and seasonal trends over the Bilate basin of the Rift Valley Lakes basins in Ethiopia. The basin is characterized by a bimodal rainfall pattern. According to the author, relatively higher variability indices were revealed during the dry season, with significant rainfall variability in the upstream as well as lesser rainfall variability during the rainy season in the downstream south of the Bilate watershed. Regarding temperature variability, the minimum average temperature was relatively more variable than the maximum average temperature.

Abegaz & Mekoya (2020) investigated rainfall variability and trends in Central Ethiopia. The author evaluated the variability of rainfall on both an annual and seasonal scale using the coefficient of variation (CV) and standard precipitation index. The author also used the Mann-Kendall test and Sen’s slope estimator to assess the rainfall trends. He found that the rainfall in North Shoa showed high variability both in space and time. The PCI (=20%) showed irregular rainfall distribution. The CV showed moderate variation in both annual and kiremt rainfall as compared to the rainfall in the Belg and Bega seasons. The Mann-Kendall test resulted in a decreasing trend in Belg and Bega seasons and an increasing trend for annual and Kiremt rainfall.

### 2.3 Hydrological Models

Hydrologic modeling is a simplified, conceptual representation of a part of the hydrologic cycle. The best model is the one that produces results that are close to reality while utilizing the fewest parameters and the lowest level of model complexity (Sorooshian, 2008). Models are primarily used to analyze various hydrological processes and predict system behavior. A model is made up of several parameters that specify its properties. The application of the hydrologic model occurs in the watershed, which is diverse and necessitates a variety of parameters, presumptions, and considerations (Belay et al., 2022).

The researcher's limited scientific knowledge in the area becomes the main source of uncertainty and inaccuracy in the proposed infrastructure development works and results in unnecessary quantification and financial losses in each component, or worse, causes damage to life and property in the vicinity. They are primarily used for hydrologic prediction and for understanding hydrologic processes. To understand hydrologic processes and the effects of anthropogenic causes and natural variability on the hydrologic system, hydrologic models have become an essential tool (Yu, 2015).

Zeberie (2019) investigated the relationship between rainfall and runoff generated under the influence of different watershed physical parameters in the Big-Akaki watershed using the SWAT model. The author uses the SCS curve number to estimate runoff from the basin surface and SWAT to delineate the basin and analyze the slope of the watershed, the soil, and land uses. The authors concluded as surface runoff has the same pattern as rainfall in the watershed and concluded that if high rainfall was recorded in the watershed, the peak runoff was inevitable.

Hamdan et al. (2021) examined Rainfall-Runoff Modeling Using the HEC-HMS model for the Al-Adhaim River Catchment, Northern Iraq. The authors use the Soil Conservation Service-Curve Number (SCS-CN), Soil Conservation Service Unit Hydrograph (SCS-UH), and Muskingum methods for loss, transformation, and routing calculations, respectively. The authors obtained results show a good agreement between observed and simulated flows, and $R^2$ was 0.9 for both calibration and verification. The correlation between simulation and observation was good, but the total volume of discharge storage for these years was slightly overestimated.

### 2.4 Classification of Hydrological Models

This section introduces the classification of existing hydrologic models and the terminology related to hydrologic modeling that has been adopted in this report.

#### 2.4.1 Lumped models

Parameters of lumped hydrologic models do not vary spatially within the basin, and thus, basin response is evaluated only at the outlet without explicitly accounting for the response of individual sub-basins. Parameters of lumped models often do not represent the physical features of hydrologic processes and usually involve a certain degree of empiricism. The impact of the spatial variability of model parameters is evaluated by using certain procedures for calculating effective values for the entire basin. The most commonly employed procedure is an area-weighted average (Haan et al., 1982). Lumped models are not usually applicable to event-scale processes. If the interest is primarily in discharge prediction only, then these models can provide just as good simulations as complex physical-based models (Ghonchepour et al., 2021).

### 2.4.2 Semi-distributed model

Parameters of semi-distributed models are partially allowed to vary in space by dividing the basin into several smaller sub-basins. There are two main types of semi-distributed models. 1) Kinematic wave theory models (KW models, such as HEC-HMS, SWAT, SWAT+), and 2) probability distributed models (PD models, such as TOPMODEL, HBV-Light). The KW models are simplified versions of the surface and/or subsurface flow equations of physically based hydrologic models (Beven, 2011). In the probability distribution models, spatial resolution is accounted for by using the probability distribution of input parameters across the basin.

### 2.4.3 Distributed Models

Parameters of distributed models are fully allowed to vary in space at a resolution usually chosen by the user. The distributed modeling approach attempts to incorporate data concerning the spatial distribution of parameter variations together with a computational algorithm to evaluate the influence of this distribution on simulated rainfall-runoff behavior. Distributed models generally require large amounts of data for parameterization in each grid cell. However, the governing physical processes are modeled in detail, and if properly applied, they can provide the highest degree of accuracy.

## 2.5 Model Selection Criteria

Numerous criteria can be used to choose the right hydrologic model. These criteria are always project-dependent since every project has its own specific requirements and needs. Further, some criteria are also user-dependent (and therefore subjective), such as the personal preference for a graphical user interface (GUI), a computer operation system (OS), input-output (I/O) management and structure, or the user’s add-on expansibility. Among the various project-dependent selection criteria, four common, fundamental ones must be answered:

1. Required model outputs are important to the project and therefore should be estimated by the model (does the model predict the variables required by the project, such as peak flow, event volume, hydrograph, long-term sequence of flows, etc.?).
2. Hydrologic processes that need to be modeled to adequately estimate the desired outputs (is the model capable of simulating stream flow, regulated reservoir operation, snow accumulation, and melt single-event or continuous processes…),
3. Availability of input data (can all the inputs required by the model be provided within the time and cost constraints of the project?),
4. Price (does the investment appear to be worthwhile for the objectives of the project?)

Based on the model selection criteria above, Hydrologic Engineering Center-Hydrologic Model System (HEC-HMS), Soil and Water Assessment Tool Plus (SWAT+), and Hydrologiska Byråns Vattenbalansavdelning Light (HBV-Light) were selected for this study.

## 2.6 Description of Hydrological Models

### 2.6.1 HEC-HMS model

Hydrologic Engineering Centre-Hydrologic Modeling System (HEC-HMS) is hydrologic modeling software developed by the US Army Corps of Engineers of the Hydrologic Engineering Centre (HEC), which contains an integrated tool for modeling hydrologic processes of dendritic watershed systems. The HEC-HMS uses a separate model to represent various components of the rainfall-runoff processes, like the loss model for calculating precipitation losses, the transform model for transforming excess precipitation into direct surface runoff, the base flow model for base flow estimation, and the routing model for routing the reach. The HEC-HMS model setup consists of four main model components: basin model, meteorological model, control specifications, and input data (time series, paired data, and gridded data) (USACE, 2021).

The basin model is used to describe the physical properties of the watershed and the topology of the stream network. It comprise the modeling components that describe canopy interception, surface storage, infiltration, surface runoff, base flow, channel routing, and lakes. Hydrologic elements are connected in a dendritic network to simulate runoff processes. The meteorological model contains rainfall, evapotranspiration, and snowmelt data. All the meteorological data analysis, for example, the precipitation required by a sub-basin element, is performed using this meteorological model component. The control specification contains start/stop timing and calculation intervals for the run. A geographic information system (GIS) can use elevation data and geometric algorithms to perform the same task much more quickly. GIS tools are being integrated directly within HEC-HMS. Current capabilities include options to delineate sub-basins and reaches from a terrain dataset.

### 2.6.2 SWAT+ model

SWAT+ is a completely restructured version of the Soil and Water Assessment Tool (SWAT) (Bieger et al., 2017) that is more flexible in terms of watershed discretization, configuration, and spatial representation of processes, as well as in defining management schedules and operation, and database maintenance. Advantages include improved anthropogenic water use and management, flexibility in managing schedules and operations, easier printing of outputs, and rapid model calibration.

SWAT+ uses the same equations as SWAT while offering more flexibility in model configuration to the user. SWAT+ introduces Land Scape Units (LSUs) to further discretize sub-basins and allow the separation of upland processes from wetlands. During model setup, sub-basins are delineated based on stream thresholds, while LSUs are delineated based on channel thresholds, as described in the user manual (Chawanda et al., 2020a). SWAT+ uses QSWAT+ interfaces for watershed delineation. The QSWAT+ interface has three main steps for SWAT+ model setup. This includes watershed delineation, creating HRU, and running the SWAT+ model in the SWAT+ editor. Potential evapotranspiration calculation method, water routing methods, and land use management are processed in the SWAT+ editor. Land use management practices are associated with plant communities, management schedules, conservation practices, curve numbers, etc.

### 2.6.3 HBV Light Model

The HBV (Hydrologiska Byran's Vattenbalansavdelning) model is a semi-distributed conceptual rainfall runoff model. The main input data to simulate daily discharge is daily rainfall, temperature, and potential evapotranspiration (Bergström, 1976a). HBV-light (Jan Seibert, 2005), a recent version of the model, has been employed in several studies in rainfall-runoff modeling across different river basins and regions (Ayalew, 2019); Birundu and Mutua, 2017).

The HBV light has four routines, which include the snowfall routine, soil moisture routine, response function routine, and routing routines (Seibert and Vis, 2012). The snowfall routine calculates snow cover and snowmelt using the degree-day method. The soil routine simulates groundwater recharge and actual evaporation as a function of actual water storage. In the response (or groundwater) routine, runoff is calculated as a function of reservoir volume. Finally, the routing routine uses a triangular weighting function to simulate the routing of runoff to the watershed. The model was selected because of its suitability, which has been demonstrated under different hydro-climatic conditions around the world ( Bergström, (1976), Lindström et al., (1997)).

### 2.7 Performance Evaluation of Hydrological Models in Simulating Rainfall Runoff

Golmohammadi et al. (2014) evaluated the performance of MIKE-SHE, APEX, and SWAT models for their ability to simulate the hydrology of the Canagagigue watershed located in the Grand River basin in southern Ontario, Canada. The "monthly $R^2$" during calibration was 0.80, 0.81, and 0.74 for MIKE SHE, APEX, and SWAT, respectively. The "monthly $R^2$" during validation was 0.64, 0.65, and 0.64 for MIKE SHE, APEX, and SWAT, respectively. The monthly RMSE during calibration was 8.70, 9.43, and 9.89 for MIKE SHE, APEX, and SWAT, respectively, and the monthly RMSE during validation was 11.42, 14.75, and 12.04 for MIKE SHE, APEX, and SWAT, respectively. The daily RMSE during calibration was 1.03, 0.95, and 1.26 for MIKE SHE, APEX, and SWAT respectively, and the daily RMSE during validation was 2.00, 2.00, and 2.19 for MIKE SHE, APEX, and SWAT, respectively. These statistical coefficients show that the daily $R^2$ (0.59, 0.44) of the fully distributed physically-based MIKE SHE model performed better than the $R^2$ (0.57, 0.41, and 0.51, 0.31) of the semi-distributed SWAT and APEX models during both calibration and validation, respectively. Based on RMSE and $R^2$ values, all three models performed better for monthly comparisons than daily ones. Monthly, the $R^2$ for APEX was slightly better than that for SWAT or MIKE-SHE. For daily predictions, all statistical parameters show better performances with the MIKE-SHE results.

Guduru et al. (2022) evaluated the performance of HEC-HMS in modeling rainfall runoff of the Meki river watershed, the rift valley basin of Ethiopia. The author selected Nash-Sutcliffe efficiency (NSE) and coefficient of determination ($R^2$) to evaluate the model's performance in modeling rainfall runoff in the watershed. The author's finding revealed that the model can perform very well (NSE = 0.83, $R^2$ = 0.91) during calibration and (NSE = 0.804, $R^2$ = 0.89) during the validation period.

Birundu and Mutua (2017) use HBV light to analyze the Mara River basin's behavior in rainfall-runoff modeling. The model tried to simulate the recession flow hydrographs, giving a representation of catchment characteristics, but it was not able to simulate well the peak flows in the catchment. The model overestimates the peak flow in the catchment. The model's performance in terms of NSE and $R^2$ was better as compared to previous rainfall-runoff modeling done using the SWAT and STREAM models.

Ayalew (2019) researched a comparative analysis of HBV light and SWAT in rainfall-runoff modeling in the Geba Catchment, Upper Tekeze Basin, Ethiopia. The researchers evaluate the performance of the HBV light and SWAT models using NSE, $R^2$, and PBIAS statistical indices. The researchers calibrate and validate the models until acceptable statistical indices reach acceptable values. The calibration results of HBV light and SWAT as evaluated by NSE, $R^{2,}$ and PBIAS are 0.707, 0.71, and 0.73, 0.81, and -11%, respectively. Moreover, an NSE, $R^{2,}$ and PBIAS of 0.71, 0.72, 0.72, 0.72, and 11% were obtained during the validation period for HBV light and SWAT models, respectively. From the results of the two models, the SWAT model was best at simulating the discharge at the catchment outlet with the highest objective function in terms of statistical analysis as compared to HBV-Light, but SWAT was less successful at predicting the uncertainty analysis of the parameters. Due to the capability of predicting the uncertainty of the parameter, the HBV Light model is selected for further water resource development and the future study of runoff simulation for the Geba Watershed.

Aliye et al. (2020) researched the Katar River Basin and the Central Rift Valley (CRV) Lake Basin of Ethiopia using the HEC-HMS and SWAT models. The authors evaluate the performance of HEC-HMS and SWAT hydrological models in simulating the rainfall runoff process for the Katar River Basin, which is the sub-catchment of the Central Rift Valley (CRV) Lake Basin of Ethiopia. The main objective of this study is to compare and assess the suitability of HEC-HMS and SWAT watershed simulation models for simulating the hydrology of the Katar river basin, the central Rift Valley Lake Basin of Ethiopia. The authors use Nash-Sutcliffe efficiency (NSE) and coefficient of determination ($R^2$) as statistical indices to assess the model performance of the HEC-HMS and SWAT models. The calibration results of HEC-HMS and SWAT as evaluated by $R^2$, and NSE were 0.88, 0.75, and 0.80, 0.69, respectively. Moreover, an $R^2$, and NSE of 0.87, 0.73, and 0.78, 0.67, respectively, were obtained during the validation period for the HEC-HMS and SWAT models. The results of statistical indices for model performance evaluation criteria showed that the simulated stream flow given by the HEC-HMS model is more satisfactory than that provided by the SWAT model.

The performance of several models has been evaluated in rainfall-runoff modeling in the upper Awash sub-basin. Zeberie (2019) conducted research on modeling rainfall runoff relationships using SWAT in the Big Akaki Watershed, Upper Awash Basin, Ethiopia. The author evaluated the SWAT capability in simulating the rainfall-runoff relation using the performance of the model for watershed calibration and validation. The values of Nash-Sutcliffe efficiency (NSE), coefficient of determination ($R^2$), and observations of the mean square error standard deviation ratio (RSR) were evaluated. Accordingly, their values showed a very good agreement with values of Nash-Sutcliffe coefficients (ENS) of 0.77 and 0.81, values of coefficient of determination ($R^2$) of 0.77 and 0.82, and observations of mean squared error standard deviation ratio (RSR) of 0.48 and 0.44 for calibration and validation, respectively. Finally, the author revealed that the surface runoff has the same pattern as the rainfall in the watershed.

Namara et al. (2020) researched rainfall-runoff modeling using HEC-HMS in the Awash Bello Catchment, Upper Awash Basin, Ethiopia. The author considers the performance of statistical indices (NSE, $R^2$, and PBIAS) during calibration and validation to compare the simulated peak flood with the observed peak flood. The model had shown good performance both during calibration and validation, with NSE = 0.855, $R^2$= 0.867 for calibration and NSE = 0.739 and $R^2$ = 0.863 for validation, respectively. PBIAS for calibration and validation were checked, and they were within the acceptable range with values of 4.59% and 5.67%, respectively. After calibration and validation, the researcher compared the peak flood from the model (573.7 $m^3$/ s), with the direct observed flow (546.4$m^3$/s) and the model provided nearly the same result as the directly observed flow. Finally, the researcher found that the model provides nearly the same result as the directly observed flow, and the HEC-HMS performs well in the simulation of peak floods in the Awash Bello catchment.

Tibebe et al. (2017) conducted research to estimate runoff at the Holetta catchment and to model rainfall-runoff relations in the area using the SWAT model in the Awash sub-basins, Ethiopia. The researcher evaluated the performance of the SWAT model using statistical indices coefficient of determination ($R^2$), Nash-Sutcliffe Efficiency (NSE), and Index of Volumetric Fit (IVF), and graphical methods. The results of statistical indices showed that

$R^2$, NSE, and IVF were 0.85, 0.84, and 102.8, respectively, for monthly calibration and 0.73, 0.67, and 108.9, respectively, for monthly validation. These indicated that the SWAT model performed well in the simulation of the hydrology of the catchment.

Maru et al. (2023) conducted a study on the Akaki catchment in Ethiopia to analyze the impact of land use land cover change (LULCC) on streamflow and surface water availability. They used the SWAT and CWB models to simulate streamflow and assess the water balance. The study found an increase in built-up and barren land areas from 1993 to 2016. The SWAT model overestimated peak flows but accurately simulated medium and low flows. Under different LULC scenarios, runoff increased in the study area. The seasonal water balance showed a decreasing trend, except for the Tseday season. The authors recommend proactive flood management measures to mitigate flood hazards.

# 3. MATERIALS AND METHODS

## 3.1 Description of the Study Area

### 3.1.1 Location

One of the sub-basins of the Upper Awash River Basin, which is located in the center of Ethiopia, is the Melka Kunture watershed. The geographical location of the Melka Kunture watershed lies between 7°52′–9.3° N and 37°57′–38°7′ E latitude and 37°57′–38°7′ E longitude at a distance of 50 km from Addis Ababa. It covers a drainage area of about 4500.42 $Km^2$, with elevations ranging from 1996m to 3565m above mean sea level. There is high population density, diverse ecology, and mainly rain-fed agriculture, which is highly vulnerable to the changing climate, which causes flooding and water shortages (Getahun et al., 2020) in the watershed.

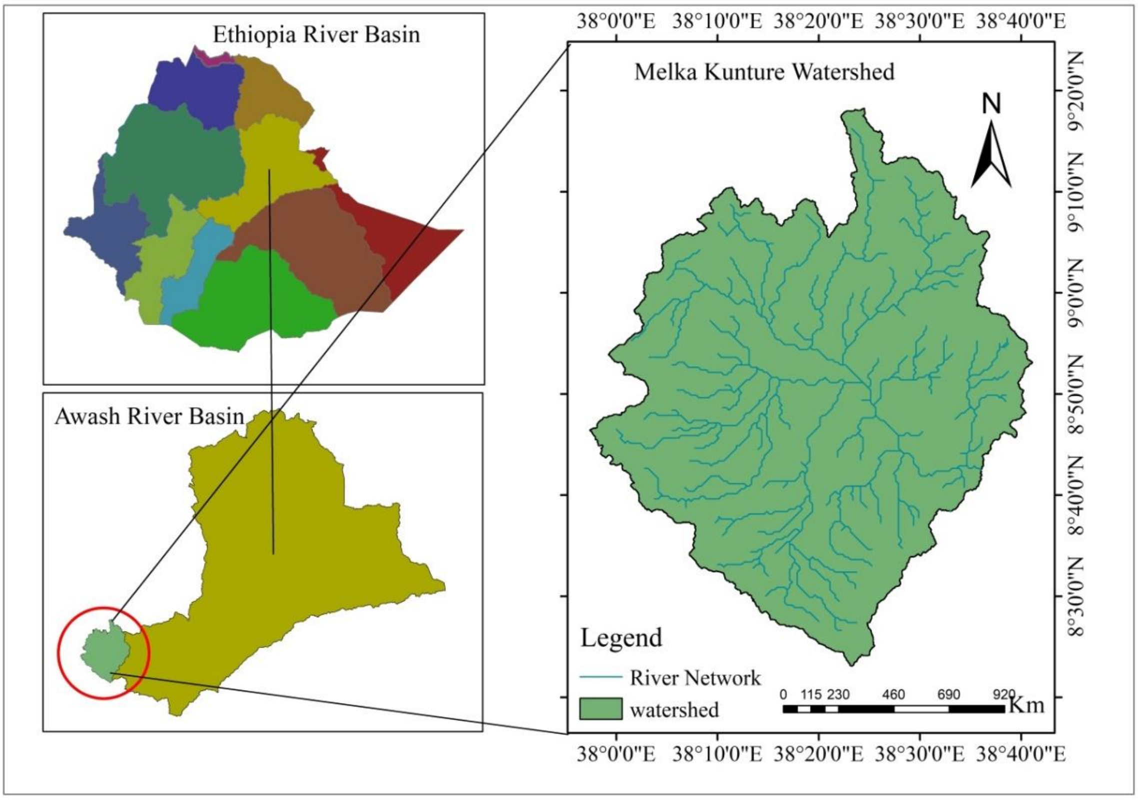


Figure 3.1: Location map of Melka Kunture watershed

### 3.1.2 Climate

The inter-tropical convergence zone's (ITCZ) movement and the Indian monsoon's year-round influence mostly dictate the Melka Kunture watershed climate (Getahun et al., 2020). Based on the movement of the inter-tropical convergence zone (ITCZ), the amount of rainfall, and the timing of the rainfall, there are three seasons in the Melka Kunture watershed. The three seasons are: Kiremt, the primary rainy season lasting from June to September; Bega, the dry season lasting from October to January; and Belg, the minor rainy season lasting from February to May.

The watershed receives a huge volume of rainfall from June to September, followed by a relatively dry season until the end of January and a small rainy season from February to the end of May (Figure 3.2). The mean annual rainfall in the Melka Kunture watershed is about 1003.32 mm, and the mean annual temperature ranges from a mean minimum temperature of 6.78 $^{0}$C to a mean maximum temperature of 27.70 $^{0}$C with a relative cold climate from November to December. The average monthly total discharge total flow distribution of the Melka Kunture watershed outlet gauging station conforms well to the mean monthly rainfall (Figure 3.3). The discharge exhibits a similar trend to that of rainfall, and the highest flows correspond to the wettest months of June, July, August, and September. The total estimated mean annual discharge of the Melka Kunture watershed was 11855.74 $m^3$/ s.

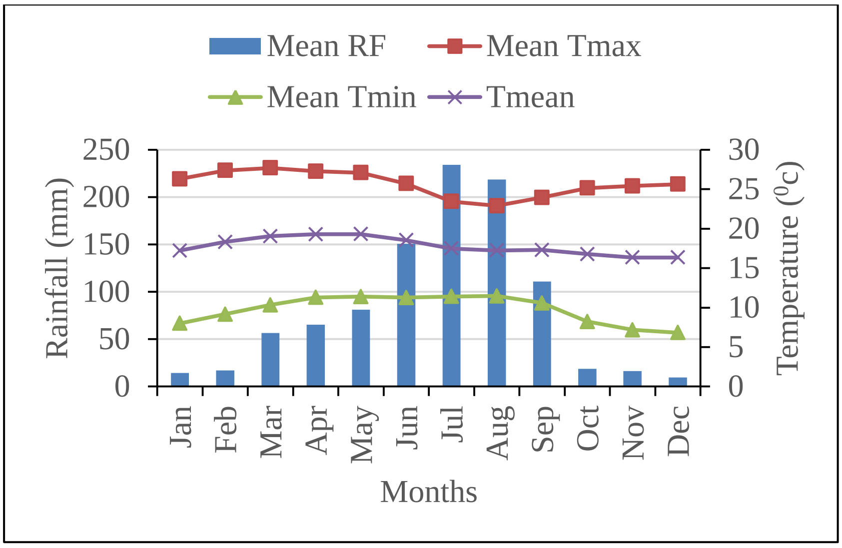


Figure 3.2: Mean monthly rainfall and temperature distribution of Melka Kunture watershed

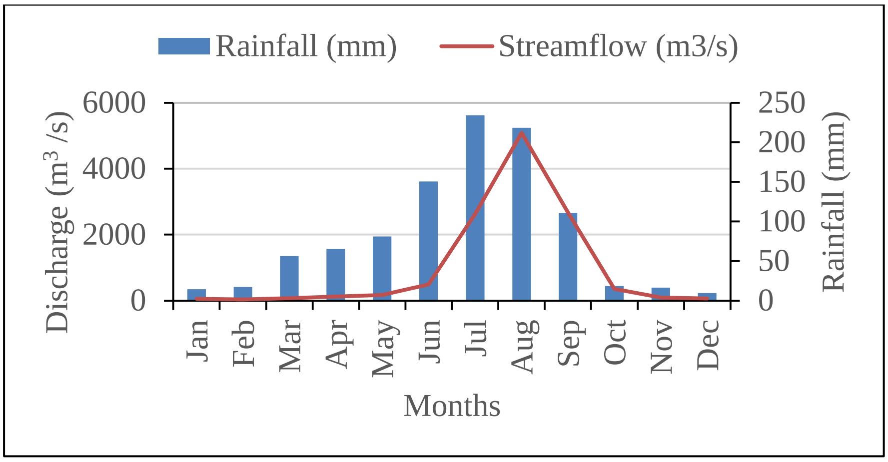


Figure 3.3: Mean monthly rainfall and discharge of Melka Kunture watershed

### 3.2 Data Collection and Analysis

Input data mainly required for simulating streamflow can be categorized into hydro-meteorological (rainfall, temperature, and streamflow) data and physiographic (digital elevation model, soil type, and land use or land cover). In this study, HEC-HMS, SWAT+, and HBV-Light models were applied to simulate the streamflow of the Melka Kunture watershed, and each model needs a different data input protocol to process and generate output. The HEC-HMS model uses the input data such as spatial data (digital elevation model, soil map, land use, and land cover), hydro-meteorological data (precipitation, temperature) and streamflow. SWAT+ model uses input data such as spatial data (digital elevation model, land use, soil) and hydro-meteorological data (precipitation, temperature, relative humidity), and HBV-Light uses spatial data (digital elevation model, land use, and land cover), hydro-meteorological data (precipitation, temperature, and streamflow), and potential evapotranspiration data.

Table 3.1: Data type and sources

| Data type | Data Sources |
|---|---|
| Digital Elevation Model | Website: https://earthexplorer.usgs.gov/ |
| Soil data | Website: https://www.fao.org/soils-portal/soil-survey/soil-maps-and-databases/faounesco-soil-map-of-the-world/en/ |
| Land use land cover | Website: https://livingatlas.arcgis.com/ |
| Meteorological data | Ethiopian Meteorological Institute (NMI) |
| Hydrological data | Ministry of Water and Energy (MoWE) |

### 3.2.1 Spatial Data

#### *3.2.1.1 Digital Elevation Model*

Topographic data are often represented in the form of a digital elevation model (DEM), where the elevations of any point in a given area at a specific spatial resolution are described. The spatial resolution of the digital elevation model used for this study is 30m x 30m. The elevation of the study area ranges from 1996m to 3565 m above mean sea level (Figure 3.4). A digital elevation model was used to delineate the watershed and analyze the drainage patterns of the land surface terrain. The watershed parameters, such as sink, flow direction, flow accumulation, and stream network, were derived from the digital elevation model. Also, sub-basin characteristics such as flow path length, basin slope, etc. were derived from the digital elevation model.

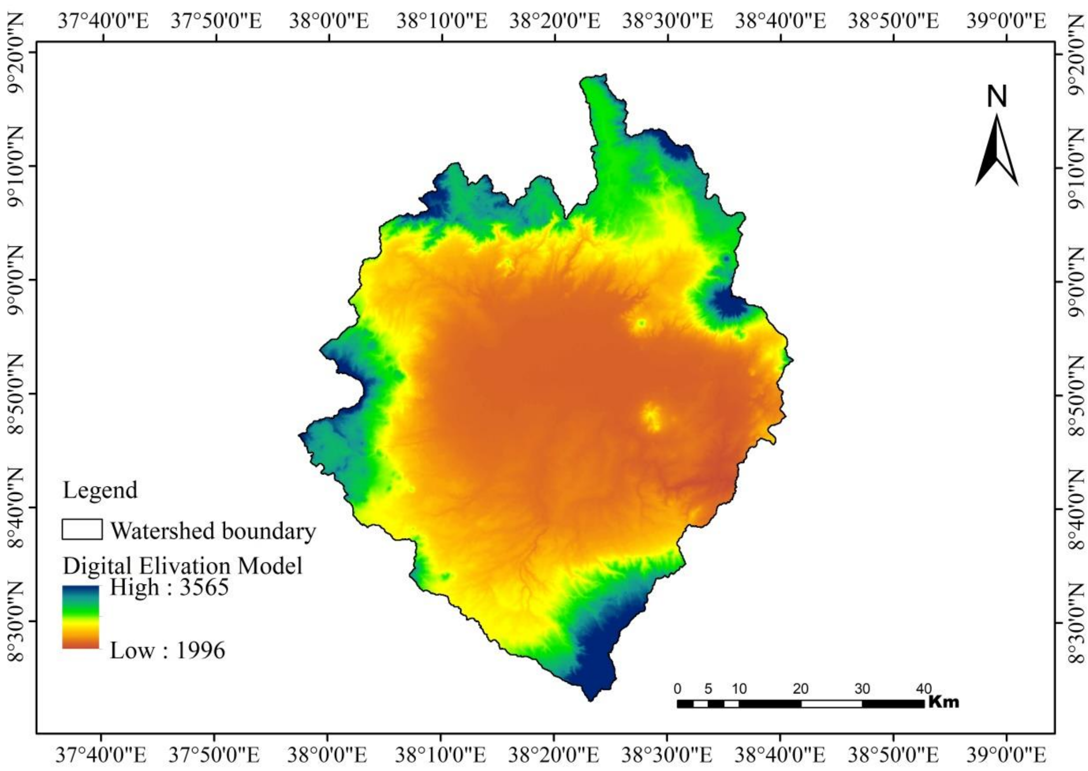


Figure 3.4: Digital elevation model of the watershed

#### *3.2.1.2 Soil Data*

Soil is the major physical watershed characteristic that governs runoff generation. The soil map of the study area was downloaded from the Food and Agriculture Organization of the United Nations (FAO) using the link in Table 3.1. According to FAO, the Melka Kunture watershed can be divided into two major soil groups (Figure 3.5). The main dominant soils in the watershed are eutric nitisols (37.82%), and pellic vertisols (62.18%).

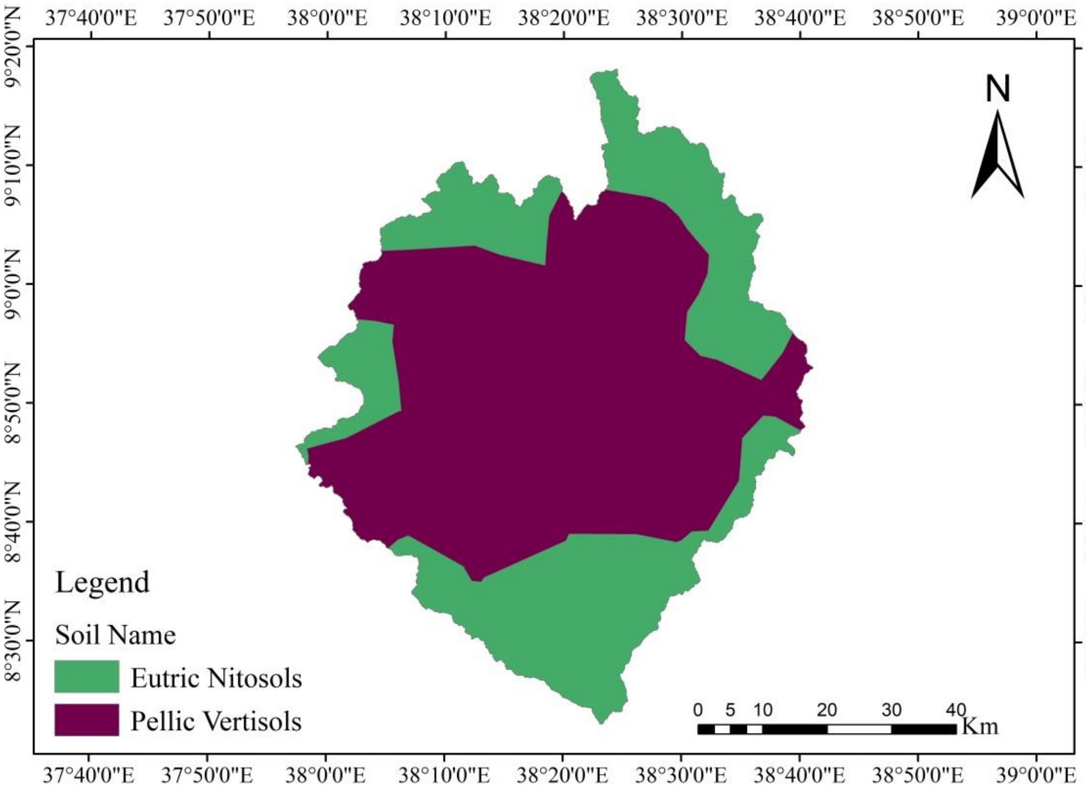


Figure 3.5: Soils map of the study area

#### *3.2.1.3 Land use and land cover*

The spatial dynamics of the hydrologic cycle at the watershed, sub-watershed, and basin levels are interrelated in studies of water resources management. Several elements, including anthropogenic and natural forces, contribute to the intensification of this cycle. Particularly, changes in land use and land cover (LULC) have a big impact on the watershed's hydrology because they change the amount and pattern of surface runoff, groundwater, and soil moisture (Beyene et al., 2018).

The spatial distribution and explicit land use and land cover parameters were essential for simulating streamflow. The change in land use and land cover is one of the major factors in the alteration of hydrological parameters in the watershed. For this study, land use data for the year 2017 was downloaded from ESRI (https://livingatlas.arcgis.com/). The maps were derived from ESA Sentinel-2 imagery at 10 meter resolution. In this watershed, the dominant land use and land cover type is agriculture/crops (87.60%), built area (6.88%), range lands (2.79%), trees (2.70%), water (0.02%), bare ground (0.02%), and others (0.0001105%).

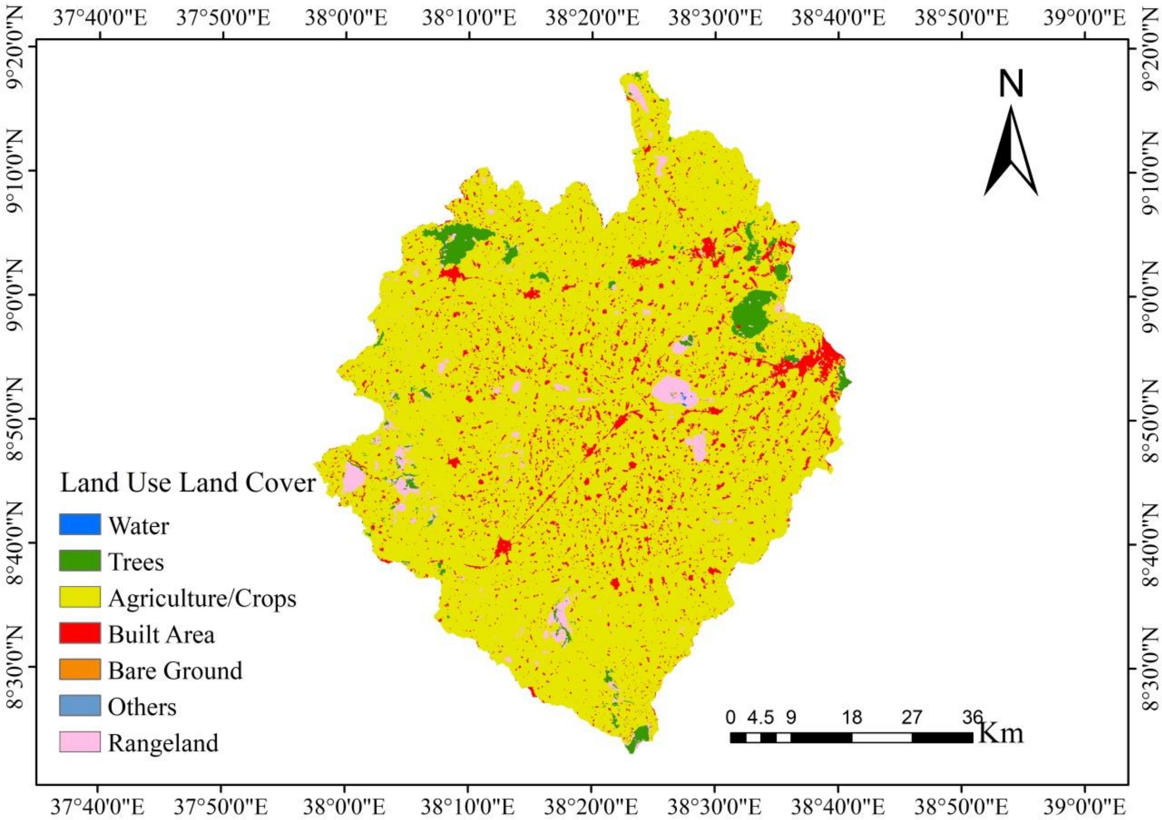


Figure 3.6: Land use and land cover map of the study area

### 3.2.2 Hydro-meteorological Data

Daily meteorological data from 2000-2015 for nine rain gauge stations (Table 3.2) situated within the Melka Kunture watershed were collected from the Ethiopian Meteorology Institute (EMI). These meteorological stations were selected depending on their length of record, recorded data availability at the station, consistency, and homogeneity of data in the watershed. Daily streamflow data from 2000-2015 at the Melka Kunture river gauging station was collected from the Ethiopian Ministry of Water and Energy (MoWE) for the successful completion of the research objective.

Table 3.2: Meteorological data for the selected stations in the study area

| Stations | Latitude (N) | Longitude (E) | Elevation (m) | Record year |
|---|---|---|---|---|
| Addisalem | 9.05 | 38.38 | 2372 | 2000-2015 |
| Asgori | 8.80 | 38.34 | 2072 | 2000-2015 |
| Bantu Liben | 8.62 | 38.36 | 2167 | 2000-2015 |
| Enselale | 8.94 | 38.44 | 2123 | 2000-2015 |
| Ginch | 9.02 | 38.13 | 2132 | 2000-2015 |
| Kimoye | 9.01 | 38.34 | 2150 | 2000-2015 |
| Teji | 8.84 | 38.38 | 2062 | 2000-2015 |
| Tulu Bolo | 8.66 | 38.21 | 2190 | 2000-2015 |
| Wolenkomi | 9.00 | 38.26 | 2165 | 2000-2015 |

#### *3.2.2.1 Filling in missing data*

One of the initial steps in any hydro-meteorological investigation is gaining access to trustworthy, high-quality data. However, data on rainfall, temperature, and streamflow are frequently incomplete. The incompleteness of these data may be caused by faulty measuring equipment, measurement mistakes, and geographic data gaps, changes in instrumentation over time, changes in measurement sites, personnel collecting the data, irregular measurement patterns, or significant recent climate changes.

Different methods are used to estimate missing rainfall (Xia et al., 1999). These methods are multiple regression analysis, arithmetic mean method, normal ratio method, aerial rainfall ratio method, inverse distance weighting method, etc. In this research, the missed meteorological data were estimated by using arithmetic and normal ratio methods by observing the nearby surrounding stations, depending on the percentage of missed rainfall at the stations. The arithmetic method is used if the normal annual precipitation at various stations is within about 10% of the normal annual precipitation at station X, but if the normal annual rainfall varies considerably more than 10%, normal ratio method is used (Silva et al., 2007). The normal ratio method is expressed by equation 3.1.

$$P_x = \frac{N_x}{M}\left[\frac{P_1}{N_1} + \frac{P_2}{N_2} + \frac{P_2}{N_3} + \cdots \frac{P_m}{N_m}\right] \tag{3.1}$$

Where, $P_x$ the missing value of rainfall is to be computed, $N_x$ is the average value of rainfall for the station in question for the recording period; $N_1$, $N_2$, $N_3$….$N_m$ is the average value of normal rainfall for the neighboring station; and $P_1$, $P_2$, $P_3$.... $P_m$, is a rainfall of the neighboring station during the missing period; and M = is the number of stations used in the computation.

#### *3.2.2.2 Estimation of area rainfall*

Within a drainage basin, rain gauge stations are evenly distributed across sub-basins, but they only provide point rainfall measurements at their specific locations. It's important to note that rainfall can vary between stations within the same watershed. To obtain an average rainfall value for the entire basin and accurately define its boundaries, the point rainfall data needs to be converted into mean areal rainfall values. To achieve this, various methods are available, including the arithmetic mean, Theissen polygon, and Isohyet methods. For this research, the Theissen polygon method was chosen to calculate the watershed's rainfall. This method offers the advantage of simplicity, making it easy to understand. Additionally, it accounts for the non-uniform distribution of meteorological stations by assigning weights based on proximity (Engida et al., 2021).

By utilizing the Theissen polygon method, it becomes possible to estimate the average annual rainfall over the desired area. This information is vital for numerous applications, including water resource management and planning.

$$P_{avg} = \frac{\sum_{i=1}^{n} P_i A_i}{\sum_{i=1}^{n} A_i} \tag{3.2}$$

Where, $P_{avg}$ is the average areal rainfall (mm), $P_i$ is the rainfall at each sub-basin (mm), and $A_i$ is the area of each sub-basin (km$^2$). The total weighted rainfall of the study area is 1003.32 mm (Table 3.3).

Table 3.3: Weighted rainfall of the study area

| Stations | Longitude (y) | Latitude (x) | Rainfall (mm) | Area (km$^2$) | Weighted Area (Wi) | Weighted rainfall (mm) |
|---|---|---|---|---|---|---|
| Addisalem | 38.383 | 9.048 | 1088.81 | 522.10 | 0.12 | 126.31 |
| Asgori | 38.335 | 8.795 | 964.23 | 337.10 | 0.07 | 72.22 |
| Bantu Liben | 38.357 | 8.618 | 1194.78 | 805.90 | 0.18 | 213.95 |
| Enselale | 38.44 | 8.937 | 662.92 | 704.79 | 0.16 | 103.82 |
| Ginch | 38.133 | 9.017 | 1097.49 | 534.57 | 0.12 | 130.36 |
| Kimoye | 38.341 | 9.013 | 998.95 | 135.91 | 0.03 | 30.17 |
| Teji | 38.375 | 8.836 | 933.99 | 377.71 | 0.08 | 78.39 |
| Tulu Bolo | 38.211 | 8.658 | 1081.29 | 764.20 | 0.17 | 183.61 |
| Wolenkomi | 38.257 | 9.004 | 912.19 | 318.15 | 0.07 | 64.49 |

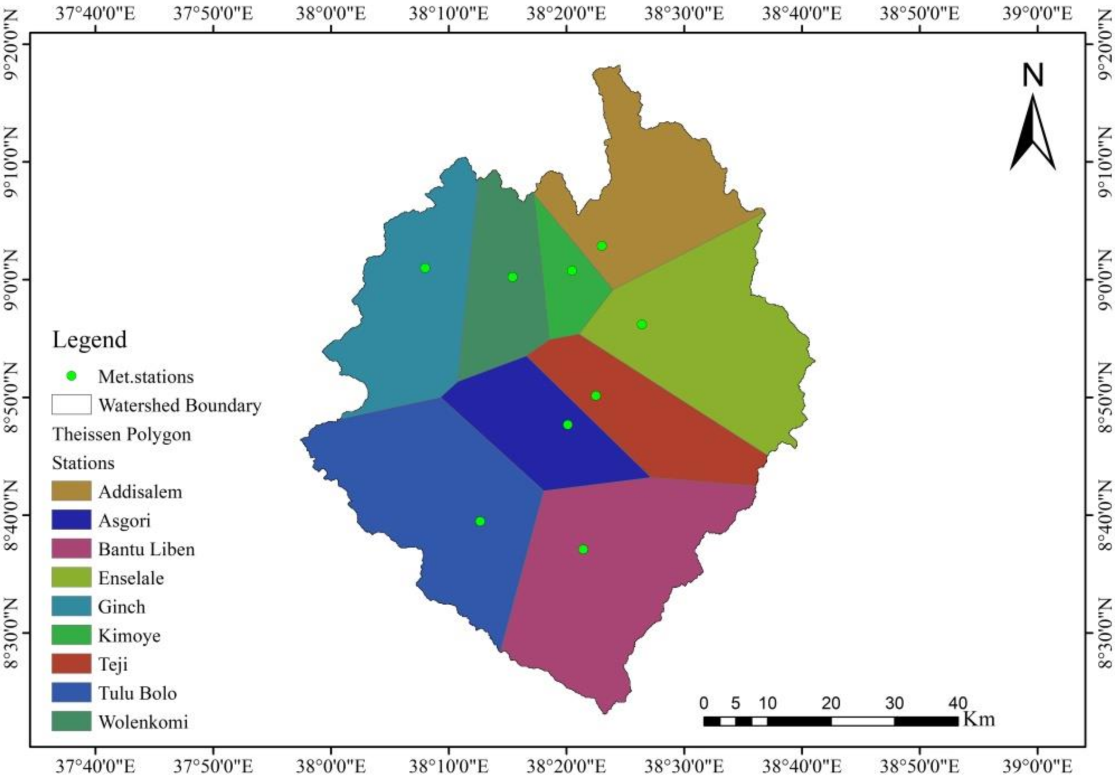


Figure 3.7: Thiessen polygon of the study area

***3.2.2.3 Estimation of potential evapotranspiration***

One of the most important parts of the hydrologic cycle is evapotranspiration. Several methods, such as the Penman-Monteith method, Hargreaves method, and Priestley-Taylor method, are included in the HEC-HMS, SWAT +, and HBV Light models. Penman-Montieth requires solar radiation, air temperature, relative humidity, and wind speed, but the Hargreaves method (Hargreaves, 1994a) requires only maximum and minimum air temperature data. In this research, the Hargreaves method was applied to calculate potential evapotranspiration because it is a simplified approach that requires only temperature data, making it suitable for Melka Kunture watershed. The potential evapotranspiration is calculated by the equation 3.3.

$$ET_o = 0.0023xR_a x(T_{mean} + 17.8)x\Delta T^{0.5} \tag{3.3}$$

Where $ET_o$ and $R_A$ have the same units. $R_A$ is the water equivalent of the terrestrial radiation ($M/m^{-2}day^{-1}$); $T_{mean}$ is the mean temperature ($^o$ C) and $\Delta T$ is a change in temperature ($^0C$)

### *3.2.2.4 Testing for consistency of data*

Inconsistency would arise in the rainfall data at a rain gauge station if conditions relevant to the recording of rainfall at the station undergo significant change during the period of record. It would be felt from the moment a significant change took place. The check for the inconsistency of the record was done by the double mass curve technique. The double mass curve is a well-known, simple tool for checking and adjusting inconsistencies in hydro-meteorological data caused by changes in observation methods or data processing (Ebru and Necati, 2012). Data on the annual or monthly mean rainfall of Station X as well as the average rainfall of the group of base stations over a long period were arranged in reverse chronological order, i.e., the latest record is the first entry and the oldest record is the last entry in the list.

Accumulated precipitation at station X ($\sum \mathrm{P_x}$) and the accumulated values of the average precipitation of the group of base stations computed from the latest records. A plot of ($\sum \mathrm{P_x}$) versus ($\sum \mathrm{P_{av}}$) for various consecutive periods is prepared. A break in the slope of this plot indicates a change in the precipitation regime at station X. Precipitation values at X beyond the period of change of regime are corrected as follows:

$$P_{cx} = P_x \frac{M_c}{M_a} \tag{3.4}$$

Where, $P_{cx}$= corrected precipitation at any period at station X, $P_x$= originally recorded rainfall for this period at X, $M_c$= corrected slope of the double mass curve, and $M_a$= original slope of the mass curve.

The consistency of recorded rainfall in the watershed at different stations was tested using the double mass curve method. The deviations between accumulated annual rainfall at individual stations and the accumulated average annual rainfall of all stations (Appendix Figure 1) for consecutive sixteen years were tested, and the result showed all stations were consistent. The correlation between accumulated annual rainfall at the individual station and the accumulated average annual rainfall of all stations was also calculated and showed a high correlation. The correlation between the cumulative rainfalls of each station and the cumulative group station average rainfall was checked (Appendix Table 1), and the result showed a very good correlation.

### *3.2.2.5 Checking the homogeneity of meteorological stations*

Homogeneity analysis is used to identify a change in the statistical properties of the time series data. The cause of change can be either natural or man-made (G. W. Belay et al., 2019). It includes alteration due to land use and rearrangement of observation stations.

Therefore, to select representative meteorological stations for any study or analysis of rainfall estimation, checking the homogeneity of a group of stations is essential. The homogeneity of selected gauging stations was determined by non-dimensionalized monthly precipitation records (equation 3.5).

$$P_i = \frac{\overline{P_i}}{\overline{P}} x100 \quad (3.5)$$

Where $P_i$ is non-dimensional precipitation for month i, $\overline{P_i}$ is the average monthly precipitation for station i, and $\bar{P}$ is the average yearly precipitation of the station.

The selected stations were plotted for comparison (Appendix Figure 2), and in all stations, the same mode and pattern were observed indicating that the selected stations are homogeneous.

#### *3.2.2.6 Homogeneity test of time series*

Frequency analysis of data requires that the data be homogeneous and independent. The restriction on homogeneity assures that the observations are from the same population. One of the tests of homogeneity is based on the cumulative deviations from the mean (Buishand, 1982).

$$S^*{}_k = \sum_{t=1}^{k} (X_t - \bar{X})\,, k = 1,2,3,4, \ldots\ldots, n \quad (3.6)$$

Where, $S^*{}_k$ are the cumulative deviations, $X_t$ is the observed value, $\bar{X}$ is the sample mean, and n is the number of records in the time series. The rescaled adjusted partial sums ($S^{**}{}_k$) are obtained as:

$$S^{**}{}_k = \frac{S^*{}_k}{D_x}\,, \quad k = 1,2,3,4, \ldots\ldots n \quad (3.7)$$

The standard deviation $D_x$ can be calculated as:

$$D_x = \sqrt{\sum_{i=1}^{n} \frac{(X_i - \bar{X})^2}{n}} \quad (3.8)$$

The cumulative deviation test statistic (Q) is estimated as:

$$Q = max|S^{**}{}_k|, 0 \leq k \leq n \quad (3.9)$$

In this study, homogeneity of the streamflow at the Melka Kunture streamflow outlet was analyzed using the RAINBOW software package (Gbaguidi, 2006). RAINBOW rescales the cumulative deviation by dividing the $S^*{}_k$'s by the sample standard deviation ($D_x$) value. By evaluating the maximum (Q) and range (R) of the rescaled cumulative deviations from the mean, the homogeneity in the data of the time series were tested. High values of Q or R are an indication that the data in the time series is not from the same population and that the fluctuations are not purely random. Critical values for the test statistic that will test the significance of the departures from homogeneity was plotted to show the variation in the significance of the data. From the test (Appendix Figure 3), it was seen that none of the three lines are crossed by the deviation line; therefore, the streamflow data series is homogeneous, and so it can be used for any further analysis.

## 3.3 Methodology

### 3.3.1 Analysis of the spatial and temporal variability of rainfall and streamflow data

Analyzing rainfall distribution, temperature, and streamflow variability in space and time is crucial for sustainable water resource management and agricultural productivity (Alemu and Bawoke, 2020). The seasonal and annual rainfall characteristics of the Melka Kunture watershed were analyzed by fundamental statistical techniques such as mean, standard deviation (SD), and coefficient of variance (CV) (Pawar et al., 2022). Additionally, the standardized rainfall anomaly index (SRAI) and precipitation concentration index (PCI) were used to evaluate the annual and seasonal distribution of rainfall.

#### *3.3.1.1 Analysis of spatiotemporal variability of rainfall*

The spatiotemporal variability of the mean annual and seasonal rainfall was interpolated between the selected weather stations to understand the spatial variability of rainfall (Habte et al., 2021). The inverse distance weighting (IDW) technique was employed for the interpolation of mean annual and seasonal rainfall using ArcGIS. This method was used in previous studies for a similar analysis (Birara, (2018); Dereje Ayalew, (2012). The spatial variability of mean annual and seasonal rainfall in the study area was evaluated using the coefficient of variation (CV). Accordingly, variability was classified as low (CV<20%), moderate (20%≤CV≤30%), and high (CV > 30%). The temporal variability was analyzed by the method below:

i. **The coefficient of variation (CV):** is a simple measure of how values deviate from the mean of the variables and is given by:

$$C_V = \frac{\sigma}{\mu} x100 \tag{3.9}$$

Where $C_V$ the coefficient of variation, $\sigma$ is the standard deviation and $\mu$ is the average meteorological variable. According to Belay et al. (2021), the degree of rainfall variability is classified as high (CV > 30), moderate (20 < CV > 30), and low (CV < 20). Hence, the higher the value of CV the higher the variability of rainfall in the study region and the reverse is also true.

**ii. Standardized rainfall anomaly index (SRAI):**

The standard rainfall anomaly index shows the dry and wet years, the nature of trends, and assesses the frequency and severity of droughts in rainfall time series. According to Lambe and Kundapura (2021) and Alemu and Bawoke (2020), the values range from extremely wet (≥ 2.00), very wet (1.50 to 1.99), moderately wet (1.00 to 1.490), near normal (-0.99 to 0.99), moderately dry (-1.00 to -1.49), severely dry (-1.50 to -1.90), and extremely dry (≤ -2.00).

$$SRAI = \frac{X_i - \bar{X}}{\sigma} \tag{3.9}$$

Where SRAI is the standard rainfall anomaly index, $X_i$ is the rainfall value time series, $\bar{X}$ is the means of the rainfall time series, and $\sigma$ is the standard deviation.

**iii. Precipitation concentration index (PCI):**

The precipitation concentration index measures the nature of precipitation's monthly, seasonal, and annual distribution. The precipitation concentration index (PCI) is used to indicate the hydrological risks of floods and droughts occasions in the study area (Belay et al., 2021) and can be calculated using equation (3.10).

$$PCI_{Annual} = \frac{\sum_{i=1}^{12} {P_i}^2}{(\sum_{i=1}^{12} P_i)^2} x100 \tag{3.10}$$

Where $PCI_{Annual}$ is the annual precipitation concentration index and $P_i$' is the individual monthly precipitation. PCI values indicated evenly distributed (<10), moderate rainfall concentration (11-15), irregularly distributed rainfall in the area (16-20), and strong irregularity rainfall distribution across the area (>20) ((Lambe and Kundapura, (2021); Melat Eshetu, (2021)).

***3.3.1.2 Analysis of temporal variability of streamflow***

Streamflow variability shows the wetness and dryness of the watershed. Hence, it is crucial to determine the variability of streamflow for Melka Kunture watershed. The spatial variability of maximum, average, and minimum streamflow in the melka Kunture watershed was evaluated using the coefficient of variation (CV). Accordingly, variability was classified as low (CV<20%), moderate (20%≤CV≤30%), and high (CV > 30%). The temporal variability was analyzed by the method below:

### 3.3.2 Hydrological Models and Model Setup

#### *3.3.2.1 HEC-HMS model*

Hydrologic Engineering Center-Hydrologic Modeling System (HEC-HMS) is a hydrologic modeling software developed by the US Army Corps of Engineers of the Hydrologic Engineering Center (HEC), which contains an integrated tool for modeling hydrologic processes of dendritic watershed systems (Hamdan et al., 2021). The Hydrologic Engineering Center-Hydrological Model System (HEC-HMS) is one such model that supports both lumped parameter-based modeling and distributed parameter-based modeling (Sahu et al., 2020).

The HEC-HMS uses a separate model to represent various components of the rainfall-runoff process, like the loss model for calculating precipitation losses, the transform model for transforming excess precipitation into a direct surface runoff, the base flow model for base flow estimation, and the routing model for routing the reach. The HEC-HMS model setup consists of four main model components: basin model, meteorological model, control specifications, and input data (time series, paired data, and gridded data) (USACE, 2021).

The basin model is used to describe the physical properties of the watershed and the topology of the stream network. It will contain the modeling components that describe canopy interception, surface storage, infiltration, surface runoff, base flow, channel routing, and lakes. Hydrologic elements are connected in a dendritic network to simulate runoff processes. The delineation process into several sub-basins is done automatically with the help of the GIS menu integrated with HEC-HMS software (Eryani et al., 2021). Hydrologic elements are used to break the watershed into manageable pieces. They are connected in a dendritic network to form a representation of the stream system. Their principal purpose is to convert atmospheric conditions into streamflow at specific locations in the watershed.

The meteorological component is also the major computational element through which precipitation input is spatially and temporally distributed over the river basin (Gebre, 2015). The Thiessen polygon technique was used to determine the gauge weights, and the following input data like daily precipitation, daily temperature, elevation, and long-term mean monthly actual potential evapotranspiration were used. Control specifications are defined in the HEC-HMS program interface to define the runtime of each model. Control specifications include the starting date and time, the ending date and time, and the computational time step.

The HEC-HMS model requires different datasets, including a Digital Elevation Model (DEM), weather data, soil type, and land uses. The Soil Conservation Service Curve Number, SCS Unit hydrograph, and Muskingum routing methods were selected for each component of the runoff process as runoff depth, direct runoff, and channel routing, respectively. These methods were chosen based on the applicability and limitations of each method, the availability of data, suitability for the same hydrologic condition, stability, wide acceptability, and well-established researcher recommendations (Tassew et al., 2019).

**i. Loss model-curve number method**

The loss models in HEC-HMS normally calculate the runoff volume by computing the volume of water that is intercepted, infiltrated, stored, evaporated, or transpired and subtracting it from the precipitation (Tassew et al., 2019). It is used for estimating excess precipitation by deducting the total losses from the total precipitation. In this study, the Soil Conservation Service Curve Number (SCS-CN) loss method (Hamdan et al., (2021); Daide et al., (2021)) was used to estimate direct runoff from specific precipitation. It is selected due to its versatility, being widely applicable in estimating runoff, requiring few input data, and providing reliable results (Guduru et al., 2022).

In the Soil Conservation Service (SCS) method, direct runoff occurs when the rainfall (mm) for the day is greater than the initial abstraction (i.e., losses like interception, depression storage, and infiltration). The Soil Conservation Service (SCS) curve number method is an empirical conceptual method developed for the computation of direct runoff using equation (3.11) under variable soil types and land uses.

$$P_e = \frac{(P - I_a)^2}{(P - I_a + S)} \tag{3.11}$$

Where $P_e$ is cumulative runoff or rainfall excess (mm), $P$ is daily rainfall (mm); $I_a$ is an initial abstraction that includes surface storage, interception, and infiltration before runoff (mm), and $S$ is the retention parameter (mm) which is calculated as equation (3.12):

$$S = 25.4\left(\frac{1000}{CN} - 10\right) \tag{3.12}$$

Where: CN is the curve number for the day. In the initial abstractions, Ia is commonly approximated as 0.2S.

$$P_e = \frac{(P - 0.2S)^2}{P + 0.8S} \quad (3.13)$$

**ii. Transform model-SCS unit hydrograph method**

The transform method allows you to specify how to convert excess rainfall to direct surface runoff. The transform prediction models in HEC-HMS simulate the process of excess rainfall direct runoff in the catchment and transform the rainfall excess into point runoff (Hamdan et al., 2021); (Daide, Afgane, Lahrach, Chaouni, Msaddek, & Elhassnaoui, 2021). In this study, the Soil Conservation Service Unit Hydrograph model will be chosen to transform excess precipitation into runoff. It is a parametric model based on the average unit hydrograph (UH) derived from gauged rainfall and runoff data from a large number of small agricultural watersheds throughout the United States. The SCS proposed the Unit Hydrograph (UH) model, which is included in the HEC-HMS program.

The lag time ($T_{lag}$) is the only input for this method. It is the time from the center of mass of excess rainfall to the hydrograph peak and is calculated based on the time of concentration $T_C$, as:

$$T_{lag} = 0.6T_C \quad (3.14)$$

Where $T_{lag}$ and $T_C$ are in a minute

The time of concentration can be estimated based on basin characteristics, including topography and the length of the reach, using the Kirpich (1940) formula (Taghvaye Salimi et al., 2016).

$$T_C = K\ L^{0.77} S^{-0.385} \quad (3.15)$$

Where $T_c$ is a time of concentration in minutes, K is a unit conversion coefficient, in which K = 0.0078 for traditional units (feet)and k = 0.0195 for SI units, L is the channel flow length, in feet or meters as dictated by K, and S is the dimensionless main channel slope whether in (ft/ft) or in (m/m)

**iii. Routing model-Muskingum method**

Flood routing is the technique of determining the flood hydrograph downstream of the river by utilizing the inflow data upstream (Sahu et al., 2020). The routing of the runoff from the outlet of the sub-basins to the outlet of the whole basin will be made by using the Muskingum routing method. From the available channel routing models in HEC-HMS, the Muskingum Routing model will be selected for this model.

The Muskingum routing method is a simple approximate method to calculate the outflow hydrograph at the downstream end of the channel from the inflow hydrograph at the upstream end. Among many models used for flood routing in rivers, this is a straightforward hydrological flood routing technique used in natural channels (Tassew et al., 2019). K and X are the two important parameters in the Muskingum methods, where K is the travel time of the flood wave passing through the routing reach and X is a dimensionless weight that corresponds to the attenuation of the flood wave as it moves through the reach, whose values vary between 0 and 0.5. K is the parameter having a unit of time. It is related to the delay between discharge peaks (Hamdan et al., 2021). K is estimated using Equation 3.16.

$$K = \frac{L}{V_w} \tag{3.16}$$

Where, $V_w$ is the flood wave velocity, which can be taken as 1.5 times the average velocity; and L is the reach length. The average velocity was obtained from the stream gauging sites.

$$\frac{dS}{dt} = I - Q \tag{3.17}$$

Where, $\frac{dS}{dt}$ rate of change of storage per unit time, I-inflow, Q–outflow

A common method of stream flow routing is the Muskingum method (McCarthy, 1939), where the storage is expressed as a function of both inflow and outflow in the reach as follows;

$$S = k[xI + (1 - x)Q] \tag{3.18}$$

Where: S – storage, x – weighted coefficient of discharge, k – flood wave travel time

**a. Terrain analysis and preparation of basin file**

The delineation of the basin was conducted by terrain processing in HEC-HMS using the GIS integrated with HEC-HMS. Filling a sink, determining flow direction and accumulation, identifying streams, specifying outlet specification and delineating watershed boundaries and sub-basin were done by GIS tools within HEC-HMS. The extraction of basin characteristics from the physical properties of the catchment was also obtained from the delineated watershed. The basin characteristics in each sub-basin were used to estimate the model parameter used in the simulation of the streamflow of the watershed. In each sub-basin, elements like surface, loss, transform, and base flow methods were used to convert rainfall to runoff.

**b. Weighted rainfall and parameters used in the HEC-HMS model**

In basin model processing, the watershed was divided into sub-basins. The sub-basin element in the HEC-MMS has only one inflow and one outflow. The Theissen polygon was used to estimate the area of rainfall in the study area. In the ArcGIS software, the Theissen polygon and sub-basin were intersected to estimate the weighted rainfall for each subbasin (Table 3.4). Outflow from the sub-basins was generated from the weighted rainfall data that has been processed in the watershed by converting excess weighted rainfall into flow (Eryani et al., 2021) (Figure 3.8), while the reach element is an element with one or more inflows originating from different elements in the model. The parameters used in this study for the HEC-HMS model are given in Table 3.5.

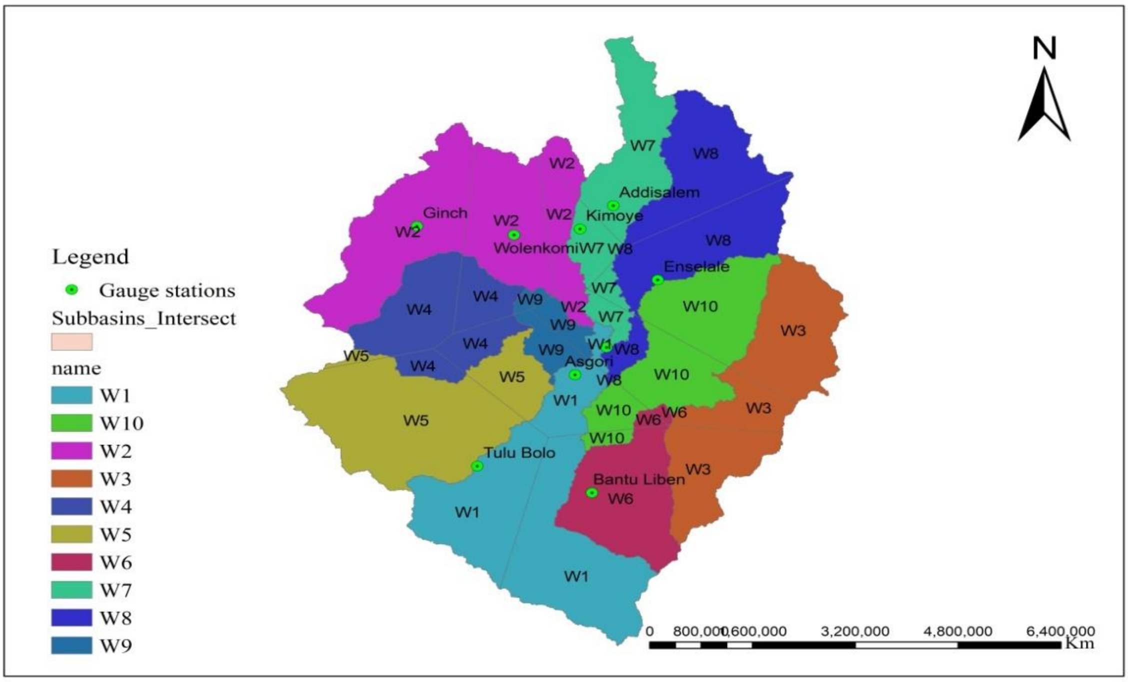


Figure 3.8: Sub-basins and Thiessen polygon with their areal coverage

Table 3.4: Metrological stations included in the Sub-basins and their percentage of areal coverage

| Name | Total Area | Station | Area | Weightage |
|---|---|---|---|---|
| W2 | 694.59 | Welenkomi | 226.23 | 0.33 |
| | | Teji | 18.27 | 0.03 |
| | | Kimoye | 74.49 | 0.11 |
| | | Ginch | 340.76 | 0.49 |
| | | Addisalem | 34.84 | 0.05 |
| W4 | 330.95 | Asgori | 58.00 | 0.18 |
| | | Welenkomi | 72.40 | 0.22 |
| | | Tulu Bolo | 35.18 | 0.11 |
| | | Ginch | 165.37 | 0.50 |
| W5 | 553.06 | Asgori | 91.89 | 0.17 |
| | | Tulu Bolo | 451.62 | 0.82 |
| | | Ginch | 9.56 | 0.02 |
| W6 | 281.50 | Asgori | 9.04 | 0.03 |
| | | Teji | 5.85 | 0.02 |
| | | Bantu Liben | 266.61 | 0.95 |
| W9 | 97.31 | Asgori | 49.28 | 0.51 |
| | | Wolenkomi | 12.70 | 0.13 |
| | | Teji | 35.33 | 0.36 |
| W10 | 413.45 | Asgori | 46.75 | 0.11 |
| | | Enselale | 212.61 | 0.51 |
| | | Teji | 137.69 | 0.33 |
| | | Bantu Liben | 16.41 | 0.04 |
| W1 | 696.96 | Asgori | 81.03 | 0.12 |
| | | Tulu Bolo | 263.76 | 0.38 |
| | | Teji | 16.60 | 0.02 |
| | | Bantu Liben | 335.57 | 0.48 |
| W7 | 334.54 | Enselale | 18.85 | 0.06 |
| | | Teji | 31.66 | 0.09 |
| | | Kimoye | 60.26 | 0.18 |
| | | Addisalem | 223.78 | 0.67 |
| W3 | 504.09 | Enselale | 235.39 | 0.47 |
| | | Teji | 95.51 | 0.19 |
| | | Bantu Liben | 173.19 | 0.34 |
| W8 | 512.66 | Asgori | 1.12 | 0.00 |
| | | Enselale | 228.41 | 0.45 |
| | | Teji | 35.19 | 0.07 |
| | | Kimoye | 1.16 | 0.00 |
| | | Addisalem | 246.77 | 0.48 |

Table 3.5: Parameter Used in HEC-HMS model

| Element | Component | Method | Parameter |
|---|---|---|---|
| Sub-basin | Surface | Simple Surface | Initial Storage<br>Maximum Storage |
| | Loss | SCS-Curve Number | Initial Abstraction<br>Curve Number<br>Impervious |
| | Transform | SCS-UH | Lag time |
| | Base Flow Models | Constant monthly | Base Flow |
| Reach | Reach Routing Method | Muskingum | K and X |

**1. Surface Method**

The ability of the land surface in the watershed to store water is represented by the surface method in the subbasins. Direct runoff will occur if the rate of rainfall exceeds the infiltration rate. Initial storage is the percentage of ground surface storage at the beginning of the simulation. Initial storage in this study is assumed to be zero because the simulation of the model starts on January 1, which is a dry month. At the same time, storage is the maximum amount of water that can be accommodated on the soil surface before surface runoff occurs. Maximum storage in the initial simulation of this study is assumed to be 9.025 mm based on the basin slope of the Melka Kunture watershed, which ranges from 5-30%.

Table 3.6: Surface Depression Storage

| Description | Slope (%) | Surface storage (mm) |
|---|---|---|
| Flat | 0-5 | 50.8 |
| Medium | 5-30 | 6.35-12.7 |
| Steep | > 30 | 1.02 |

Source: (Eryani et al., 2021).

**2. Loss Method**

Water loss in the watershed from rainfall to surface runoff was simulated by the loss method. The process of rainfall loss due to land use and soil type through infiltration and evapotranspiration was simulated in the loss method model. This study uses the SCS-CN method. The parameters used in the SCS-CN method were initial abstraction, curve number, and impervious (Hamdan et al., 2021). In the curve number method, the runoff is directly proportional to the precipitation, with the assumption that the runoff is produced after the initial abstraction of 20% of the potential maximum storage (Tassew et al., 2019).

The curve number value was calculated based on the land cover type and soil type in the ArcGIS software. The value of the curve number ranges from 0 to 100. The value of CN zero indicates that there is no runoff occurrence, and CN value 100 indicates that the rainfall will become full runoff (Daide, Afgane, Lahrach, Chaouni, Msaddek, & Elhasnaoui, 2021) and the watershed condition is under flooding. The rainfall loss, which occurs through the runoff and infiltration processes, is determined using the SCS-CN method. The percentage of imperviousness for each sub-basin was manually adjusted by trial and error and automatically optimized to get the best fit.

Table 3.7: Loss parameter for the Melka Kunture watershed model

| Sub-basins | Initial Abstraction | Mean Curve Number | %impervious |
|---|---|---|---|
| W1 | 12.676 | 80.03 | 6.5 |
| W2 | 11.846 | 81.09 | 6.5 |
| W3 | 11.234 | 81.89 | 6.5 |
| W4 | 11.151 | 82.00 | 6.5 |
| W5 | 11.166 | 81.98 | 6.5 |
| W6 | 11.44 | 82.62 | 6.5 |
| W7 | 11.692 | 81.29 | 6.5 |
| W8 | 11.893 | 81.03 | 6.5 |
| W9 | 11.47 | 81.58 | 6.5 |
| W10 | 12.384 | 80.40 | 6.5 |

**3. Transform Method**

The transform method in the HEC-HMS model simulates the process from rain to flow hydrograph. In this case, the soil conservation service unit hydrograph model was chosen to transform excess precipitation into runoff. It is a parametric model based on the average Unit Hydrograph (UH) derived from gauged rainfall and runoff data of a large number of small agricultural watersheds throughout the United States (Tassew et al., 2019). The SCS proposed the unit hydrograph model, and it is included in the HEC-HMS program. The lag time (Tlag) is the only input parameter for this method. Lag time is the time interval between the center of the mass of rain and the time of peak discharge (Abdessamed et al., 2018).

Table 3.8: Lag time calculation for each sub-basin

| Subbasins | Graph Type | Lag time(min) |
|---|---|---|
| W1 | Standard | 186.164 |
| W2 | Standard | 141.518 |
| W3 | Standard | 125.188 |
| W4 | Standard | 117.698 |
| W5 | Standard | 166.566 |
| W6 | Standard | 126.939 |
| W7 | Standard | 166.376 |
| W8 | Standard | 144.884 |
| W9 | Standard | 114.608 |
| W10 | Standard | 133.848 |

**4. Base Flow**

The sub-basin element conceptually represents infiltration, surface runoff, and subsurface processes interacting together. The actual subsurface calculations were performed by a base flow method contained within the sub-basins.

Table 3.9: Monthly baseflow ($m^3/s$)

| Sub-basins | Jan | Feb | Mar | Apr | May | Jun | Jul | Aug | Sep | Oct | Nov | Dec |
|---|---|---|---|---|---|---|---|---|---|---|---|---|
| W1 | 0.25 | 0.19 | 0.22 | 0.37 | 0.50 | 1.21 | 7.41 | 19.73 | 13.42 | 1.44 | 0.48 | 0.32 |
| W2 | 0.25 | 0.19 | 0.22 | 0.37 | 0.50 | 1.21 | 7.38 | 19.66 | 13.38 | 1.44 | 0.47 | 0.32 |
| W3 | 0.18 | 0.14 | 0.16 | 0.27 | 0.37 | 0.88 | 5.36 | 14.27 | 9.71 | 1.04 | 0.34 | 0.23 |
| W4 | 0.12 | 0.09 | 0.10 | 0.18 | 0.24 | 0.57 | 3.52 | 9.37 | 6.37 | 0.69 | 0.23 | 0.15 |
| W5 | 0.20 | 0.15 | 0.17 | 0.30 | 0.40 | 0.96 | 5.88 | 15.65 | 10.65 | 1.15 | 0.38 | 0.26 |
| W6 | 0.10 | 0.08 | 0.09 | 0.15 | 0.20 | 0.49 | 2.99 | 7.97 | 5.42 | 0.58 | 0.19 | 0.13 |
| W7 | 0.12 | 0.09 | 0.10 | 0.18 | 0.24 | 0.58 | 3.55 | 9.47 | 6.44 | 0.69 | 0.23 | 0.16 |
| W8 | 0.19 | 0.14 | 0.16 | 0.27 | 0.37 | 0.89 | 5.45 | 14.51 | 9.87 | 1.06 | 0.35 | 0.24 |
| W9 | 0.04 | 0.03 | 0.03 | 0.05 | 0.07 | 0.17 | 1.03 | 2.75 | 1.87 | 0.20 | 0.07 | 0.05 |
| W10 | 0.15 | 0.11 | 0.13 | 0.22 | 0.30 | 0.72 | 4.39 | 11.70 | 7.96 | 0.86 | 0.28 | 0.19 |

**5. Routing method**

The Muskingum routing method is a simple approximate method to calculate the outflow hydrograph at the downstream end of the channel from the inflow hydrograph at the upstream end. Muskingum is a straightforward hydrological flood routing technique used in natural channels (Tassew et al., 2019). The reach routing method conceptually represents the condition of the river channel in the watershed. This research uses the Muskingum method to route the river channel in the watershed.

Table 3.10: Reach routing method using the Muskingum method

| Reach | Initial Type | Muskingum K (hr) | Muskingum X |
|---|---|---|---|
| R1 | Discharge = Inflow | 2.367 | 0.500 |
| R2 | Discharge = Inflow | 0.016 | 0.026 |
| R3 | Discharge = Inflow | 0.016 | 0.350 |
| R4 | Discharge = Inflow | 0.016 | 0.500 |
| R5 | Discharge = Inflow | 85.827 | 0.44 |
| R6 | Discharge = Inflow | 45.482 | 0.5 |
| R7 | Discharge = Inflow | 107.12 | 0.5 |

**6. Model calibration and validation**

To get reliable output, hydrological models need to be calibrated and validated using the observed streamflow data (Sahu et al., 2020). Model calibration is the process of optimizing the model parameters to get a good goodness of fit between the simulated and observed streamflow hydrographs. In this case, model calibration was done by using the estimated parameters to achieve a good fit between simulated and observed streamflow data. The automatic calibration through optimization trials available in the HEC-HMS model was used for optimizing the model parameters. Model calibration was done using two-third (2000-2010) of the streamflow data. In the presence of these data, optimization of the parameters was done using a systematic search method that yielded a good fit between the simulated and observed streamflow.

HEC-HMS version 4.9 has two different approaches to model parameter optimization: deterministic and stochastic. Deterministic optimization begins with initial parameter estimates and adjusts them so that the simulated results match the observed data as closely as possible. Stochastic optimization produces a collection of equally probable parameter sets that represent a sample from the joint distribution of the parameter population.

There are three search methods (differential evolution, simplex, and univariate algorithms) in HEC-HMS 4.9 that optimizes parameter values. In this case, the simplex search method was used for the optimization of the parameter during calibration. The HEC-HMS model also has a variety of objective functions to measure the goodness of fit between the simulated and observed streamflow data in different ways, such as root mean square error (RMSE), peak weighted RMSE, percent error in peak discharge, percent error in discharge volume, the sum of square residuals, the variance of absolute residuals, first-lag autocorrelation, etc. In this case, the root mean square error (RMSE) objective function was used to account for the error between the simulated and observed streamflow because it gave better results than the others at the calibration. The model was validated using the optimized parameters found during the calibration. One-third of the remaining streamflow data (2011-2015) was used to check the goodness of fit between the simulated and observed streamflow data.

#### *3.3.2.2 SWAT+ model*

The interface of the SWAT+ model complies with a QGIS extension that integrates a wide range of available geospatial data to represent the characteristics of the watershed at the hydrological response unit (HRU) level rather than the sub-basin level. In the model, the impacts of spatial heterogeneity of topography, land use, soil, and slope on catchment hydrology were described in subdivisions at the watershed level. The Melka Kunture watershed was divided into 15 sub-basins, each with its own set of 97 landscape units (Figure 3.14). The sub-basins are further partitioned into hydrological response units (HRU) based on the soil types, land use types, and slope classes that allow a high level of spatial detail in simulations. The model simulates the hydrology at HRU using the water balance equation (equation 3.19).

The SWAT+ is a completely restructured version of the Soil and Water Assessment Tool (SWAT) (Bieger et al., 2017). It is more flexible in terms of watershed discretization, configurations and spatial representation of processes, as well as in defining management schedules and operations, and database maintenance. Advantages include improved anthropogenic water use and management, flexibility in managing schedules and operations, easier printing of outputs, and rapid model calibration. The model is very effective at simulating streamflow.

SWAT+ uses the same equations as SWAT while offering more flexibility in model configuration to the user. The daily water balance in each HRU is calculated based on daily rainfall, runoff, evapotranspiration, and infiltration and return flow from the subsoil and from the flow of groundwater (Setegn et al., 2008). In SWAT+, the hydrological cycle and processes were simulated using the water balance equation 3.19.

$$SW_{ti} = SW_{0i} + \sum_{i=1}^{t} \left(R_{dayi} - Q_{surfi} - E_{ai} - W_{seepi} - Q_{gwi}\right) \quad (3.19)$$

where $SW_{ti}$ is the final soil water content (mm of $H_2O$) on a day I, $SW_{0i}$is the initial soil water content on a day i (mm of $H_2O$)), t is the time (days), $R_{dayi}$ is the amount of precipitation on a day i (mm of $H_2O$), $Q_{surfi}$ is the amount of surface runoff on a day i (mm of $H_2O$), $E_{ai}$ is the amount of evapotranspiration on a day i (mm of $H_2O$), $W_{seepi}$ is the amount of water entering the vadose zone from the soil profile on a day i (mm of $H_2O$), and $Q_{gwi}$ is the amount of return flow on the day (mm of $H_2O$) (Pulighe et al., 2021).

There are different methods to estimate surface runoff. In this case, the SCS curve number method was used to estimate surface runoff. The Hargreaves method was used for estimating potential evapotranspiration (PET).

The soil conservation service curve number method is given in equation 3.20.

$$Q_{surf} = \frac{\left(R_{dayi} - 0.2S\right)^2}{\left(R_{dayi} + 0.8S\right)} \quad (3.20)$$

Where: S is the retention parameter (mm). The retention parameter is defined by equation 3.21

$$S = 25.4\left(\frac{100}{CN} - 10\right) \quad (3.21)$$

The SCS curve number is a function of the soil’s permeability, land use, and antecedent soil water conditions.

**i. Delineation of the watershed**

Watershed delineation involves the use of the digital elevation model (DEM) to calculate a flow direction and a flow accumulation map (Chawanda et al., 2020b). Stream and channel thresholds are applied to the flow accumulation map to drive stream and channel networks, respectively. In this case, the watershed is delineated by drawing the outlet at the main outlet of the stream. Figure 3.9 showed the sub-basins generated after watershed delineation for Melka Kunture watershed using QGIS software.

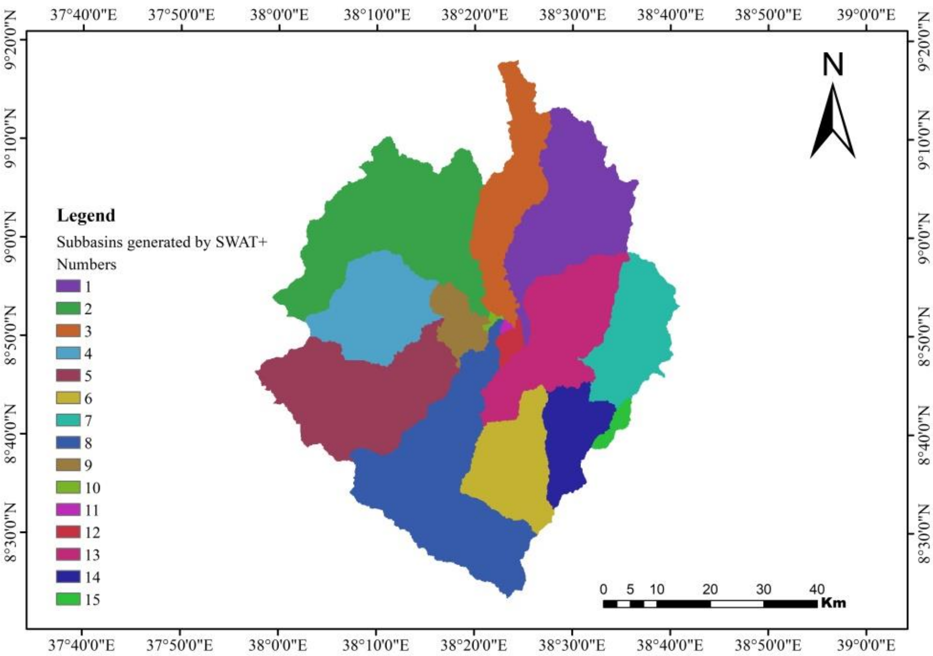


Figure 3.9: Sub-basins generated by the SWAT+ model for the study area

Topographic parameters (elevation and slope) were generated during watershed delineation processes. During model setup, sub-basins are delineated based on stream thresholds, while LSUs are delineated based on channel thresholds, as described in the user manual (Chawanda et al., 2020a). The subbasins were generated from the digital elevation model of the study area. Accordingly, the elevation of the watershed ranges from 1996 to 3565 a.m.s.l. QSWAT+ introduces Land Scape Units (LSUs) to further discretize sub-basins and allow the separation of upland processes from wetlands. The three options that are used to delineate landscape units are buffer stream, DEM inversion, and branch length. In this study, DEM inversion was used to calculate ridges since the slope of the watershed is medium.

**ii. Hydrologic Response Unit (HRU) analysis**

SWAT+ used hydrological response units (HRU) analyses, which are divisions of sub-basins into smaller units, each of which has a land use/soils/slope range combination in the QSWAT+ Tool. The land use map and its lookup table were set into the model using the hydrologic response unit (HRU) analysis toolbar. Similarly, the soil map and its lookup table were provided to the model. A soil database is also provided in the model to analyze the hydrologic response unit. After the characterization of the land use and soil maps in the basin, multiple slope classes can be set. The number of slope classes can be entered at the user's convenience. Figure 3.10 showed slope class generated in QSWAT+ as 0% - 5.12%, 5.13% - 12.82%, 12.83% - 24.09%, 24.10% - 40.49%, and > 40.49%.

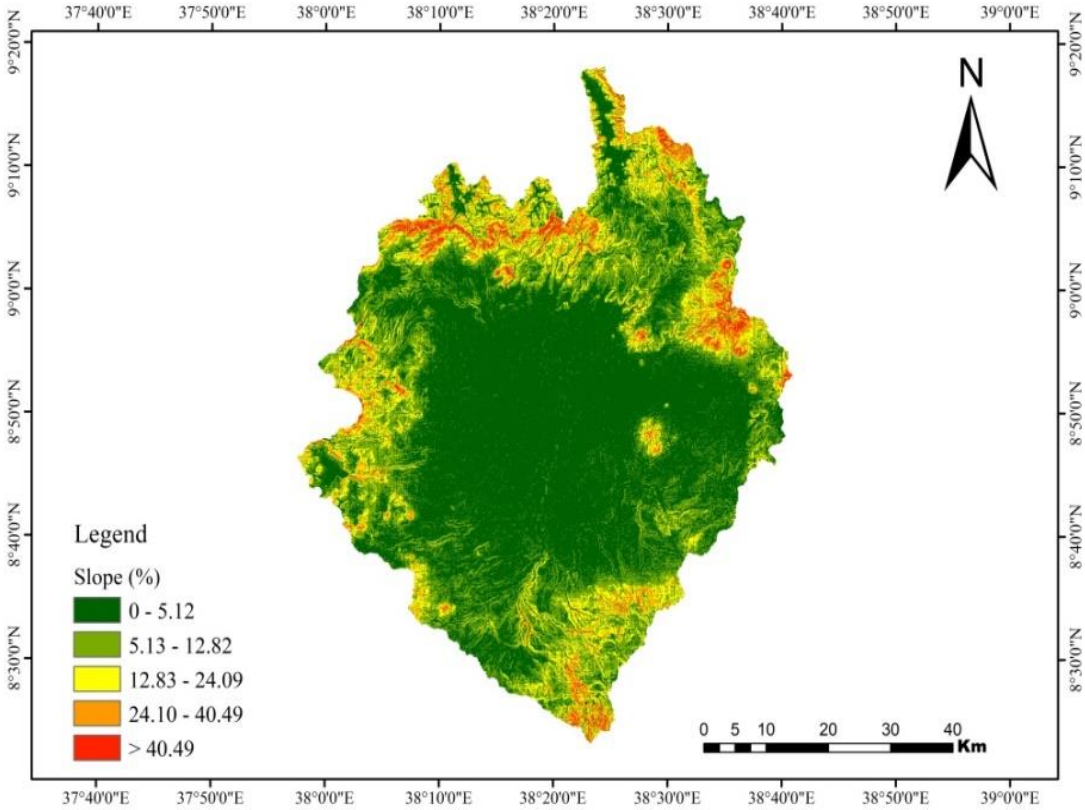


Figure 3.10: slope classes generate by QSWAT+ tools

**iii. Model sensitivity analysis, calibration, and validation**

**a) Model sensitivity analysis**

Sensitivity analysis investigates the sensitivity of a parameter to the simulation results at a certain parameter value. A sensitivity analysis was performed to identify the model's most sensitive parameters for calibration (Bajpai, 2018). The SWAT+ Toolbox version v0.4.5, which is an independent tool from SWAT+, was used to analyse sensitivity, calibration and validation of the streamflow.

In SWAT+ Toolbox v0.4.5, the well-known sensitivity analysis methods are Sobol, Fourier amplitude, Random Balance Design Fourier amplitude, and Delta moment independent measures. In this case, the Sobol sensitivity analysis method was chosen because of its popularity in estimating significant sensitive parameters based on the P factor and t-test (Tumsa et al., 2022a).

**b) Model Calibration and validation**

Model calibration is the process of standardizing simulated values by using deviations from observed values for a particular area to derive correction factors that can be applied to generate simulated values that are consistent with the observed values. Such empirical corrections are common in modeling, and it is understood that every hydrologic model should be tested against observed data, preferably from the watershed under study, to understand the level of reliability of the model (Muthukrishnan et al., 2006).

Dynamically Dimensioned search (DDS) method integrated with the SWAT+ toolbox v0.4.5 was used to calibrate the models. It is an automatic calibration technique developed for complex watershed simulation models, such as SWAT (Yen et al., 2016). In this model, one year of streamflow data was used for the warm-up period (2000), and two-thirds (2001–2015) of the observed streamflow data, were used for model calibration. Thus, the calibration was performed for a period of ten years (2001–2010) of streamflow data. The model was validated using the adjusted parameters found during the calibration. The streamflow data 2011 to 2015 was used to check the goodness of fit between the simulated and observed streamflow data.

Table 3.11: Dynamically dimensioned search algorithms and calibrate value of SWAT+ Parameters

| Parameters | object | Min_value | Calibrated value | Max-value | Units |
|---|---|---|---|---|---|
| awc | sol | 0.01 | 0.354 | 1 | mm_H2Omm |
| Cn2 | hru | -30 | -23.99 | 10 | |
| canmx | hru | 0 | 87.553 | 100 | mm/H2O |
| Flow_min | aqu | 0 | 9.075 | 10 | M |
| ovn | hru | -20 | -4.495 | 20 | M |
| Gwflow_lte | hlt | 0 | 4.734 | 10 | Mm |
| Gwdeep_lte | hlt | 0 | 2.426 | 10 | mm |
| Gw_lte | hlt | 0 | 9151.315 | 10000 | mm |
| bf_max | aqu | 0 | 0.768 | 2 | mm |
| Tc_lte | hlt | -30 | -7.24 | 30 | min |
| Revap_co | aqu | 0.02 | 0.04 | 0.2 | |
| epco | hru | 0 | 0.476 | 1 | |
| alpha | aqu | 0 | 0.02 | 1 | day |
| slope | hru | 0 | 0.95 | 1 | m/m |
| Cn3_swf | hru | -20 | 24.065 | 30 | |
| esco | hru | 0 | 0.853 | 1 | |

### *3.3.2.3 HBV-Light model*

The Hydrologiska Byråns Vattenbalansavdelning Light (HBV-Light) model is a semi-distributed conceptual rainfall-runoff model applied to simulate stream flow using daily precipitation, temperature, and a monthly estimate of potential evaporation as the main input (Bergström, 1976b). This model separates the catchment into different elevation and vegetation zones, as well as into different sub-cat9chments. The model consists of four different routines; the snow routine (not considered in this research), the soil routine, the response routine, and the routing routine (Seibert and Vis, 2012). In the snow routine, snow accumulation and snowmelt are computed by the degree-day method. In the soil, routine groundwater recharge and actual evaporation are simulated as functions of actual water storage. In the response (or groundwater) routine, runoff is computed as a function of water storage. Finally, in the routing routine, a triangular weighting function was used to simulate the routing of the runoff to the catchment outlet. The central equations of the HBV model and more detailed descriptions of the model can be found elsewhere (Seibert, (1999); Jan Seibert, (2005), Seibert and Vis, 2012)).

HBV light (Jan Seibert, 2005), a new version of the model, has been employed in several studies in rainfall-runoff modeling on river basins (Ayalew, (2019); Burundi and Mutua, (2017)). The HBV-Light model, which is a semi-distributed conceptual model, is one of the rainfall-runoff models selected for simulating streamflow for Melka Kunture watershed hydrology because of its suitability, which has been demonstrated under different hydro climatic conditions around the world (Birundu and Mutua, 2017). A short description of the HBV-Light development procedure is given below:

The model simulates daily discharge using daily rainfall, temperature, and potential evaporation as inputs. Precipitation is simulated to be either snow or rain depending on whether the temperature is above or below a threshold temperature, TT [°C]. All precipitation simulated to be snow, i.e., falling when the temperature is below TT, is multiplied by a snowfall correction factor, SFCF [-]. Snowmelt is calculated with the degree-day method (Equation 3.22). Meltwater and rainfall are retained within the snowpack until they exceed a certain fraction, CWH [-], of the water equivalent of the snow. Liquid water within the snowpack refreezes according to Equation 3.23.

Rainfall and snowmelt (P) are divided into the water filling the soil box and groundwater recharge depending on the relation between the water content of the soil box (SM [mm]) and its largest value (FC [mm]) (Equation 3.24). Actual evaporation from the soil box equals the potential evaporation if SM/FC is above LP [-], while a linear reduction is used when SM/FC is below LP (Equation 3.25). Groundwater recharge is added to the upper groundwater box (SUZ [mm]). PERC [mm $d^{-1}$] defines the maximum percolation rate from the upper to the lower groundwater box (SLZ [mm]). Runoff from the groundwater boxes is computed as the sum of two or three linear outflow equations depending on whether SUZ is above a threshold value, UZL [mm], or not (Equation 3.26). This runoff is finally transformed by a triangular weighting function defined by the parameter MAXBAS (Equation 3.27) to give the simulated runoff [mm $d^{-1}$].

If different elevation zones have been used, the changes in precipitation and temperature with elevation are calculated using the two parameters PCALT [%/100 m] and TCALT [ºC / 100 m] (Equations 3.28 and 3.29). The long-term mean of the potential evaporation, $E_{Pot}$, M for a certain day of the year can be corrected to its value at day t, $E_{pot}$ (t), by using the deviations of the temperature, *T(t),* from its long-term mean, $T_M$, and a correction factor, CET [°$C^{-1}$] (Equation 3.30).

$$Snowmelt = CFMAX(T(t) - TT) \qquad (3.22)$$

$$refreezing = CFR\ CFMAX\big(TT - T(t)\big) \qquad (3.23)$$

$$\frac{recharge}{P(t)} = \left(\frac{SM(t)}{FC}\right)^{BETA} \qquad (3.24)$$

$$E_{act} = E_{pot} * min\left(\frac{SM(t)}{FC * LP}, 1\right) \qquad (3.25)$$

$$Q_{GW}(t) = K_2 SLZ + K_1 SUZ + K_0\ max(SUZ - UZL, 0) \qquad (3.26)$$

$$Q_{sim}(t) = \sum_{i=1}^{MAXBAS} c(i)\ Q_{GW}(t - i + 1) \qquad (3.27)$$

$$where \quad c(i) = \int_{i=1}^{i} \frac{2}{MAXBAS} - \left|u - \frac{MAXBAS}{2}\right| \frac{4}{MAXBAS^2} du$$

$$P(h) = P_0 \left(1 + \frac{PCALT(h - h_0)}{10000}\right) \qquad (3.28)$$

$$T(h) = T_0 - \frac{TCALT(h - h_0)}{100} \qquad (3.29)$$

$$E_{pot}(t) = (1 + C_{ET}(T(t) - T_M))E_{pot,M} \qquad (3.30)$$

$$but\ 0 \leq E_{pot}(t) \leq 2E_{pot,M}$$

Where P (t) is the precipitation at time t, FC is the field capacity, BETA is a parameter that determines the relative contribution to runoff from rain or snow melt, $ET_{act}$ is the actual evapotranspiration, $ET_{pot}$ is the potential evapotranspiration, LP is the soil moisture value above which $ET_{act}$ reaches $ET_{pot}$, QGW is the groundwater recharge, $Q_{sim}$ is the simulated runoff, and Ki is the recession constant. The main calibration parameters for the HBV-Light model are listed in Table 3.12.

Table 3.12: Parameters and their ranges during GAP optimization of HBV-Light model

| Routine | Parameters | Description | Range | Optimized value |
|---|---|---|---|---|
| Soil moisture routine | FC | Maximum soil moisture storage (mm) | 100-550 | 550 |
| | LP | Soil moisture value above which $ET_{act}$ reaches $ET_{pot}$ (mm) | 0.3-0.1 | 0.49 |
| | Beta | The parameter that determines the relative contribution to runoff from rain or snow melt (_) | 1-5 | 1.19 |
| Response routine | PERC | Maximum percolation to lower zone (mm/day) | 0-4 | 3.18 |
| | UZL | Threshold parameter (mm) | 0-70 | 69.99 |
| | $K_o$ | Recession coefficient ($day^{-1}$) | 0.1-0.5 | 0.1 |
| | $K_1$ | Recession coefficient ($day^{-1}$) | 0.01-0.2 | 0.04 |
| | $K_2$ | Recession coefficient ($day^{-1}$) | 0.00005-0.1 | $5x10^{-5}$ |
| Routing routine | MAXBAS | Triangular weighing function | 1-2.5 | 1.93 |

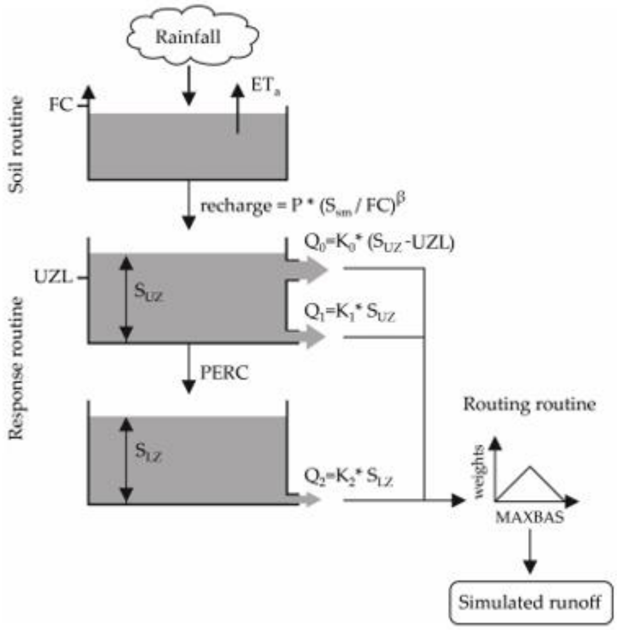


Figure 3.11: Model structure of HBV-Light (Koutsouris et al., 2017)

### i. HBV-light model input

The conceptual HBV-Light model computes streamflow from observed daily rainfall, mean daily temperature, mean daily estimates of potential evapotranspiration, and streamflow data. The daily annual rainfall was calculated by the Theissen polygon method. The potential evapotranspiration for the study area was estimated by the Hargreaves method. The Hargreaves method had been selected because it requires less meteorological data, i.e., maximum and minimum temperature, compared to other methods (Hargreaves, 1994b). The watershed classification of land use and area elevations was also used as inputs into the model. Accordingly, the Melka Kunture watershed was classified into ten elevation-vegetation zones. The model uses a warm-up period of one year to set state variable values according to the preceding meteorological conditions and parameter sets (Vis et al., 2015).

### ii. Model calibration and validation

The HBV-light model was applied to the Melka Kunture watershed using daily time series data. The watershed was classified into ten elevation-vegetation zones. Rainfall and temperature time series data were compiled for different elevation zones with a lapse rate of 10 percent and 0.6 $^{0}$C /100m, respectively. The daily potential evapotranspiration input data was calculated using Hargreaves method. In this case, the first year of input data measurement was used for the warm-up of the model to estimate the initial state variables.

The rest of the data was used for both calibration and validation of the model. As a result, model calibration was done using two-thirds of the data (2001-2010), and model validation was done using one-third of the observed streamflow data (2011-2015).

The Genetic Algorithm and Powell Optimization (GAP) algorithm, which is integrated within the HBV-Light model, was used for calibration, resulting in 500,000 different parameterizations. The GAP algorithm produces reasonably good results in finding a global solution to the observed function (Vidmar et al., 2020). The parameter ranges used in GAP optimization are defined in Table 3.4. Finally, the model was validated (2011–2015) using the parameters optimized during model calibration.

### 3.3.3 Models Performance Evaluation Criteria

To calibrate and validate the models and for comparison purposes, some quantitative information is required to measure model performance (Golmohammadi et al., 2014). Statistical metrics such as coefficient of determination ($R^2$), Nash-Sutcliffe efficiency (NSE), and percent bias (PBIAS) were used to evaluate the models performance in simulating streamflow of Melka Kunture watershed.

**The coefficient of determination ($R^2$)** is an indication of the strength of the relationship between the observed and simulated values (Santhi et al., 2001). The coefficient of determination (Equation 3.31) will be used to assess whether the simulations have reproduced the observed variability of the natural hydrologic process while minimizing the overall deviation. $R^2$ ranges between 0 and 1, with higher values indicating less error variance, and typically values greater than 0.5 are considered acceptable (Moriasi et al., 2007a).

$$R^2 = \frac{[\sum_{i=1}^{N}(Q_{obs} - \bar{Q}_{obs})(Q_{sim} - \bar{Q}_{sim})]^2}{\sum_{i=1}^{N}(Q_{obs} - \bar{Q}_{obs})^2 \sum_{i=1}^{N}(Q_{sim} - \bar{Q}_{sim})^2} \tag{3.31}$$

The **Nash-Sutcliffe efficiency (NSE)** is a normalized statistic that determines the relative magnitude of the residual variance compared to the measured data variance (Nash and Sutcliffe, 1970). Nash-Sutcliffe efficiency indicates how well the plot of observed versus simulated data fits the 1:1 line (Santhi et al., 2001).

NSE ranges from $-\infty$ (worst fit) to one (perfect match between simulation and observation). Values between 0 and 1 are generally viewed as acceptable levels of performance, whereas values $\leq 0$ indicate that the mean observed value is a better predictor than the simulated value, which indicates unacceptable performance (Moriasi et al., 2007). NSE is calculated using equation 3.32.

$$NSE = 1 - \frac{\sum_{i=1}^{N}(Q_{Sim} - Q_{Obs})^2}{\sum_{i=1}^{N}(Q_{Obs} - \bar{Q}_{Obs})^2} \tag{3.32}$$

Where $Q_{obs}$ is the observation record at time step i; $Q_{sim}$ is the simulated modeling response at time step I; $\bar{Q}_{obs}$ is the average observation record at time step i, and N is the number of total simulation time steps.

**Percent bias (PBIAS):** quantifies the average tendency of the simulated data to be larger or smaller than their observed counterparts (Gupta et al., 1999). Low-magnitude values of PBIAS indicate accurate model simulation, with 0.0 being the optimal value. According to Gupta et al., 1999), positive values denotes model underestimation bias while negative values denote model overestimation bias. When calculating PBIAS, use equation 3.33:

$$PBIAS = \frac{\sum_{i=1}^{N}(Q_{obs} - Q_{sim})}{\sum_{i=1}^{N} Q_{obs}} * 100\% \tag{3.33}$$

Where, $PBIAS$ the deviation of the data being evaluated is expressed as a percentage.

Table 3.13: General performance ratings for a recommended statistic for the monthly time step for streamflow (Moriasi et al., 2007)

| Performance Rating | NSE | RSR | PBIAS |
|---|---|---|---|
| Very Good | 0.75 < NSE ≤ 1.00 | 0.00 < RSR ≤ 0.50 | -10 ≤ PBIAS ≤ 10 |
| Good | 0.65 < NSE≤0.75 | 0.50 < RSR ≤ 0.60 | ±10 ≤ PBIAS < ±15 |
| Satisfactory | 0.50 < NSE ≤ 0.65 | 0.60 < RSR ≤ 0.70 | ±15 ≤ PBIAS < ±25 |
| Unsatisfactory | NSE ≤ 0.50 | RSR > 0.70 | PBIAS ≥ ±25 |

### 3.3.4 Model comparison and selection of suitable hydrological models

The application of hydrological models, whether simple or complex, depends on how well they can reproduce the response of the system (Jaiswal et al., 2020). To compare model performance in producing stream flow, research based on well-calibrated and validated hydrological models was conducted (Nguyen Khoi, 2015a). Model comparison was done after calibration and validation of the models at the watershed outlet. For comparison purposes, some quantitative information is required to measure model performance (Golmohammadi et al., 2014). Statistical metrics such as NSE, $R^2$, and PBIAS were used to evaluate the models' performance in simulating streamflow for selecting an appropriate hydrological model.

## 3.4 Conceptual Framework of the Study

Following a thorough data analysis of meteorological and hydrological data, time series data was organized according to the specifications of each model. In the next stage, model parameter sensitivity analysis, calibration, and validation were done. Calibration and validation were done by dividing the data into two-thirds for calibration and one-third for validation. Finally, the models were compared using the simulated streamflow generated depending on the performance evaluation of the models.

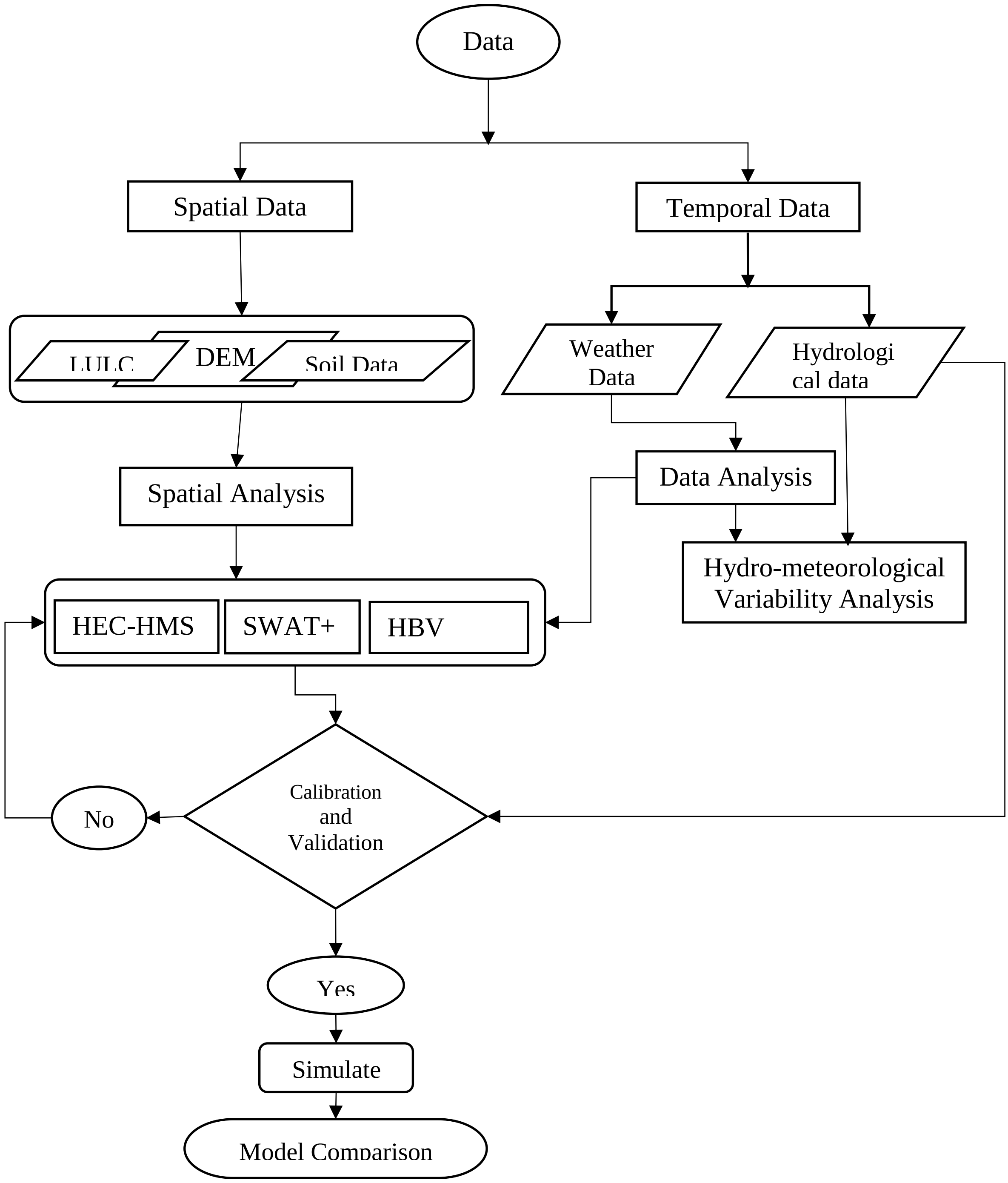


Figure 3.12: Conceptual framework of the study

# 4. RESULTS AND DISCUSSION

## 4.1 Rainfall Characteristics over Melka Kunture Watershed

The results presented in Figure 4.1 indicate that there is no significant difference in rainfall patterns between the nine rainfall stations and the study area. The seasonal rainfall regimes were presented in Figure 4.1. The first rainy season, known as the small rainy season, occurs from February to May, with the highest rainfall amounts typically observed in April. This period experiences relatively lower but still significant rainfall. The second rainy season, referred to as the main rainy season, takes place from June to September, with the peak of rainfall occurring in July. This season is characterized by more substantial rainfall amounts and is considered the primary rainy period.

During the Bega season, which spans from October to January, the watershed receives a minimal amount of rainfall. This period is typically associated with lower precipitation levels compared to the two main rainy seasons. These findings provide valuable insights into the temporal distribution of rainfall, which is crucial for understanding the hydrological processes and water resource management in the region.

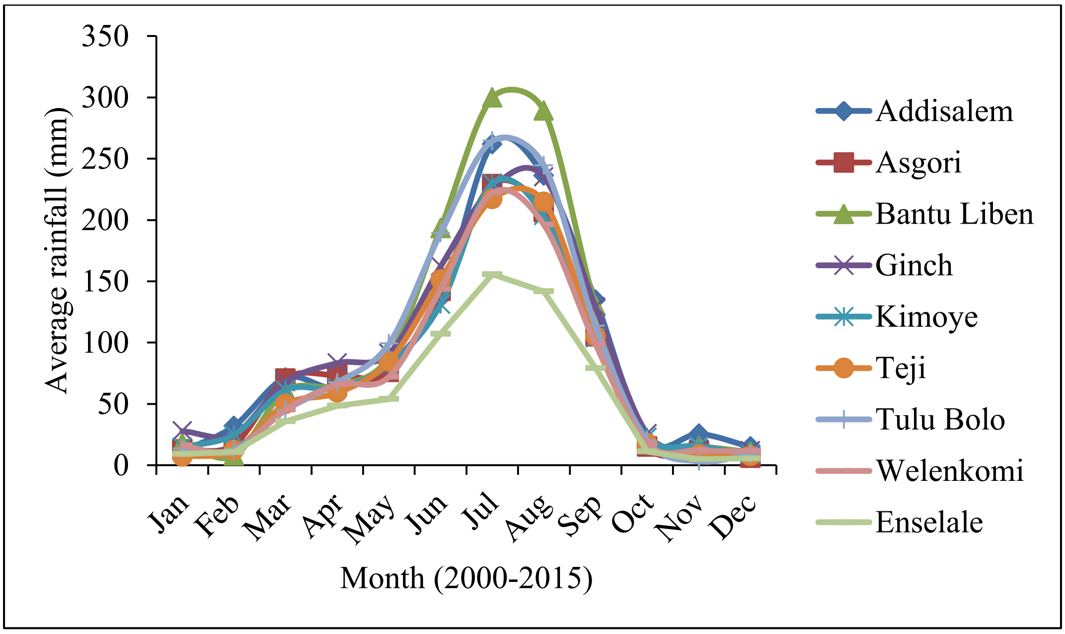


Figure 4.1: Mean monthly rainfalls of the selected stations in the Melka Kunture watershed

## 4.2 Spatial and temporal variability of rainfall

### 4.2.1 Spatial variations of rainfall

For the annual and seasonal rainfall over the Melka Kunture watershed, the nine stations' spatial variances were interpolated. The spatial distribution of long-term (2000–2015) mean annual rainfall showed a higher occurrence of rainfall in the southern parts compared to the northern parts, with a spatial variability of 15.46% (Figure 4.2). Similar trends were observed in the Kiremt season (June–September), with a spatial variability of 16.64%. The highest mean rainfall was observed at Bantu Liben, while the lowest mean rainfall was observed at Enselale station in the Melka Kunture watershed during the annual and kiremt season (Table 4.1).

In the Belg season (February–May), higher rainfall was observed in the northwest part compared to the other parts, with a spatial variability of 17.44%. The highest rainfall (267.56 mm) of the Belg season was observed at Ginch, while the lowest mean annual rainfall (148.79 mm) was at Enselale station in the Melka Kunture watershed. In the Bega season (October–January), the occurrence of higher rainfall was observed in the northern part of the study area, with a spatial variability of 36.75%. The highest rainfall (100.19mm) was observed at Kimoye, while the lowest rainfall (30.56 mm) was observed at Enselale station in the Melka Kunture watershed. In general, the spatial variability of rainfall in the Melka Kunture watershed shows low rainfall variability (CV <20%) in annual and seasonal cases, except in the Bega season (CV >30%). Previous studies on spatial variability showed similar results during the major rainy season (Kiremt) and the low rainy season (Belg) as well as annually in the respective study area (Getahun, Li, et al., 2020).

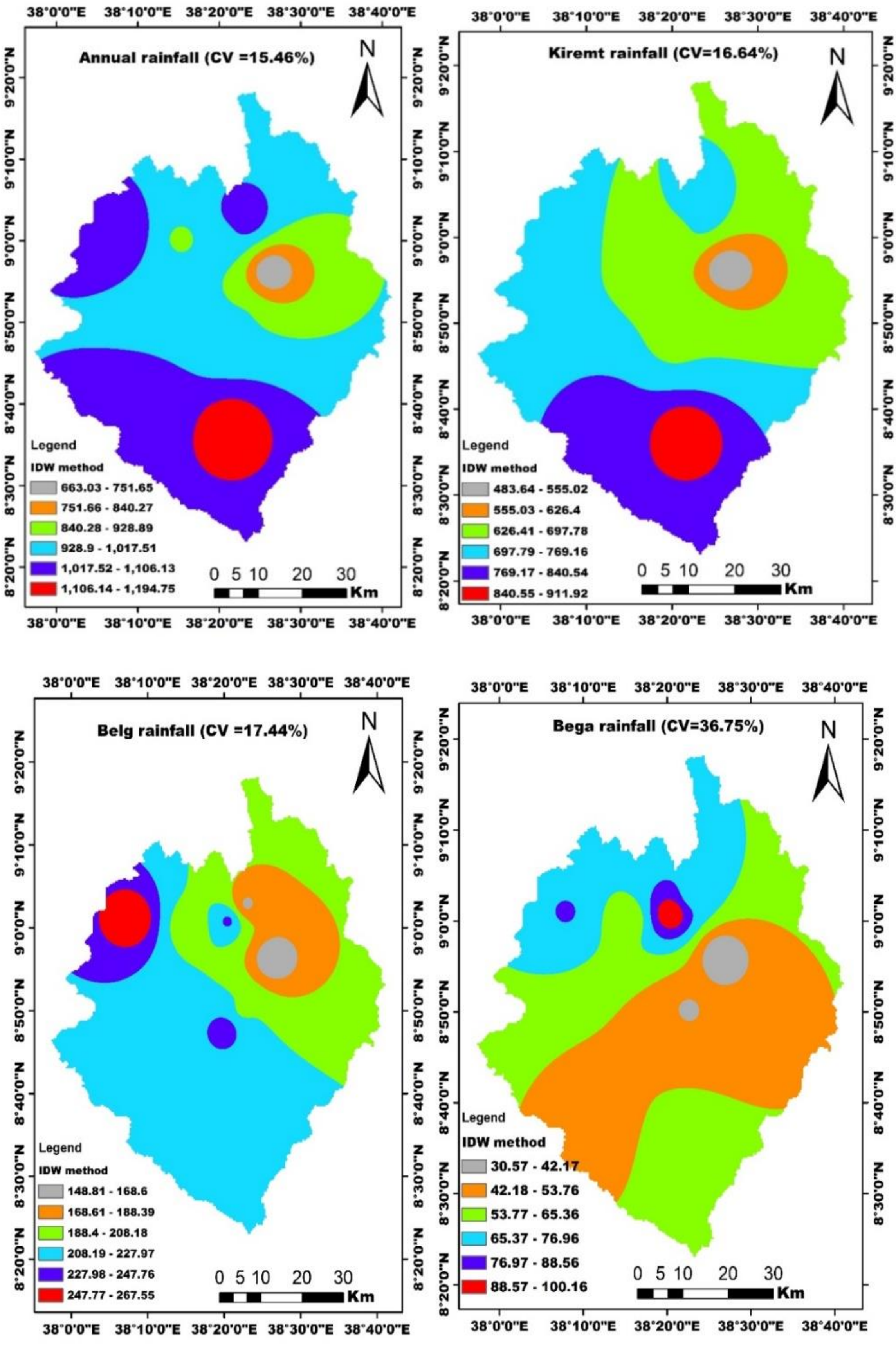


Figure 4.2: Spatial distribution and variability of mean annual and seasonal rainfall of Melka Kunture watershed (2000 - 2015)

### 4.2.2 Temporal variations of rainfall

Analyses of the long-term annual rainfall records from 2000-2015, as presented in Table 4.1, provide insights into the variation of rainfall across the nine stations in the study area. Based on the coefficient of variation (CV), which measures the relative variability of rainfall, the stations Addisalem, Asgori, Teji, and Wolenkomi can be categorized as low (< 20%) variation, and Bantu Liben, Ginch, Kimoye, and Tulu Bolo could be categorized as moderate (20% < CV < 30%) variation, while Enselale categorized as high (CV >30%) rainfall variation. This higher rainfall variation indicates that there is a greater degree of fluctuation or variability in the amount of rainfall over a given time period.

Seasonally, the rainfall pattern in the study area varies from low to high variability. In the Belg and Bega seasons, there is high (CV > 30%) rainfall variability in all stations. In the Kiremt season, Addisalem, Asgori, Kimoye, Teji, and Wolenkomi could be categorized as low (<20%) rainfall variation, and Bantu Liben, Ginch, and Tulu Bolo could be categorized as moderate (20 < CV < 30%) rainfall variation and Enselale could be categorized as high (> 30%) rainfall variation in the study area. The seasonal rainfall at Belg showed a high degree of variability for all stations, unlike the rainfall at the kiremt season. The high variability of rainfall in the small rainy season is very prone to risk for rain-fed agriculture and almost all of the stations in the study watershed clearly indicate high (35.80% - 60.89%) ranges of rainfall variability. Similar result has also been found by (Bekele et al. (2017), Melat Eshetu (2021)) also revealed that there is low to moderate ranges of rainfall variation annually and in the Kiremt season while in the Belg season high rainfall variation were occurred. This is inconsistent with the study by (Belay et al., 2021, Dereje Ayalew, 2012) which identifies high variation of rainfall seasonally and low to moderate during kiremt season and annually. The high variability of rainfall in belg season will cause unfavorable condition for agricultural production (Melat Eshetu, 2021a).

These findings provide valuable information about the long-term rainfall patterns and their variability within the study area. Understanding the seasonal and station-specific variation is crucial for effective water resource management and planning in the region.

Table 4.1: Seasonal and annual variability of rainfall gauging stations

| Station | Annual | | Belg season | | Kiremt Season | | Bega Season | |
|---|---|---|---|---|---|---|---|---|
| | Mean | CV | mean | CV | mean | CV | Mean | CV |
| Addisalem | 1088.81 | 13.84 | 165.58 | 50.70 | 768.56 | 13.82 | 72.56 | 119.62 |
| Asgori | 964.23 | 15.08 | 236.83 | 52.36 | 682.30 | 10.99 | 45.11 | 92.89 |
| Bantu Liben | 1194.78 | 28.65 | 221.63 | 60.89 | 911.94 | 26.04 | 61.20 | 92.28 |
| Enselale | 662.92 | 36.17 | 148.79 | 51.81 | 483.57 | 34.67 | 30.56 | 69.04 |
| Ginch | 1097.49 | 27.53 | 267.56 | 49.84 | 752.09 | 26.57 | 77.85 | 60.37 |
| Kimoye | 998.95 | 20.53 | 231.02 | 38.68 | 667.74 | 9.92 | 100.19 | 181.74 |
| Teji | 933.99 | 15.83 | 205.60 | 45.08 | 687.75 | 12.70 | 40.64 | 65.26 |
| Tulu Bolo | 1081.29 | 20.37 | 224.13 | 41.73 | 811.63 | 21.46 | 45.54 | 93.49 |
| Wolenkomi | 912.19 | 14.21 | 194.30 | 35.80 | 660.40 | 13.26 | 57.49 | 58.55 |

The standard rainfall anomaly index for each station in the Melka Kunture watershed was presented in the appendix Table 2. The station in the watershed experienced extremely wet and extremely dry years (Figure 4.3). Asgori, Ginch, Kimoye, Teji, Tulu Bolo, and Wolenkomi stations showed extremely wet (SRAI > 2.0) conditions during the years of 2013, 2006, 2011, 2010, 2013, and 2006, respectively, and their respective standard rainfall anomaly indexes were 2.25, 3.49, 3.11, 2.07, 2.74, and 2.01. This indicates that the observed rainfall is significantly above the long-term average rainfall for a specific location on a given time period. Addisalem and Bantu Liben stations showed extremely dry (SRAI < -2.0) conditions during 2015 and 2010, respectively, and their respective standard rainfall anomaly indexes were -2.06 and -2.27. This indicates that the observed rainfall is significantly below the long-term average rainfall for a specific location on a given time period. This study is inconsistent with the study by Hiben et al. (2022) which was conducted at Ghba river, Ethiopia. There is a variation of SRAI compared with the result obtained; this is due to study location and the variability of hydro climatic condition in the study area.

Generally, the annual standard rainfall anomaly index was explained in percentage, and most of the stations annual standard rainfall anomaly index showed near-normal rainfall conditions (68.75% to 87.50%) in all stations (Figure 4.4).

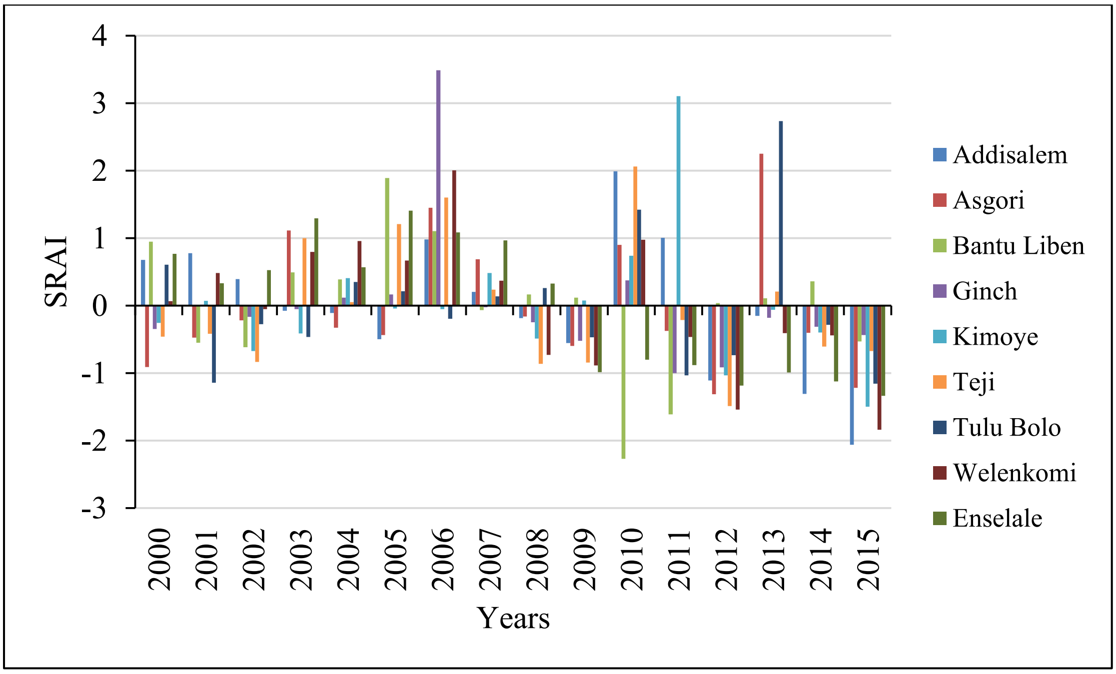


Figure 4.3: Standard rainfall anomaly indexes of the stations

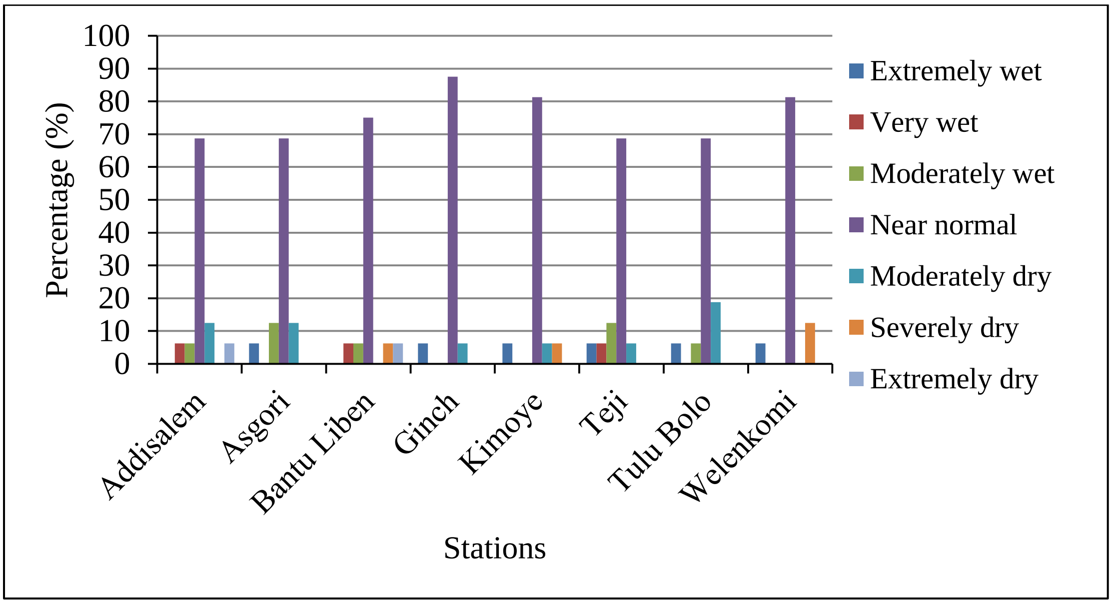


Figure 4.4: Percentage of standard rainfall anomaly index in all stations

The annual precipitation concentration index was calculated depending on the annual and seasonal periods. According to Lambe and Kundapura (2021) and Melat Eshetu (2021), the calculated PCI values indicated evenly distributed (PCI < 10%), moderate rainfall concentration (PCI is between 11% and 15%), irregularly distributed rainfall in the area (PCI is between 16 and 20), and strong irregularity in rainfall distribution across the area (PCI > 20%). The annual Precipitation Concentration Index (PCI) of Addisalem, and Ginch, and Kimoye stations showed moderate rainfall concentration, while asgori, Bantu Liben, Teji, Tulu Bolo, wolenkomi, and Enselale stations showed irregular rainfall distribution in the Melka Kunture watershed (Figure 4.5). This is caused due to climate zone, weather stations, Topography, variations in rainfall intensity, and climate change within the study period. Seasonally, all stations in the Melka Kunture watershed showed strong irregularities in rainfall (Figure 4.5). This is because of the seasons are characterized by varying weather patterns, including differences in rainfall amounts, duration, and intensity. This irregularity in rainfall may cause droughts, floods, and landslides in the watershed.

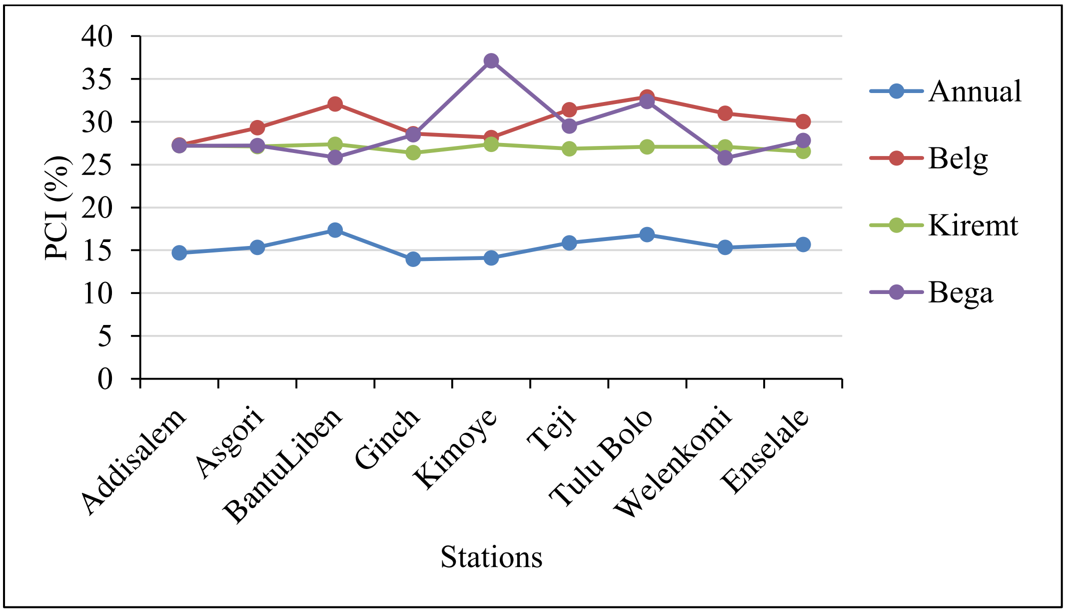


Figure 4.5: Annual and seasonal precipitation index of Melka Kunture watershed

### 4.2.3 Temporal variations of Streamflow

The mean monthly maximum, minimum, and average streamflow of the Melka Kunture streamflow watershed are shown in Figure 4.6. From November to June the mean monthly streamflow was low and increase in June, as the highest flow was observed in August. The maximum mean monthly streamflow was low from November to April, with at least one maximum event from April to November. The peak streamflow was 555.18, 167.48, and 1238 $m^3/s$ in August for maximum, average, and minimum streamflow, respectively. The lowest streamflow was 5.45$m^3/s$ in December for maximum streamflow, 1.4$m^3/s$ in February for average streamflow, and 0.28$m^3/s$ in March for minimum streamflow.

The result of the variability analysis (Table 4.2) in maximum flow showed that there was high variability (CV >30%) on both an annual and seasonal basis, except for the Kiremt season, which showed moderate (20% < CV < 30%) flow variability. In average flow, annual and Kiremt seasons showed moderate (20% < CV < 30%) flow variability, and Belg and Bega seasons showed high (CV >30%) flow variability. During the minimum flow, the annual and Bega seasons showed moderate (20% < CV < 30%) flow variability, and the Kiremt and Belg seasons showed high (CV > 30%) flow variability at the Melka Kunture streamflow gauging station. Similar study conducted in Modjo sub-basin has indicated that a very high variability for both annual and seasonal basis (Melat Eshetu, 2021) for maximum, minimum and average discharge. There is a variation of maximum, minimum and average, this is due to hydro-meteorological variations and heterogeneity of the land use land cover in the study area. A comparable was reported in Bilate watershed Rift valley region of Ethiopia (Y. Orke & Li, 2021). The higher variability of streamflow was observed during Belg and Bega seasons.

Table 4.2: Maximum, minimum, and average discharge variability characteristics of Melka Kunture watershed.

| | Annual | | Belg | | Kiremt | | Bega | |
|---|---|---|---|---|---|---|---|---|
| | Mean | CV | Mean | CV | Mean | CV | Mean | CV |
| Maximum streamflow | 347.80 | 33.79 | 50.99 | 89.45 | 849.70 | 28.09 | 52.90 | 65.42 |
| Minimum stream flow | 0.67 | 27.92 | 4.32 | 36.96 | 123.57 | 44.05 | 8.54 | 23.67 |
| Average flow | 32.61 | 23.76 | 13.27 | 64.02 | 361.72 | 26.15 | 18.69 | 45.34 |

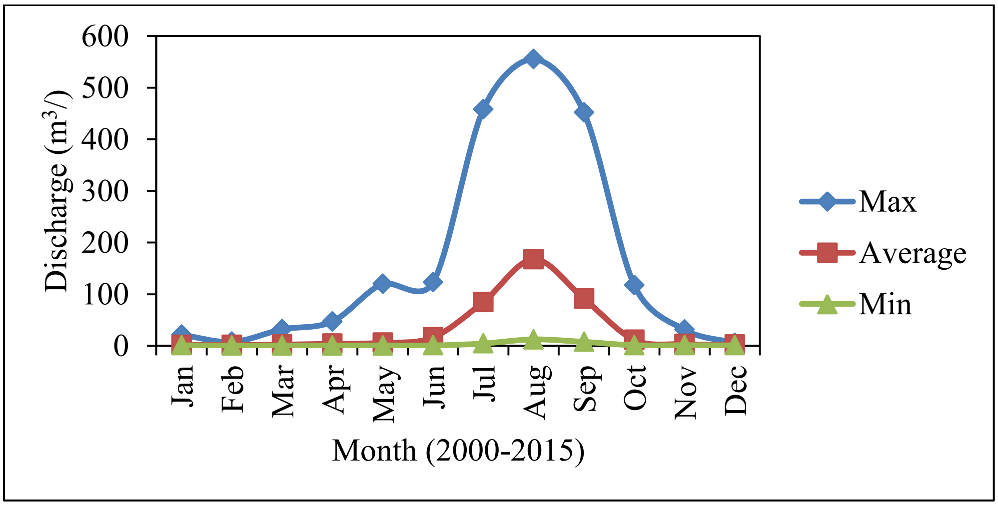


Figure 4.6: The mean monthly maximum, minimum, and average river discharge of the Melka Kunture streamflow watershed

## 4.2 Performance of Hydrological models in simulating streamflow

### 4.2.1 HEC-HMS Model

The basin model plays a crucial role in HEC-HMS (Hydrologic Engineering Center's Hydrologic Modeling System) as it simulates the streamflow dynamics across the entire watershed. In the case of the Melka Kunture watershed, the basin model was developed by delineating nine subbasins and seven reaches using a GIS tool integrated with the HEC-HMS model. Figure 3.12 provides a schematic representation of the basin model for the Melka Kunture watershed, illustrating the subbasins and reaches within the system. This visual representation helps understand the spatial organization of the watershed and the flow pathways. The basin model incorporates three key components: the loss model, transform model, and routing model. These components work together to simulate streamflow for the subbasins and reaches within the watershed.

The loss model accounts for the various processes that result in the loss of water from the watershed, such as evaporation and infiltration. It helps estimate the amount of water that does not contribute to the streamflow. The transform model focuses on transforming the rainfall input into direct runoff. It considers factors like soil type, land use, and vegetation cover to estimate the portion of rainfall that becomes runoff. The routing model is responsible for simulating the movement of water through the stream network. It considers factors such as channel characteristics, slope, and hydraulic properties to determine the flow dynamics and travel times within the watershed.

Tables 3.6 to 3.10 present the estimated parameters for the different methods used in the simulation within the basin model. These tables likely provide details on specific parameters related to the loss model, transform model, and routing model, allowing for a comprehensive understanding of the modeling approach and parameterization used in the study. Overall, the basin model, with its subbasins, reaches, and integrated components, serves as a fundamental framework for simulating streamflow and understanding the hydrological processes within the Melka Kunture watershed.

#### *4.2.1.1 HEC-HMS model calibration*

Figure 4.7 presents a visual comparison of the hydrographs of simulated and observed streamflow during the calibration period. The figure illustrates a close agreement between the simulated and observed streamflow, indicating that the model was able to capture the key characteristics of the streamflow dynamics. The agreement in terms of streamflow distribution was considered acceptable. To further evaluate the model's performance, several objective functions were utilized. These included the Nash-Sutcliffe efficiency (NSE), root mean square error standard deviation (RSR), coefficient of determination ($R^2$), root mean square error (RMSE), and PBIAS objective functions. These objective functions provide quantitative measures of the model's accuracy in replicating the observed streamflow.

Table 4.3 presents the values of these objective functions, allowing for an assessment of the model's performance. The NSE, RSR, $R^2$, and RMSE values provide insights into the model's ability to reproduce the observed streamflow patterns and minimize the differences between simulated and observed data. By utilizing these objective functions and assessing the agreement between simulated and observed streamflow, the calibration process aimed to optimize the model parameters and improve the model's performance in simulating streamflow dynamics for the Melka Kunture watershed.

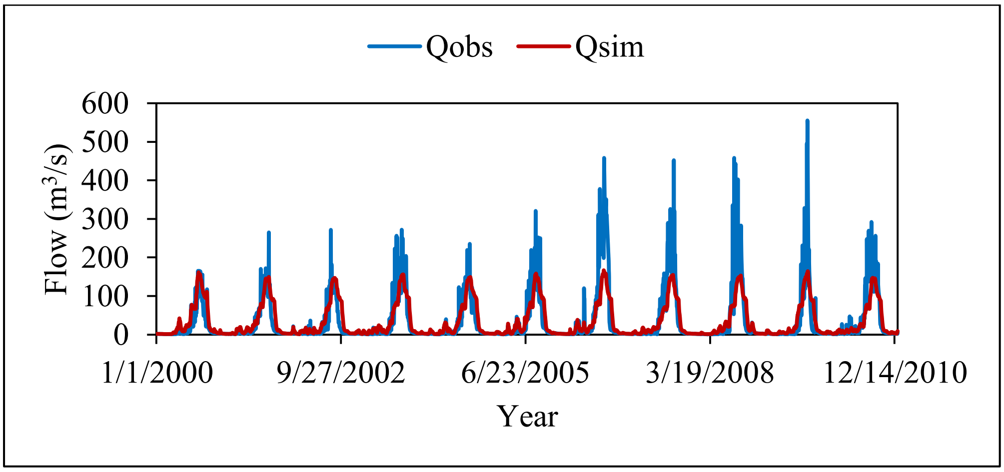


Figure 4.7: Comparison of observed streamflow hydrograph calibration periods

#### *4.2.1.2 HEC-HMS model validation*

During the validation phase, streamflow data from the period 2011 to 2015 were used to assess the performance of the calibrated model. The parameters obtained during the calibration process were applied to the model for this validation. Figure 4.8 presents a comparison between the simulated and observed streamflow hydrographs after the validation process. This visual representation allows for an evaluation of the model's ability to replicate the observed streamflow patterns during the validation period.

Table 4.3 provides the results of the evaluation parameters for the validation phase. These parameters include the coefficient of determination ($R^2$), Nash-Sutcliffe efficiency (NSE), root mean square error (RMSE), root mean square error standard deviation (RMSE Std.

Dev.), and percent bias (PBIAS). These metrics are commonly used to assess the accuracy and performance of hydrological models.

By evaluating these parameters and comparing the simulated and observed streamflow hydrographs, the validation process aims to assess the accuracy and reliability of the calibrated model during the specified validation period. These evaluation parameters provide valuable insights into the model's performance in replicating the observed streamflow dynamics for the Melka Kunture watershed.

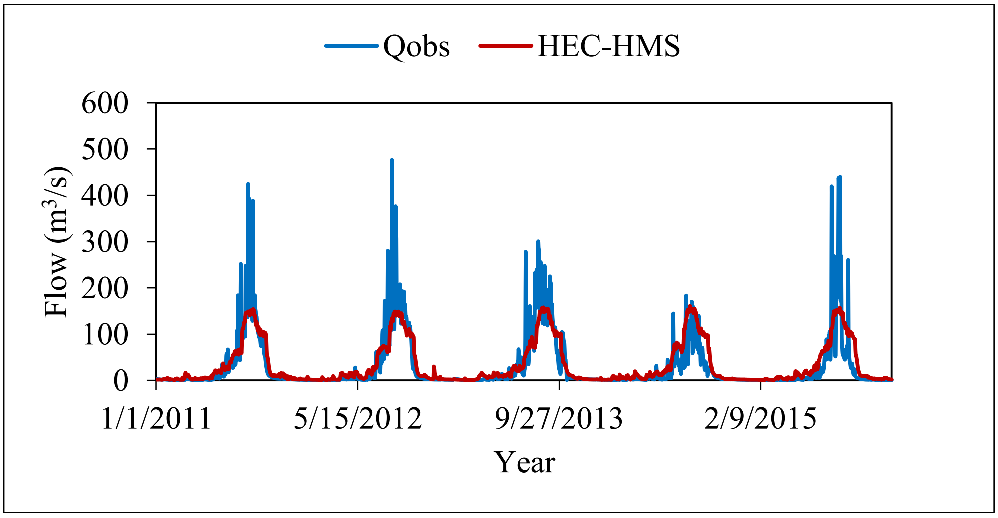


Figure 4.8: Comparison of simulated and observed streamflow validation periods

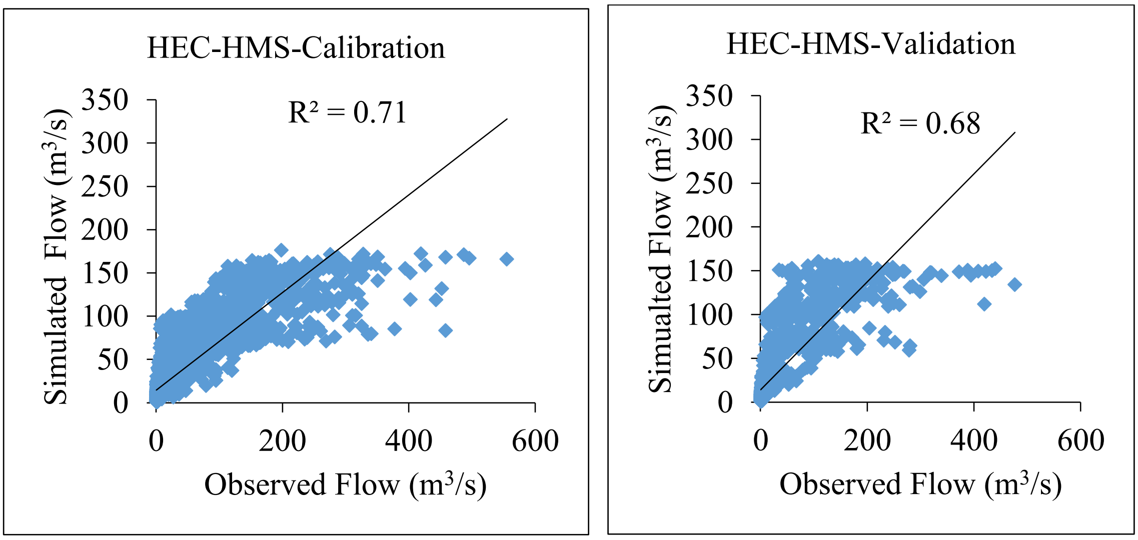


Figure 4.9: The scatter plot of the simulated and observed streamflow for the calibration and validation periods

#### *4.2.1.3 HEC-HMS Performance Evaluation*

The model experienced calibration and validation processes to assess its performance, with the optimization trial tool used for automatic parameter calibration. Table 4.3 presents the performance ratings of the model parameters. The performance rating criteria showed that, the model's $R^2$ and NSE values fall within the good range for both calibration and validation. Regarding PBIAS, the model demonstrates a very good performance during calibration by slightly overestimating the streamflow volume.

During validation, the model shows a very good performance by underestimating the streamflow. Based on the obtained results, it can be concluded that the model is acceptable for further hydrological studies. The proximity of the trend line to the simulated streamflow values indicates a good correlation between the simulated and observed streamflow values. This suggests that the model is capable of slightly capturing the streamflow dynamics.

To visualize the comparison between the actual and simulated streamflow, Figure 4.9 displays a scatter plot for both the calibration and validation periods. This plot provides a graphical representation of the agreement between the observed and simulated streamflow values, allowing for a visual assessment of the model's performance. Considering the positive evaluation results, the good correlation between simulated and observed streamflow, and the visual representation in Figure 4.9, the model can be deemed reliable and suitable for use in future hydrological studies within the context of the Melka Kunture watershed.

Comparing HEC-HMS applicability in simulating streamflow to findings by Geyisa Namara et al. (2020), there is a variation in $R^2$, NSE, and PBIAS, which could be caused using different hydro-meteorological data. HEC-HMS hydrological model achieved $R^2$, NSE, and PBIAS values during calibration (1990-2005) and validation (2006-2015) 0.867, 0.855 and 4.59% and 0.863, 0.739, and 5.67% in the upper Awash sub-basin at Awash Bello gauged station. This variation could be happen due to the longer length of hydro-meteorological data used in the study area (1990-2015). The other factor for the variation of the result is that as the basin is more divided to small sub-basin the more the accuracy of the streamflow simulation. The SCS-CN loss method, SCS-UH, constant and monthly baseflow method, are the best fit performed methods of the hydrological processes of loss, direct runoff transformation and baseflow part of the model. In this watershed curve number and initial abstraction are the most sensitive parameter.

Sime (2022) has also indicated that the curve number is the most sensitive parameter in the Katar watershed rift valley, Ethiopia. Aliye et al. (2020) evaluate the performance of HEC-HMS and SWAT models in simulating the rainfall-Runoff process for data scarce region of Ethiopia Rift Valley Lake basin. The HEC-HMS $R^2$ and NSE value during calibration and validation was 0.88 and 0.75 and 0.87 and 0.73 respectively. Again, this variation could be attributed due to heterogeneity of the land use land cover as well their similarity is that both model use SCS-Curve Number and give satisfactory result. Therefore, HEC-HMS model is applicable in simulating the streamflow for Melka Kunture watershed.

Table 4.3: Statistical performance evaluation value of daily simulated and observed streamflow hydrograph by the HEC-HMS model during calibration and validation

| Performance criteria | $R^2$ | NSE | $NSE_{log}$ | RMSE | PBIAS | RSR |
|---|---|---|---|---|---|---|
| Calibration period (2000-2010) | 0.71 | 0.68 | 0.70 | 37.53 | -0.1 | 0.6 |
| Validation period (2011-2015) | 0.68 | 0.68 | 0.71 | 139.69 | 6.39 | 0.6 |

### 4.2.2 SWAT+ Model Result

#### *4.2.2.1 SWAT+ Sensitivity Analysis*

The Sobol sensitivity analysis method, implemented in the SWAT+ Toolbox v0.4.5 software, was utilized to identify the most sensitive parameters for the Melka Kunture watershed (Table 4.4). Sensitivity analysis ranked the parameters based on their highest sensitivity index values. The two most sensitive parameters were the available water content in the soil (awc) and the soil conservation service runoff curve number for moisture condition II (cn2), with sensitivity index values of 0.77 and 0.23, respectively.

Additional parameters, although having a relatively smaller impact on hydrologic response prediction, were identified as significantly sensitive for calibration. These parameters include maximum canopy storage (canmx) and minimum flow (flow-min), with sensitivity index values of 0.025 and 0.012, respectively. While their individual impacts are comparatively lower, they were still considered important in conjunction with other flow-governing parameters.

In summary, the sensitivity analysis using the Sobol method highlighted the critical role of parameters such as available water content in the soil (awc) and soil conservation service runoff curve number for moisture condition II (cn2) in predicting the hydrologic response of the Melka Kunture watershed. Parameters with relatively smaller impacts, namely maximum canopy storage (canmx) and minimum flow (flow-min) were also identified as significant and included in the calibration analysis process alongside other relevant flow-related parameters.

Table 4.4: Sobol's sensitivity indices for SWAT+ Parameters in Melka Kunture river watershed

| Parameters | object | Min-value | Max-value | Units | Sensitivity | Rank |
|---|---|---|---|---|---|---|
| awc | sol | 0.01 | 1 | Mm_H2Omm | 0.77 | 1 |
| Cn2 | hru | 25 | 98 | | 0.23 | 2 |
| canmx | hru | 0 | 100 | Mm/H2O | 0.025 | 3 |
| Flow_min | aqu | 0 | 10 | M | 0.012 | 4 |
| ovn | hru | 0.01 | 30 | M | 0 | NS |
| Gwflow_lte | hlt | 0 | 10 | mm | 0 | NS |
| Gwdeep_lte | hlt | 0 | 10 | mm | 0 | NS |
| Gw_lte | hlt | 0 | 10 | mm | 0 | NS |
| bf_max | aqu | 0 | 2 | mm | 0 | NS |
| Tc_lte | hlt | 1 | 84600 | min | 0 | NS |
| Revap_co | aqu | 0.02 | 0.2 | | -0.00094 | 5 |
| epco | hru | 0 | 1 | | -0.00097 | 6 |
| alpha | aqu | 0 | 1 | day | -0.011 | 7 |
| slope | hru | 0 | 1 | m/m | -0.22 | 8 |
| Cn3_awf | Hru | 0 | 1 | | -0.34 | 9 |
| esco | hru | 0 | 1 | | -0.36 | 10 |

NS: Not sensitive; and the parameter with the most sensitive value is shown in bold type

#### *4.2.2.2 SWAT+ Calibration*

The calibration process was conducted automatically using the dynamically dimensioned search (DDS) method. It is an optimization technique that dynamically adjusts the number of decisions variables considered at the given iteration to efficiently explore the search space. The calibration process involved optimizing the model parameters to achieve the best fit between the simulated streamflow and the observed streamflow data. Specifically, the calibration was performed using the two-thirds portion of the observed streamflow data, covering the ten-year period from 2001 to 2010 (Figure 4.10). This period provided a significant dataset for calibrating the model and fine-tuning its parameters to accurately represent the streamflow dynamics of the Melka Kunture watershed.

By utilizing a warm-up period and selecting a substantial portion of the observed streamflow data for calibration, the model was able to capture the hydrological processes and refine its parameterization to improve its performance in simulating streamflow for the Melka Kunture watershed. During calibration the underestimation or overestimation of streamflow by SWAT+ model in different years were observed. This was due to input data accuracy, model structure and complexity, spatial and temporal variability, uncertainty in climate and weather patterns and system complexity and nonlinearities. In general, it is important to note that no hydrologic model can perfectly replicate all aspects of real-world hydrological processes. Model limitations, uncertainties in input data, and natural variability in hydrological systems contribute to the underestimation or overestimation of streamflow in different years.

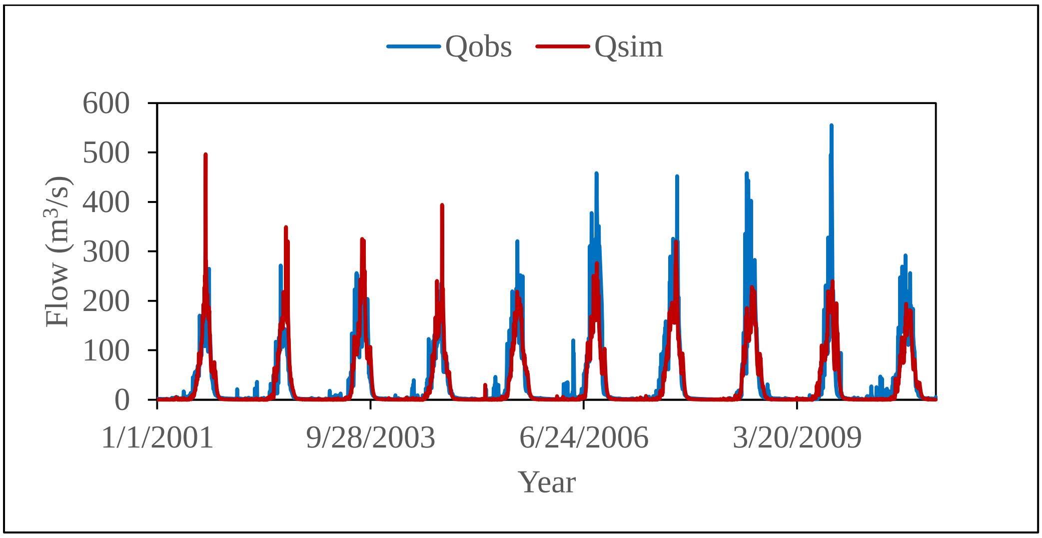


Figure 4.10: Comparison of daily simulated and observed streamflow calibration periods

#### *4.2.2.3 SWAT+ validation*

To check the model input parameters used in the calibrated model, a validation process was conducted using the same input parameters as those used during the calibration procedure. The purpose of validation was to evaluate the model's performance using streamflow data that were not included in the calibration period. For the validation process, daily observed streamflow data of five year period (2011-2015) were utilized as input data (Figure 4.11). These data represented an independent dataset that had not been used during the calibration period. By employing this separate set of streamflow observations, the model's ability to accurately predict streamflow patterns beyond the calibration period could be assessed. During validation, underestimation and overestimation of streamflow by SWAT+ model in different years were also observed. This was due to model limitations, uncertainties in input data, and natural variability in hydrological systems contribute to the underestimation or overestimation of streamflow in different years.

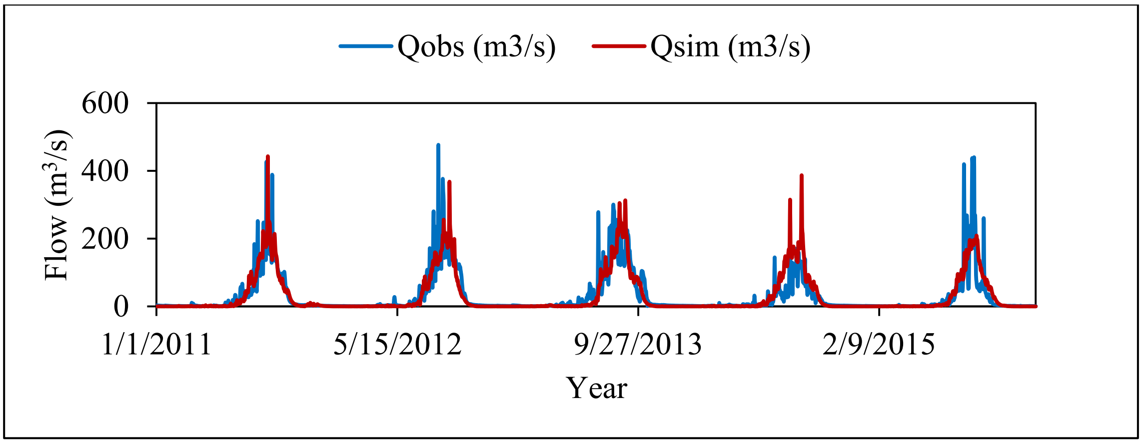


Figure 4.11: Comparison of daily simulated and observed streamflow validation periods

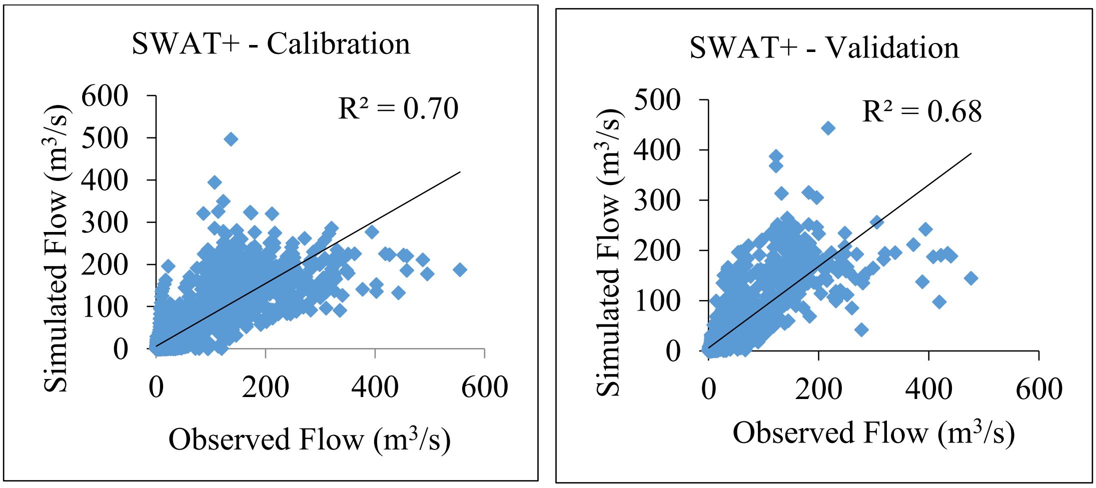


Figure 4.12: The scatter plot of the actual and simulated streamflow for the calibration and validation periods

***4.2.2.4 SWAT+ Performance Evaluation***

The performance of the SWAT+ model was evaluated using various statistical parameters to assess its accuracy. Table 4.5 provides the values of the statistical parameters obtained during the calibration and validation processes. Key indicators such as the coefficient of determination ($R^2$), Nash-Sutcliffe efficiency (NSE), and percent bias (PBIAS) were calculated to evaluate the model's performance.

For the calibration period, the computed values of $R^2$, NSE, and PBIAS were 0.71, 0.70, and 9.35, respectively. These values indicate a reasonably good agreement between the simulated and observed streamflow for the calibration period. The model captured a significant portion of the variability in the streamflow data, as evidenced by the high $R^2$

and NSE values. However, there was a slight underestimation of streamflow, indicated by the positive PBIAS value

During the validation period, the estimated values of $R^2$, NSE, and PBIAS were 0.68, 0.66, and -0.48, respectively. These values also demonstrate a good level of agreement between the simulated and observed streamflow. However, there was a slight overestimation of streamflow during the validation period, as indicated by the negative PBIAS value. The scatter plot in Figure 4.12 illustrates the comparison between the actual and simulated streamflow for both the calibration and validation periods. The proximity of the trend line to the simulated streamflow values suggests a strong correlation between the simulated and observed streamflow values. This further confirms the model's ability to replicate the streamflow dynamics satisfactorily.

Previous study by Tumsa et al. (2022) showed that SWAT+ model capability in simulating streamflow under land use land cover change in Guder catchment, Ethiopia. The value of $R^2$, NSE, and PBIAS during calibration and validation showed satisfactory result in simulating monthly observed streamflow of the catchment. Study by Abate et al. (2023) also revealed that the applicability of SWAT+ model in data scarce region of upper Danakil Basin, Ethiopia.

Overall, the statistical parameters and the scatter plot analysis indicate that the SWAT+ model performed well in simulating streamflow for the Melka Kunture watershed. The model's high $R^2$ and NSE values, along with the close agreement between the simulated and observed streamflow, support its suitability for future hydrological research in the area.

Table 4.5: Performance statistics for daily streamflow simulation of SWAT+ model during calibration and validation

| Performance criteria | $R^2$ | NSE | $NSE_{log}$ | RMSE | PBIAS |
|---|---|---|---|---|---|
| Calibration period (2001-2010) | 0.71 | 0.70 | 0.19 | 37.53 | 9.49 |
| Validation period (2011-2015) | 0.68 | 0.66 | -2.07 | 35.57 | -0.48 |

### 4.2.3 HBV-Light model

#### *4.2.3.1 HBV-Light model calibration and validation*

The HBV-Light model was applied to simulate streamflow in the Melka Kunture watershed using streamflow data from the years 2000 to 2015. The year 2000 was utilized as a warm-up period to estimate the initial state variables of the model. To calibrate the

HBV-Light model, two-thirds of the streamflow data (2001 to 2010) were employed. This calibration period allowed for adjusting the model parameters to optimize its performance. The calibration process was conducted automatically using the Genetic Algorithm and Powell (GAP) optimization technique, which efficiently searches for the optimal parameter values.

Following the calibration phase, one-third of the streamflow data (2011 to 2015) was used for model validation. This independent dataset was used to assess the model's performance and evaluate its ability to accurately replicate streamflow patterns that were not used during the calibration process. During the calibration, the model parameters were optimized using the Genetic Algorithm and Powell (GAP) method. The specific parameter values and optimization results can be found in Table 3.4.

By utilizing a warm-up period, dividing the data into calibration and validation sets, and employing the GAP optimization technique, the HBV-Light model was able to capture the characteristics of streamflow in the Melka Kunture watershed and provide reliable simulations. During calibration and validation, underestimation and overestimation of streamflow by HBV-Light model in different years were also observed. This was due to model limitations, uncertainties in input data, and natural variability in hydrological systems contribute to the underestimation or overestimation of streamflow in different years.

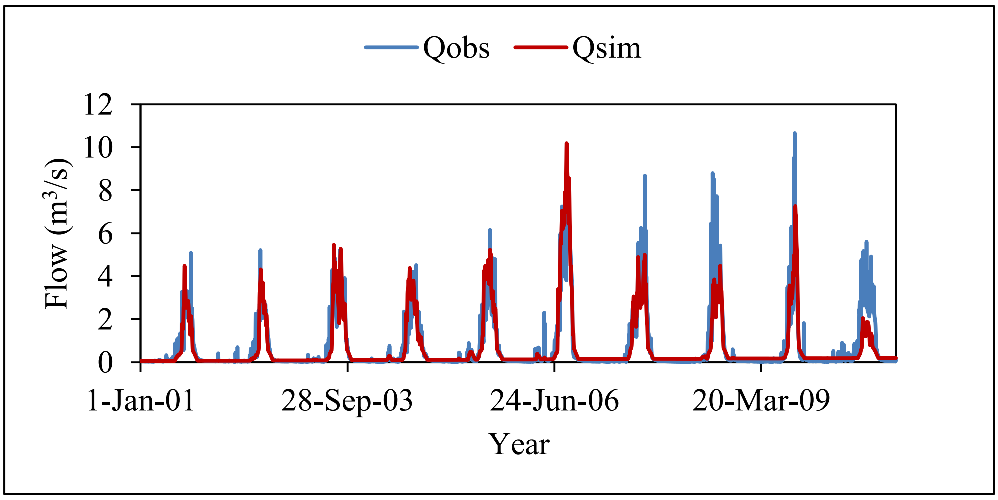


Figure 4.13: Comparison of daily simulated and observed streamflow during calibration in HBV-light model

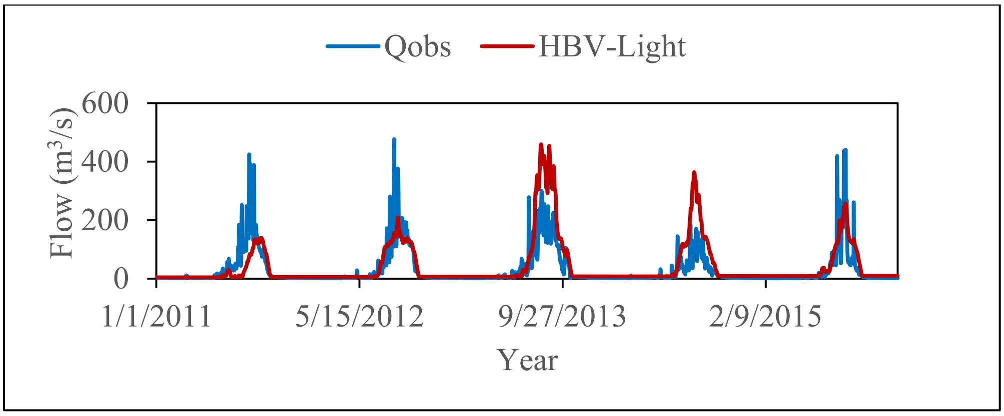


Figure 4.14: Comparison of daily simulated and observed streamflow during validation in HBV-light model

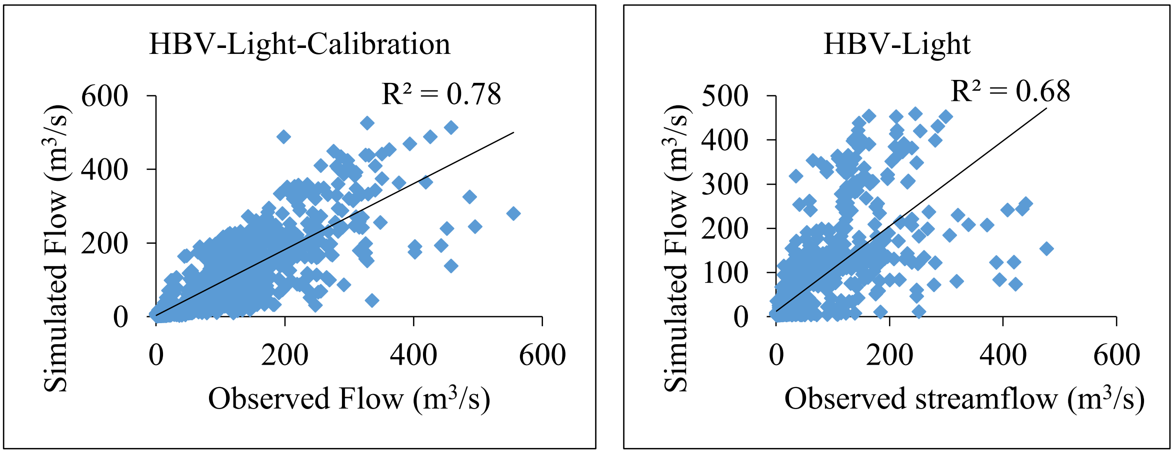


Figure 4.15: The scatter plot of observed and simulated streamflow during calibration and validation periods by HBV-Light model

#### *4.2.3.2 HBV-Light performance evaluation*

HBV-Light demonstrated strong performance in modeling streamflow for the Melka Kunture watershed during both the calibration and validation periods, as indicated in Table 4.6. For the calibration period, the model achieved an $R^2$ value of 0.78, indicating a very good fit between the simulated and observed streamflow. The Nash-Sutcliffe efficiency ($R_{eff}$) value of 0.80 further confirms the model's ability to satisfactorily simulate streamflow patterns. Additionally, the volume error value of 0.94 suggests a minimal deviation in the total volume of simulated daily streamflow compared to the observed data.

During the validation period, HBV-Light maintained its strong performance with an $R^2$ value of 0.68, indicating a good correlation between the simulated and observed streamflow. The $R_{eff}$ value of 0.68 signifies the model's ability to capture the variability in streamflow. The volume error value of 0.99 indicates a very close agreement between the total volume of simulated and observed streamflow. The model underestimates the volume both during calibration and validation.

The model's consistent performance in meeting the standards for good performance over both the calibration and validation periods (Table 4.6) demonstrates its reliability in representing streamflow dynamics in the Melka Kunture watershed. This is further supported by the trend line in Figure 4.15, which closely aligns with the simulated streamflow values, indicating a strong correlation between the model's predictions and the observed streamflow. Generally, the results show that the HBV-Light model can reproduce daily historical streamflow with an acceptable accuracy. Previous study by (Abebe & Kebede, 2017) show similar result. Similarly, Budhathoki et al. (2023) applied HBV-Light to simulate daily streamflow contribution on water balance in Himalayan river basin, Nepal. The $R^2$, NSE and PBIAS value during calibration 0.77, 0.77, and -3% and 0.87, 0.82, and -21% respectively. This show the agreement between simulated and observed daily streamflow is close. Therefore, HBV-Light model is applicable in simulating the daily streamflow of Melka Kunture watershed.

Table 4.6: Performance statistics for daily streamflow simulation of HBV-light during calibration and validation periods after GAP optimization

| Performance criteria | $R^2$ | NSE | $NSE_{log}$ | PBIAS/VE | KGE |
|---|---|---|---|---|---|
| Calibration period (2001-2010) | 0.78 | 0.8 | 0.64 | 0.94 | 0.87 |
| Validation period (2011-2015) | 0.68 | 0.68 | 0.51 | 0.99 | 0.75 |

### 4.3 Comparison of HEC-HMS, SWAT+, and HBV-Light models' performance in simulating streamflow in the Melka Kunture watershed

The streamflow prediction capacity of the HEC-HMS, SWAT+, and HBV-Light models was compared with observed streamflow data for the Melka Kunture watershed. The comparison was conducted over the calibration period from 2001 to 2010. Figure 4.16 illustrates the daily simulated and measured streamflow for this period, showcasing the performance of each model.

Additionally, the statistical performance of the parameters used in streamflow simulation was assessed for each model. The selected criteria for comparison were the coefficient of determination ($R^2$), Nash-Sutcliffe efficiency (NSE), and percent bias (PBIAS). Table 4.7 provides a summary of the daily statistical performance achieved by the HEC-HMS, SWAT+, and HBV-Light models during both the calibration and validation periods.

By examining Figure 4.16, one can visually compare the simulated streamflow generated by each model with the observed streamflow. This allows for an assessment of their accuracy and performance. Table 4.7 complements the visual analysis by presenting quantitative measures, such as $R^2$, NSE, and PBIAS, which provide further insights into the models' ability to replicate streamflow patterns.

Based on the $R^2$, NSE, and PBIAS values, all three models performed relatively well during calibration period (with $R^2$ = 0.71, NSE = 0.677, and PBIAS = -0.1 for HEC-HMS; $R^2$ = 0.71, NSE = 0.669, and PBIAS = 9.349 for SWAT+; and $R^2$ = 0.78, NSE = 0.80 and PBIAS = 0.94 for HBV-Light models for daily streamflow simulations). HBV-Light achieved the highest performance value, indicating very good performance, while HEC-HMS and SWAT+ obtained good ratings based on the $R^2$, NSE, and PBIAS criteria. During the validation period, all three models achieved good ratings based on the $R^2$, NSE, and PBIAS criteria (with $R^2$ = 0.68, NSE = 0.676, and PBIAS = 6.39 for HEC-HMS, $R^2$ = 0.68, NSE = 0.66, and PBIAS = -0.48 for SWAT+, and $R^2$ = 0.68, NSE = 0.68, and PBIAS = 0.99 for HBV-Light models for daily streamflow simulations). HBV-Light maintained its good performance, while HEC-HMS and SWAT+ also showed satisfactory result.

In summary, based on the provided performance rating criteria, HBV-Light consistently demonstrated better performance compared to HEC-HMS and SWAT+ during both the calibration and validation periods. HBV-Light achieved very good ratings, while HEC-HMS and SWAT+ obtained good ratings for most of the evaluation criteria (Table 4.7).

Table 4.7: Performance statistics for daily streamflow simulation using HEC-HMS, SWAT+, and HBV-light models in the calibration and validation periods

| Models | Performance criteria | $R^2$ | NSE | $NSE_{log}$ | RMSE/RSR | PBIAS/VE |
|---|---|---|---|---|---|---|
| HEC-HMS | Calibration period | 0.71 | 0.677 | 0.70 | 37.53/0.6 | -0.1 |
| | Validation period | 0.68 | 0.676 | 0.71 | 139.69/0.6 | 6.39 |
| SWAT+ | Calibration period | 0.71 | 0.696 | 0.19 | 37.554. | 9.349 |
| | Validation period | 0.68 | 0.66 | -2.07 | 35.57 | -0.475 |
| HBV-Light | Calibration period | 0.78 | 0.80 | 0.64 | - | 0.94 |
| | Validation period | 0.68 | 0.68 | 0.51 | - | 0.99 |

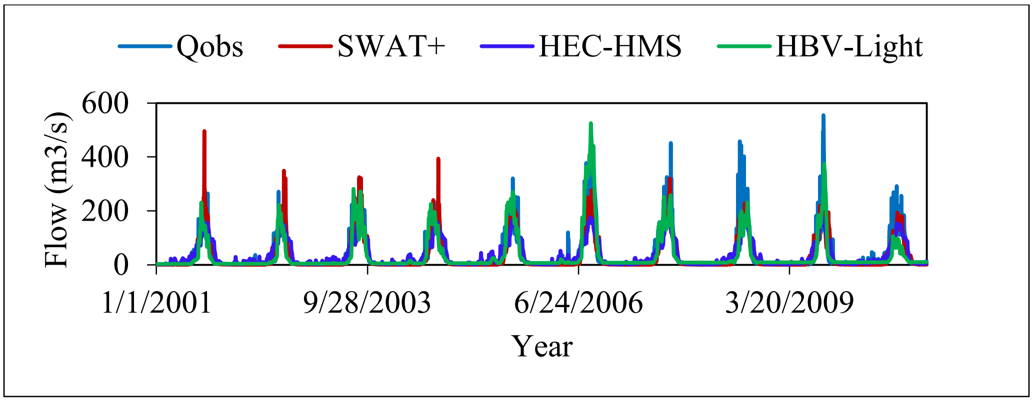


Figure 4.16: Comparison of daily observed and simulated hydrographs for the HEC-HMs, SWAT+, and HBV-Light models for the calibration period

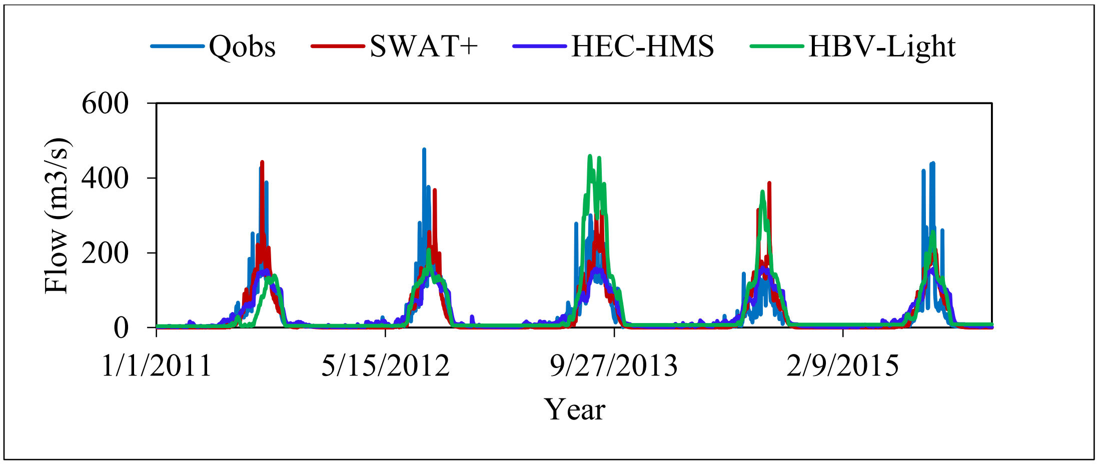


Figure 4.17: Comparison of daily observed and simulated hydrographs for the HEC-HMs, SWAT+, and HBV-Light models for the validation period

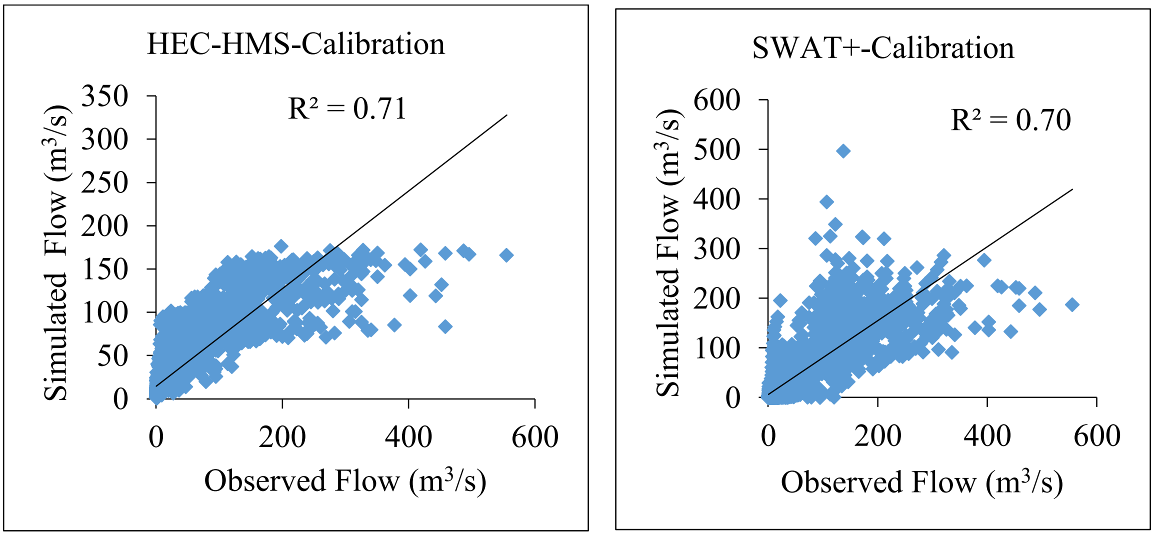

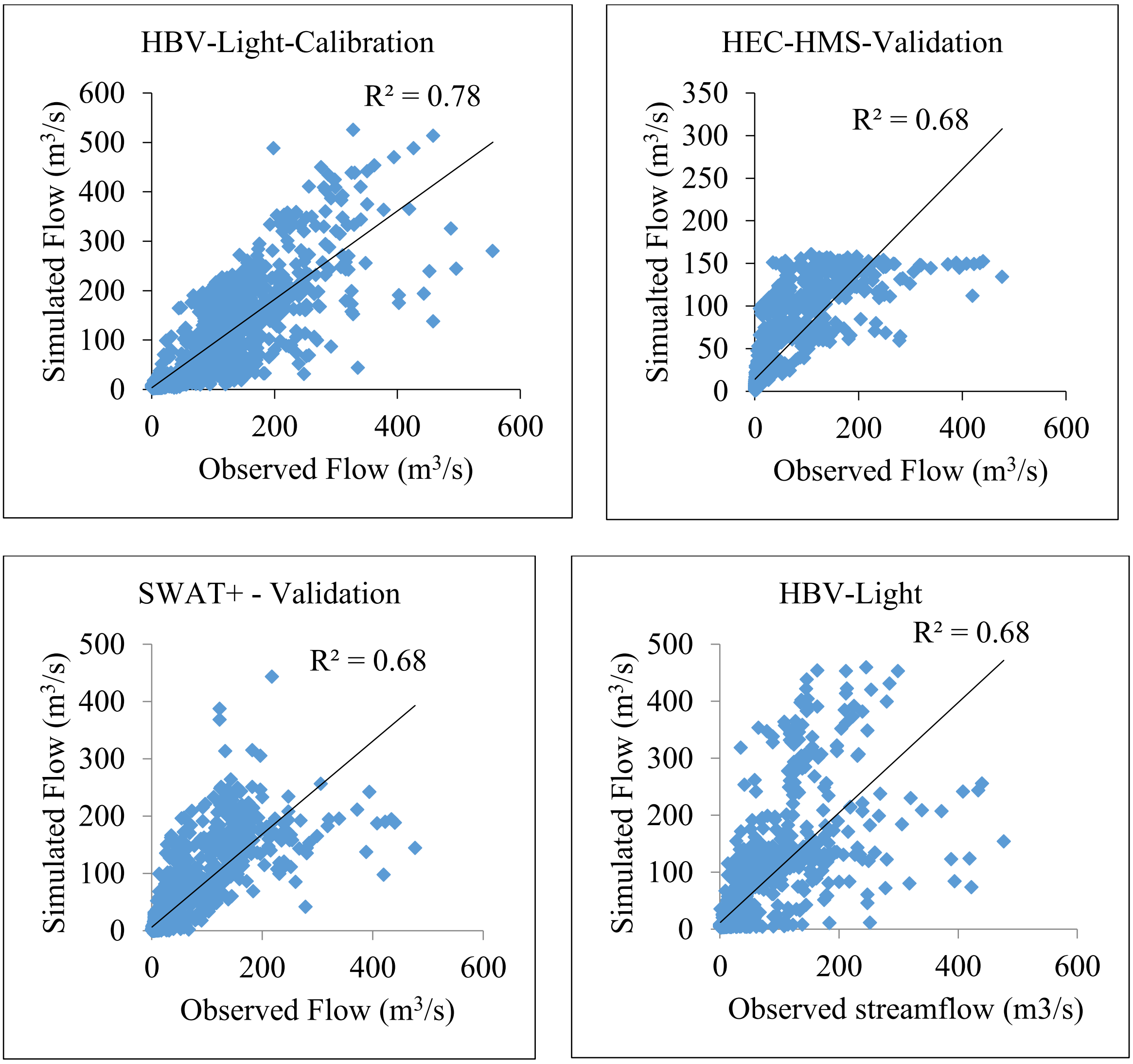


Figure 4.18: The scatter plot of observed and simulated streamflow during calibration and validation periods

The low streamflow simulation performance of HEC-HMS, SWAT+, and HBV-Light were assessed using Nash-Sutcliffe logarithm (NSElog). NSElog is an adaptation of Nash-Sutcliffe efficiency that incorporates the logarithm of flow data (Oudin et al., 2006). It is utilized to evaluate the accuracy of hydrological models in simulating low streamflow conditions, which refer to periods of relatively low water flow in streams.

By comparing the observed low streamflow values with those simulated by each model, the Nash-Sutcliffe efficiency logarithm (Table 4.7) provides valuable insights into how well the models capture the characteristics of low streamflow. In this study, the performance of HEC-HMS, SWAT+, and HBV-Light in simulating low streamflow was assessed during both the calibration and validation periods. During the calibration period, the NSElog values were found to be 0.70, 0.19, and 0.64 for HEC-HMS, SWAT+, and

HBV-Light, respectively. These values suggest that HEC-HMS exhibited the highest level of agreement between observed and simulated low streamflow, followed by HBV-Light, while SWAT+ showed comparatively weaker performance.

Similarly, during the validation period, the Nash-Sutcliffe efficiency logarithm (NSElog) values were 0.71, -2.07, and 0.51 for HEC-HMS, SWAT+, and HBV-Light, respectively. Once again, HEC-HMS demonstrated the best performance, maintaining a consistently good agreement with the observed low streamflow. On the other hand, SWAT+ exhibited a significant decline in its performance, indicating poor agreement, and HBV-Light showed a moderate level of agreement.

Based on these statistical performance metrics, it can be concluded that the HEC-HMS model outperformed both SWAT+ and HBV-Light in simulating low streamflow conditions during both the calibration and validation periods. However, it's important to consider other evaluation factors and metrics to gain a comprehensive understanding of the models' overall performance in various hydrological aspects.

# 5. CONCLUSION AND RECOMMENDATION

## 5.1 Conclusion

The main purpose of this study was to analyze variations in rainfall and streamflow and evaluating the performance of HEC-HMS, SWAT+, and HBV-Light models in simulating streamflow to find suitable model for hydrological modeling in Melka Kunture watershed. The variability of historical rainfall and streamflow of the watershed was analyzed using coefficient of variation (CV), standard rainfall anomaly (SRAI), and precipitation concentration index (PCI) in the period 2000-2015.

The variation of rainfall within the watershed ranges from low to high seasonally and annually. The CV for streamflow also showed from moderate to high seasonally and annually. The result of the annual SRAI showed the rainfall within the watershed ranges from extremely wet to extremely dry, but mostly all stations get near normal rainfall annually. The annual PCI result within watershed ranges from irregular to moderate rainfall distribution, while seasonally, the PCI within the watershed showed strong irregularities of rainfall distribution.

Calibration and validation of the models were conducted by using daily observed streamflow at Melka Kunture streamflow outlet in the period 2000-2015. The results of calibration and validation suggest that the three models could simulate fairly well the streamflow for Melka Kunture watershed. The comparison of HEC-HMS, SWAT+, and HBV-Light models in generating streamflow in the 2000-2015 periods shows that HBV-Light is the most suitable for hydrological modeling with high accuracy.

However, when considering the simulation of low streamflow simulation conditions, the HEC-HMS model outperformed both SWAT+ and HBV-Light. It exhibits better performance in capturing the hydrological processes associated with low streamflow, which is crucial for effective water resource management in the watershed. This highlights the significance of selecting an appropriate hydrological model for specific watershed characteristics and objectives.

## 5.2 Recommendation

Based on the results found and challenges faced during this particular research execution period the following recommendations are forwarded:

- ✓ The models should be tested for further simulations, particularly under changing environmental conditions such as climate and land use land cover alterations.
- ✓ HEC-HMS, SWAT+, and HBV-Light were used in this study to simulate streamflow in the Melka Kunture watershed upper awash sub-basin. They gave satisfactory result during calibration and validation. Currently, machine learning technique has gained significant importance in hydrological modeling due to their ability to analyze complex and non-linear relationships within hydrological processes. They can learn from historical data and make predictions without relying heavily on explicit equations or assumptions. Machine learning models can effectively handle uncertainty associated with input data and model parameters and require less computational effort once trained. Therefore, for further simulations of the streamflow of Melka Kunture watershed additional research should be conducted comparing the performance of physically based model with the machine learning technique.
- ✓ .It is worth noting that the use of fully distributed hydrological models like MIKE SHE was limited in this study due to data constraints within the watershed. MIKE SHE requires gridded hydro-meteorological and high spatial resolution data to account for the variability in terrain, land cover, soil properties, and hydrological processes. In the feature using this model is important in planning, designing and development of strategies in water resources management in the Melka Kunture watershed if the gridded hydro-meteorological data and high spatial resolution data are prepared.

# REFERENCES


Abate, B. Z., Assefa, T. T., Tigabu, T. B., Abebe, W. B., & He, L. (2023). Hydrological Modeling of the Kobo-Golina River in the Data-Scarce Upper Danakil Basin, Ethiopia. *Sustainability*, *15*(4), Article 4. https://doi.org/10.3390/su15043337

Abbott, M. B., Bathurst, J. C., Cunge, J. A., O'Connell, P. E., & Rasmussen, J. (1986). An introduction to the European Hydrological System — Systeme Hydrologique Europeen, "SHE", 2: Structure of a physically-based, distributed modelling system. *Journal of Hydrology*, *87*(1), 61–77. https://doi.org/10.1016/0022-1694(86)90115-0

Abdessamed, D., Bouanani, A., & Babahamed, K. (2018). Modelling rainfall runoff relations using HEC-HMS in a semi-arid region: Case study in Ain Sefra watershed, Ksour Mountains (SW Algeria). *Journal of Water and Land Development*, *36*, 45–55. https://doi.org/10.2478/jwld-2018-0005

Abebe, E., & Kebede, A. (2017). Assessment of Climate Change Impacts on the Water Resources of Megech River Catchment, Abbay Basin, Ethiopia. *Open Journal of Modern Hydrology*, *7*(2), Article 2. https://doi.org/10.4236/ojmh.2017.72008

Abegaz, W. B., & Mekoya, A. (2020). Rainfall Variability and Trends over Central Ethiopia. *International Journal of Environmental Sciences & Natural Resources*, *24*(4), 49–57. https://doi.org/10.19080/IJESNR.2020.24.556144

Abera, F., Asfaw, D., & Nigussie, A. (2017). Trend and Variability Analysis of Rainfall & Stream Flow Series at Tekeze River Basin, Ethiopia. *International Journal of Scientific and Engineering Research*, *8*, 665–680.

Alemu, M. M., & Bawoke, G. T. (2019). Analysis of spatial variability and temporal trends of rainfall in Amhara region, Ethiopia. *Journal of Water and Climate Change*, *11*(4), 1505–1520. https://doi.org/10.2166/wcc.2019.084

Alemu, M. M., & Bawoke, G. T. (2020). Analysis of spatial variability and temporal trends of rainfall in Amhara region, Ethiopia. *Journal of Water and Climate Change*, *11*(4), 1505–1520. https://doi.org/10.2166/wcc.2019.084

Aliye, M. A., Aga, A. O., Tadesse, T., & Yohannes, P. (2020). Evaluating the Performance of HEC-HMS and SWAT Hydrological Models in Simulating the Rainfall-Runoff Process for Data Scarce Region of Ethiopian Rift Valley Lake Basin. *Open Journal of Modern Hydrology*, *10*(04), Article 04. https://doi.org/10.4236/ojmh.2020.104007

Aliye, M., Aga, A., Danbara, T., & Aga, P. (2020). Evaluating the Performance of HEC-HMS and SWAT Hydrological Models in Simulating the Rainfall-Runoff Process for Data Scarce Region of Ethiopian Rift Valley Lake Basin. *Open Journal of Modern Hydrology*, *10*, 105–122. https://doi.org/10.4236/ojmh.2020.104007

Al-Weshah, D.-R., Tarekegn, D., & Mtalo, F. (2018). Rainfall Runoff Modeling in Upper-Awash Sub-Basin. *African Review (Dar Es Salaam, Tanzania)*.

Aredo, M. (2020). Review of Rainfall-Runoff Modelling in Ethiopia. *Journal of Engineering Mathematics*, *01*, 23–31.

Ayalew, A. T. (2019). Rainfall - Runoff Modeling: A Comparative Analyses: Semi Distributed HBV Light and SWAT Models in Geba Catchment, Upper Tekeze

Basin, Ethiopia. *American Journal of Science, Engineering and Technology*, *4*(2), Article 2. https://doi.org/10.11648/j.ajset.20190402.12

Bajpai, O. (2018). Modeling and assessing land-use and hydrological regimes to future land-use scenario for sustainable watershed management in a semi-arid region of southern India. *International Journal of Conservation Science*. https://www.academia.edu/38009220/Modeling_and_assessing_land_use_and_hydrological_regimes_to_future_land_use_scenario_for_sustainable_watershed_management_in_a_semi_arid_region_of_southern_India

Bekele, D., Alamirew, T., Kebede, A., Zeleke, G., & Melese, A. M. (2017). Analysis of rainfall trend and variability for agricultural water management in Awash River Basin, Ethiopia. *Journal of Water and Climate Change*, *8*(1), 127–141. https://doi.org/10.2166/wcc.2016.044

Belay, A., Demissie, T., Recha, J. W., Oludhe, C., Osano, P. M., Olaka, L. A., Solomon, D., & Berhane, Z. (2021a). Analysis of Climate Variability and Trends in Southern Ethiopia. *Climate*, *9*(6), 96. https://doi.org/10.3390/cli9060096

Belay, A., Demissie, T., Recha, J. W., Oludhe, C., Osano, P. M., Olaka, L. A., Solomon, D., & Berhane, Z. (2021b). Analysis of Climate Variability and Trends in Southern Ethiopia. *Climate*, *9*(6), Article 6. https://doi.org/10.3390/cli9060096

Belay, G. W., Azeze, M., & Melesse, A. M. (2019). Reservoir operation analysis for Ribb reservoir in the Blue Nile basin. In *Extreme Hydrology and Climate Variability* (pp. 191–211). Elsevier. https://doi.org/10.1016/B978-0-12-815998-9.00016-6

Belay, Y. Y., Gouday, Y. A., & Alemnew, H. N. (2022). Comparison of HEC-HMS hydrologic model for estimation of runoff computation techniques as a design input: Case of Middle Awash multi-purpose dam, Ethiopia. *Applied Water Science*, *12*(10), 237. https://doi.org/10.1007/s13201-022-01764-7

Bergström, S. (1976a). Development and Application of a Conceptual Runoff Model for Scandinavian Catchments. In *SMHI Rep. RHO 7: Vol. 134 pp.*

Bergström, S. (1976b). Development and Application of a Conceptual Runoff Model for Scandinavian Catchments. In *SMHI Rep. RHO 7: Vol. 134 pp.*

Beven, K. J. (2011). *Rainfall-Runoff Modelling: The Primer*. John Wiley & Sons.

Beyene, S. K., Mohammed, Ing. A., & Pingale, Dr. S. (2018). Impact of Land Use/Land Cover Change on Watershed Hydrology: A Case Study of Upper Awash Basin, Ethiopia. *Ethiopian Journal of Water Science and Technology (EJWST)*, *1*, 4–27.

Bieger, K., Arnold, J. G., Rathjens, H., White, M. J., Bosch, D. D., Allen, P. M., Volk, M., & Srinivasan, R. (2017). Introduction to SWAT+, A Completely Restructured Version of the Soil and Water Assessment Tool. *JAWRA Journal of the American Water Resources Association*, *53*(1), 115–130. https://doi.org/10.1111/1752-1688.12482

Birara, H. (2018). Trend and variability analysis of rainfall and temperature in the Tana basin region, Ethiopia. *Journal of Water and Climate Change*. https://www.academia.edu/52118149/Trend_and_variability_analysis_of_rainfall_and_temperature_in_the_Tana_basin_region_Ethiopia

Birundu, A. M., & Mutua, B. M. (2017). Analyzing the Mara River Basin Behaviour through Rainfall-Runoff Modeling. *International Journal of Geosciences*, *08*(09), 1118–1132. https://doi.org/10.4236/ijg.2017.89064

Budhathoki, B. R., Adhikari, T. R., Shrestha, S., & Awasthi, R. P. (2023). Application of hydrological model to simulate streamflow contribution on water balance in Himalaya river basin, Nepal. *Frontiers in Earth Science*, *11*. https://www.frontiersin.org/articles/10.3389/feart.2023.1128959

Buishand, T. A. (1982). Some methods for testing the homogeneity of rainfall records. *Journal of Hydrology*, *58*(1–2), 11–27. https://doi.org/10.1016/0022-1694(82)90066-X

Chathuranika, I., Gunathilake, M., Baddewela, P., Sachinthanie, E., Babel, M., Shrestha, S., Jha, M., & Rathnayake, U. (2022). Comparison of Two Hydrological Models, HEC-HMS and SWAT in Runoff Estimation: Application to Huai Bang Sai Tropical Watershed, Thailand. *Fluids*, *7*, 1–17. https://doi.org/10.3390/fluids7080267

Chawanda, C. J., George, C., Thiery, W., Griensven, A. van, Tech, J., Arnold, J., & Srinivasan, R. (2020a). User-friendly workflows for catchment modelling: Towards reproducible SWAT+ model studies. *Environmental Modelling & Software*, *134*, 104812. https://doi.org/10.1016/j.envsoft.2020.104812

Chawanda, C. J., George, C., Thiery, W., Griensven, A. van, Tech, J., Arnold, J., & Srinivasan, R. (2020b). User-friendly workflows for catchment modelling: Towards reproducible SWAT+ model studies. *Environmental Modelling & Software*, *134*, 104812. https://doi.org/10.1016/j.envsoft.2020.104812

Daide, F., Afgane, R., Lahrach, A., Chaouni, A.-A., Msaddek, M., & Elhasnaoui, I. (2021). Application of the HEC-HMS hydrological model in the Beht watershed (Morocco). *E3S Web of Conferences*, *314*, 05003.

Daide, F., Afgane, R., Lahrach, A., Chaouni, A.-A., Msaddek, M., & Elhassnaoui, I. (2021). Application of the HEC-HMS hydrological model in the Beht watershed (Morocco). *E3S Web of Conferences*, *314*, 05003. https://doi.org/10.1051/e3sconf/202131405003

Dereje Ayalew. (2012a). Variability of rainfall and its current trend in Amhara region, Ethiopia. *African Journal of Agricultural Research*, *7*(10). https://doi.org/10.5897/AJAR11.698

Dereje Ayalew. (2012b). Variability of rainfall and its current trend in Amhara region, Ethiopia. *AFRICAN JOURNAL OF AGRICULTURAL RESEEARCH*, *7*(10). https://doi.org/10.5897/AJAR11.698

Ebru, E., & Necati, A. (2012). Homogeneity and Trend Analysis of Hydrometeorological Data of the Eastern Black Sea Region, Turkey. *Journal of Water Resource and Protection*, *2012*. https://doi.org/10.4236/jwarp.2012.42012

Engida, T. G., Nigussie, T. A., Aneseyee, A. B., & Barnabas, J. (2021). Land Use/Land Cover Change Impact on Hydrological Process in the Upper Baro Basin, Ethiopia. *Applied and Environmental Soil Science*, *2021*, 1.

Eryani, G. A. P., Amerta, I. M. S., & Jayantari, M. W. (2021). Model Calibration Parameter Using Optimization Trial in HEC-HMS for Unda Watershed. *IOP*

*Conference Series: Earth and Environmental Science*, *930*(1), 012040. https://doi.org/10.1088/1755-1315/930/1/012040

Gbaguidi, F. (2006). *RAINBOW - a software package for hydrometeorological frequency analysis and testing the homogeneity of historical data sets*. https://www.academia.edu/51143818/RAINBOW_a_software_package_for_hydrometeorological_frequency_analysis_and_testing_the_homogeneity_of_historical_data_sets

Gebre, S. L. (2015). Application of the HEC-HMS Model for Runoff Simulation of Upper Blue Nile River Basin. *Journal of Waste Water Treatment & Analysis*, *06*(02). https://doi.org/10.4172/2157-7587.1000199

Getahun, Ming-Hsu Li, & Pei-Yuan Chen. (2020). Assessing Impact of Climate Change on Hydrology of Melka Kuntrie Subbasin, Ethiopia with Ar4 and Ar5 Projections. *Water*, *12*(5), Article 5. https://doi.org/10.3390/w12051308

Geyisa Namara, W., Adugna Damise, T., & Gudu Tufa, F. (2020a). Rainfall Runoff Modeling Using HEC-HMS: The Case of Awash Bello Sub-Catchment, Upper Awash Basin, Ethiopia. *International Journal of Environment*, *9*(1), 68–86. https://doi.org/10.3126/ije.v9i1.27588

Geyisa Namara, W., Adugna Damise, T., & Gudu Tufa, F. (2020b). Rainfall Runoff Modeling Using HEC-HMS: The Case of Awash Bello Sub-Catchment, Upper Awash Basin, Ethiopia. *International Journal of Environment*, *9*(1), 68–86. https://doi.org/10.3126/ije.v9i1.27588

Ghonchepour, D., Sadoddin, A., Bahremand, A., Croke, B., Jakeman, A., & Salmanmahiny, A. (2021). A methodological framework for the hydrological model selection process in water resource management projects. *Natural Resource Modeling*, *34*(3), e12326. https://doi.org/10.1111/nrm.12326

Golmohammadi, G., Prasher, S., Madani, A., & Rudra, R. (2014). Evaluating three hydrological distributed watershed models: MIKE-SHE, APEX, SWAT. *Hydrology*, *1*, 20–39. https://doi.org/10.3390/hydrology1010020

Guduru, J., Boru, N., Rabba, Z., & Namara, W. (2022). Rainfall-runoff modeling using HEC-HMS model for Meki River watershed, rift valley basin, Ethiopia. *Journal of African Earth Sciences*, *197*, 104743. https://doi.org/10.1016/j.jafrearsci.2022.104743

Gui, H., Wu, Z., & Zhang, C. (2021). Comparative Study of Different Types of Hydrological Models Applied to Hydrological Simulation. *CLEAN – Soil, Air, Water*, *49*(8), 2000381. https://doi.org/10.1002/clen.202000381

Gupta, H., Sorooshian, S., & Yapo, P. (1999). Status of Automatic Calibration for Hydrologic Models: Comparison With Multilevel Expert Calibration. *Journal of Hydrologic Engineering - J HYDROL ENG*, *4*. https://doi.org/10.1061/(ASCE)1084-0699(1999)4:2(135)

Haan, C. T., H.P. Johnson, & D.L. Brakenslek. (1982). *Hydrological Modeling of Small Watershed*. 18.

Habte, A., Mamo, G., Worku, W., Ayalew, D., & Gayler, S. (2021). Spatial Variability and Temporal Trends of Climate Change in Southwest Ethiopia: Association with

Farmers’ Perception and Their Adaptation Strategies. *Advances in Meteorology*, *2021*, e3863530. https://doi.org/10.1155/2021/3863530

Hamdan, A. N. A., Almuktar, S., & Scholz, M. (2021). Rainfall-Runoff Modeling Using the HEC-HMS Model for the Al-Adhaim River Catchment, Northern Iraq. *Hydrology*, *8*(2), 58.

Hargreaves, G. H. (1994a). Defining and Using Reference Evapotranspiration. *Journal of Irrigation and Drainage Engineering*, *120*(6), 1132–1139. https://doi.org/10.1061/(ASCE)0733-9437(1994)120:6(1132)

Hargreaves, G. H. (1994b). Defining and Using Reference Evapotranspiration. *Journal of Irrigation and Drainage Engineering*, *120*(6), 1132–1139. https://doi.org/10.1061/(ASCE)0733-9437(1994)120:6(1132)

Hiben, M. G., Gebeyehu Awoke, A., & Adugna Ashenafi, A. (2022). Hydroclimatic Variability, Characterization, and Long Term Spacio-Temporal Trend Analysis of the Ghba River Subbasin, Ethiopia. *Advances in Meteorology*, *2022*, e3594641. https://doi.org/10.1155/2022/3594641

*International conference on water and the environment: Development issues for the 21st century, 26-31 January 1992, Dublin, Ireland : the Dublin statement and report of the conference*. (1992). World Meteorological Organization.

Jaiswal, R. K., Ali, S., & Bharti, B. (2020). Comparative evaluation of conceptual and physical rainfall–runoff models. *Applied Water Science*, *10*(1), 48. https://doi.org/10.1007/s13201-019-1122-6

Jan Seibert. (2005). *Seibert, J. (2005) HBV Light Version 2. User’s Manual. Department of Physical Geography and Quaternary Geology, Stockholm University, Stockholm.* Vdocument.In. https://vdocument.in/hbv-manual-2005.html

Kidanewold, B., Seleshi, Y., & Melesse, A. (2014). Surface Water and Groundwater Resources of Ethiopia: Potentials and Challenges of Water Resources Development. In *Nile River Basin: Ecohydrological Challenges, Climate Change and Hydropolitics* (pp. 97–118). https://doi.org/10.1007/978-3-319-02720-3_6

Koutsouris, A., Seibert, J., & Lyon, S. (2017). Utilization of Global Precipitation Datasets in Data Limited Regions: A Case Study of Kilombero Valley, Tanzania. *Atmosphere*, *8*, 246. https://doi.org/10.3390/atmos8120246

Lambe, B. T., & Kundapura, S. (2021). Analysis of meteorological variability and tendency over Bilate basin of Rift Valley Lakes basins in Ethiopia. *Arabian Journal of Geosciences*, *14*(23), 2692. https://doi.org/10.1007/s12517-021-08962-8

Lindström, G., Johansson, B., Persson, M., Gardelin, M., & Bergström, S. (1997). Development and test of the distributed HBV-96 hydrological model. *Journal of Hydrology*, *201*(1), 272–288. https://doi.org/10.1016/S0022-1694(97)00041-3

Malede, D. A., Agumassie, T. A., Kosgei, J. R., Linh, N. T. T., & Andualem, T. G. (2022). Analysis of rainfall and streamflow trend and variability over Birr River watershed, Abbay basin, Ethiopia. *Environmental Challenges*, *7*, 100528. https://doi.org/10.1016/j.envc.2022.100528

Maru, H., Haileslassie, A., Zeleke, T., & Teferi, E. (2023). Analysis of the impacts of land use land cover change on streamflow and surface water availability in Awash

Basin, Ethiopia. *Geomatics, Natural Hazards and Risk*, *14*(1), 1–25. https://doi.org/10.1080/19475705.2022.2163193

McCarthy, G. T. (1939). *Unit hydrograph and flood routing*. Army Engineer District, Providence. https://scholar.google.com/scholar_lookup?title=unit+hydrograph+and+flood+routing&author=McCarthy%2C+Gerald+T.&publication_year=1939

Melat Eshetu. (2021a). Hydro-climatic Variability and Trend Analysis of Modjo River Watershed, Awash River Basin of Ethiopia. *Journal of Environment and Earth Science*. https://www.academia.edu/72677589/Hydro_climatic_Variability_and_Trend_Analysis_of_Modjo_River_Watershed_Awash_River_Basin_of_Ethiopia

Melat Eshetu. (2021b). Hydro-climatic Variability and Trend Analysis of Modjo River Watershed, Awash River Basin of Ethiopia. *Journal of Environment and Earth Science*. https://doi.org/10.7176/JEES/11-9-04

Mitiku, A. B., Woldyohanes, B., Mekonnen, S. A., Mekonnen, K., & Tadesse, A. (2020). The need for integrated flood management approach from social, economic and environmental perspectives: The case of Upper Awash River Basin. *International Journal of Water Resources and Environmental Engineering*, *12*(3), 57–70. https://doi.org/10.5897/IJWREE2020.0935

Moriasi, J. G. Arnold, M. W. Van Liew, R. L. Bingner, R. D. Harmel, & T. L. Veith. (2007a). Model Evaluation Guidelines for Systematic Quantification of Accuracy in Watershed Simulations. *Transactions of the ASABE*, *50*(3), 885–900. https://doi.org/10.13031/2013.23153

Moriasi, J. G. Arnold, M. W. Van Liew, R. L. Bingner, R. D. Harmel, & T. L. Veith. (2007b). Model Evaluation Guidelines for Systematic Quantification of Accuracy in Watershed Simulations. *Transactions of the ASABE*, *50*(3), 885–900. https://doi.org/10.13031/2013.23153

Muthukrishnan, S., Harbor, J., Lim, K. J., & Engel, B. A. (2006). *Calibration of a Simple Rainfall-runoff Model for Long-term Hydrological Impact Evaluation*. *18*(2), 8.

Namara, W. G., Damise, T. A., & Tufa, F. G. (2020). Rainfall Runoff Modeling Using HEC-HMS: The Case of Awash Bello Sub-Catchment, Upper Awash Basin, Ethiopia. *International Journal of Environment*, *9*(1), Article 1. https://doi.org/10.3126/ije.v9i1.27588

Nash, J. E., & Sutcliffe, J. V. (1970). River flow forecasting through conceptual models part I — A discussion of principles. *Journal of Hydrology*, *10*(3), 282–290. https://doi.org/10.1016/0022-1694(70)90255-6

Nguyen Khoi, D. (2015a). Comparison of the HEC-HMS and SWAT Hydrological Models in Simulating Streamflow. *Tạp Chí Khoa Học và Công Nghệ*, *53*, 189–195.

Nguyen Khoi, D. (2015b). Comparison of the HEC-HMS and SWAT Hydrological Models in Simulating the Streamflow. *Tạp Chí Khoa Học và Công Nghệ*, *53*, 189–195.

Orke, Y. A., & Li, M.-H. (2021). Hydroclimatic Variability in the Bilate Watershed, Ethiopia. *Climate*, *9*(6), Article 6. https://doi.org/10.3390/cli9060098

Orke, Y., & Li, M.-H. (2021). Hydroclimatic Variability in the Bilate Watershed, Ethiopia. *Climate*, *9*, 98. https://doi.org/10.3390/cli9060098

Oudin, L., Andréassian, V., Mathevet, T., Perrin, C., & Michel, C. (2006). Dynamic averaging of rainfall-runoff model simulations from complementary model parameterizations. *Water Resources Research*, *42*(7). https://doi.org/10.1029/2005WR004636

Parra, V., Fuentes-Aguilera, P., & Muñoz, E. (2018). Identifying advantages and drawbacks of two hydrological models based on a sensitivity analysis: A study in two Chilean watersheds. *Hydrological Sciences Journal*, *63*(12), 1831–1843. https://doi.org/10.1080/02626667.2018.1538593

Pawar, U., Karunathilaka, P., & Rathnayake, U. (2022). Spatio-Temporal Rainfall Variability and Concentration over Sri Lanka. *Advances in Meteorology*, *2022*, e6456761. https://doi.org/10.1155/2022/6456761

Pulighe, G., Lupia, F., Chen, H., & Yin, H. (2021). Modeling Climate Change Impacts on Water Balance of a Mediterranean Watershed Using SWAT+. *Hydrology*, *8*(4), Article 4. https://doi.org/10.3390/hydrology8040157

Sahu, S., Pyasi, s. K., Galkate, R., & Shrivastava, R. (2020). Rainfall-Runoff Modelling using HEC-HMS Model for Shipra River Basin in Madhya Pradesh, India. *International Journal of Current Microbiology and Applied Sciences*, *9(08)*, 3440–3449. https://doi.org/10.20546/ijcmas.2020.908.398

Santhi, C., Arnold, J. G., Williams, J. R., Dugas, W. A., Srinivasan, R., & Hauck, L. M. (2001). Validation of the Swat Model on a Large Rwer Basin with Point and Nonpoint Sources1. *JAWRA Journal of the American Water Resources Association*, *37*(5), 1169–1188. https://doi.org/10.1111/j.1752-1688.2001.tb03630.x

Seibert, J. (1999). *Conceptual runoff models—Fiction or representation of reality?* 52.

Seibert, J., & Vis, M. J. P. (2012). Teaching hydrological modeling with a user-friendly catchment-runoff-model software package. *Hydrology and Earth System Sciences*, *16*(9), 3315–3325. https://doi.org/10.5194/hess-16-3315-2012

Serur, A. B. (2023). Performance evaluation of hydrological model in simulating streamflow and water balance analysis: Spatiotemporal calibration and validation in the upper Awash sub-basin in Ethiopia. *Sustainable Water Resources Management*, *9*(2), 48. https://doi.org/10.1007/s40899-023-00827-0

Setegn, S. G., Srinivasan, R., & Dargahi, B. (2008). Hydrological Modelling in the Lake Tana Basin, Ethiopia Using SWAT Model. *The Open Hydrology Journal*, *2*(1), 49–62. https://doi.org/10.2174/1874378100802010049

Silva, R. P. D., Dayawansa, N. D. K., & Ratnasiri, M. D. (2007). A comparison of methods used in estimating missing rainfall data. *Journal of Agricultural Sciences – Sri Lanka*, *3*(2), Article 2. https://doi.org/10.4038/jas.v3i2.8107

Sime, C. H. (2022). *Performance of Semi-Distributed Hydrological Models in Stream Flow Simulation* [Preprint]. In Review. https://doi.org/10.21203/rs.3.rs-2004447/v1

Sorooshian, S. (Ed.). (2008). *Hydrological modelling and the water cycle: Coupling the atmospheric and hydrological models*. Springer.

Taghvaye Salimi, E., Nohegar, A., Malekian, A., Hosseini, M., & Holisaz, A. (2016). Estimating time of concentration in large watersheds. *Paddy and Water Environment*, *15*, 123–132. https://doi.org/10.1007/s10333-016-0534-2

Tassew, B., Belete, M., & Miegel, K. (2019). Application of HEC-HMS Model for Flow Simulation in the Lake Tana Basin: The Case of Gilgel Abay Catchment, Upper Blue Nile Basin, Ethiopia. *Hydrology*, *6*, 21. https://doi.org/10.3390/hydrology6010021

Thapa, B. R., Ishidaira, H., Pandey, V. P., & Shakya, N. M. (2017). A multi-model approach for analyzing water balance dynamics in Kathmandu Valley, Nepal. *Journal of Hydrology: Regional Studies*, *9*, 149–162. https://doi.org/10.1016/j.ejrh.2016.12.080

Tibebe, M., Melesse, A., & Asfaw, D. (2017). Rainfall-runoff relation and runoff estimation for Holetta River, Awash subbasin, Ethiopia using SWAT model. *International Journal of Water Resources and Environmental Engineering*, *9*, 102–112. https://doi.org/10.5897/IJWREE2015.0601

Tumsa, B. C., Kenea, G., & Tola, B. (2022a). The application of SWAT+ model to quantify the impacts of sensitive LULC changes on water balance in Guder catchment, Oromia, Ethiopia. *Heliyon*, *8*(12), e12569. https://doi.org/10.1016/j.heliyon.2022.e12569

Tumsa, B. C., Kenea, G., & Tola, B. (2022b). The application of SWAT+ model to quantify the impacts of sensitive LULC changes on water balance in Guder catchment, Oromia, Ethiopia. *Heliyon*, *8*(12), e12569. https://doi.org/10.1016/j.heliyon.2022.e12569

USACE. (2021). *HEC-HMS User's Manual v4.8*. https://www.hec.usace.army.mil/confluence/hmsdocs/hmsum/4.8

Vidmar, A., Brilly, M., Sapač, K., & Kryžanowski, A. (2020). *Efficient Calibration of a Conceptual Hydrological Model Based on the Enhanced Gauss–Levenberg–Marquardt Procedure*. 20.

Vis, M., Knight, R., Pool, S., Wolfe, W., & Seibert, J. (2015). Model Calibration Criteria for Estimating Ecological Flow Characteristics. *Water*, *7*(5), Article 5. https://doi.org/10.3390/w7052358

Xia, Y., Fabian, P., Stohl, A., & Winterhalter, M. (1999). Forest climatology: Estimation of missing values for Bavaria, Germany. *Agricultural and Forest Meteorology*, *96*(1), 131–144. https://doi.org/10.1016/S0168-1923(99)00056-8

Yen, H., Jeong, J., & Smith, D. R. (2016). Evaluation of Dynamically Dimensioned Search Algorithm for Optimizing SWAT by Altering Sampling Distributions and Searching Range. *JAWRA Journal of the American Water Resources Association*, *52*(2), 443–455. https://doi.org/10.1111/1752-1688.12394

Yu, Z. (2015). Hydrology, Floods and Drought/ Model and Prediction. In *Encyclopedia of Atmospheric Sciences* (pp. 217–223). Elsevier. https://doi.org/10.1016/B978-0-12-382225-3.00172-9

Zeberie, W. (2019). Modelling of Rainfall-Runoff Relationship in Big-Akaki Watershed, Upper Awash Basin, Ethiopia. *Undefined*. https://www.semanticscholar.org/paper/Modelling-of-Rainfall-Runoff-Relationship-in-Upper-Zeberie/6b6a9e22df9fd5704e5db326d119a56c3e301de9

Zhang, L., & Yang, X. (2018). Applying a Multi-Model Ensemble Method for Long-Term Runoff Prediction under Climate Change Scenarios for the Yellow River Basin, China. *Water*, *10*(3), Article 3. https://doi.org/10.3390/w10030301

# APPENDIX

## Appendix Table

Appendix Table 1: The correlation between the cumulative rainfalls of each station and the cumulative group station average rainfall

| Stations | Addisalem | Asgori | Batu Liben | Ginch | Hidi Sekoke | Kimoye | Teji | Tulu Bolo | Welenkomi | Enselale |
|---|---|---|---|---|---|---|---|---|---|---|
| $R^2$ | 0.999 | 0.999 | 0.998 | 0.999 | 0.9995 | 0.997 | 0.999 | 0.998 | 0.999 | 0.999 |

Appendix Table 2: Standard rainfall anomaly index

| Year | Addisalem | Asgori | Bantu Liben | Ginch | Kimoye | Teji | Tulu Bolo | Welenkomi | Enselale |
|---|---|---|---|---|---|---|---|---|---|
| 2000 | 0.68 | -0.91 | 0.95 | -0.35 | -0.25 | -0.46 | 0.61 | 0.07 | 0.77 |
| 2001 | 0.78 | -0.47 | -0.55 | 0.02 | 0.07 | -0.42 | -1.14 | 0.48 | 0.33 |
| 2002 | 0.39 | -0.22 | -0.62 | -0.17 | -0.67 | -0.83 | -0.27 | -0.05 | 0.53 |
| 2003 | -0.07 | 1.12 | 0.49 | -0.05 | -0.41 | 1.00 | -0.46 | 0.80 | 1.30 |
| 2004 | -0.11 | -0.32 | 0.39 | 0.12 | 0.41 | 0.05 | 0.35 | 0.96 | 0.57 |
| 2005 | -0.50 | -0.44 | 1.89 | 0.17 | -0.04 | 1.21 | 0.22 | 0.67 | 1.41 |
| 2006 | 0.98 | 1.45 | 1.11 | 3.49 | -0.05 | 1.60 | -0.19 | 2.01 | 1.09 |
| 2007 | 0.20 | 0.69 | -0.07 | -0.02 | 0.49 | 0.24 | 0.14 | 0.37 | 0.97 |
| 2008 | -0.18 | -0.16 | 0.17 | -0.24 | -0.49 | -0.86 | 0.26 | -0.73 | 0.33 |
| 2009 | -0.55 | -0.60 | 0.12 | -0.52 | 0.08 | -0.84 | -0.47 | -0.88 | -0.98 |
| 2010 | 1.99 | 0.90 | -2.27 | 0.38 | 0.74 | 2.07 | 1.42 | 0.98 | -0.80 |
| 2011 | 1.01 | -0.37 | -1.61 | -1.00 | 3.11 | -0.21 | -1.03 | -0.46 | -0.88 |
| 2012 | -1.11 | -1.31 | 0.04 | -0.91 | -1.03 | -1.49 | -0.73 | -1.54 | -1.18 |
| 2013 | -0.15 | 2.25 | 0.11 | -0.18 | -0.06 | 0.21 | 2.74 | -0.41 | -0.99 |
| 2014 | -1.31 | -0.40 | 0.36 | -0.31 | -0.40 | -0.60 | -0.28 | -0.44 | -1.12 |
| 2015 | -2.06 | -1.22 | -0.53 | -0.43 | -1.50 | -0.67 | -1.15 | -1.84 | -1.34 |

Apendix Table 3: Percentage of the standard rainfall anomaly index of the stations

| Condition | Addis-alem | Asgori | Bantu Liben | Ginch | Kimoye | Teji | Tulu Bolo | Welen-komi |
|---|---|---|---|---|---|---|---|---|
| Extremely wet | 0.00 | 6.25 | 0.00 | 6.25 | 6.25 | 6.25 | 6.25 | 6.25 |
| Very wet | 6.25 | 0.00 | 6.25 | 0.00 | 0.00 | 6.25 | 0.00 | 0.00 |
| Moderately wet | 6.25 | 12.50 | 6.25 | 0.00 | 0.00 | 12.50 | 6.25 | 0.00 |
| Near normal | 68.75 | 68.75 | 75.00 | 87.50 | 81.25 | 68.75 | 68.75 | 81.25 |
| Moderately dry | 12.50 | 12.50 | 0.00 | 6.25 | 6.25 | 6.25 | 18.75 | 0.00 |
| Severely dry | 0.00 | 0.00 | 6.25 | 0.00 | 6.25 | 0.00 | 0.00 | 12.50 |
| Extremely dry | 6.25 | 0.00 | 6.25 | 0.00 | 0.00 | 0.00 | 0.00 | 0.00 |

Appendix Table 4: Average rainfall and precipitation concentration index for stations in the Melka Kunture watershed

| Station | Annual | | Belg | | Kiremt | | Bega | |
|---|---|---|---|---|---|---|---|---|
| | Rainfall | PCI | Rainfall | PCI | Rainfall | PCI | Rainfall | PCI |
| Addisalem | 1103.96 | 14.70 | 247.69 | 27.28 | 768.56 | 27.23 | 72.56 | 27.22 |
| Asgori | 961.70 | 15.35 | 236.83 | 29.30 | 682.30 | 27.11 | 45.11 | 27.23 |
| BantuLiben | 1214.33 | 17.34 | 221.63 | 32.09 | 911.94 | 27.37 | 61.20 | 25.85 |
| Ginch | 1109.41 | 13.94 | 267.56 | 28.61 | 752.09 | 26.38 | 77.85 | 28.49 |
| Kimoye | 995.14 | 14.12 | 231.02 | 28.17 | 667.74 | 27.37 | 100.19 | 37.13 |
| Teji | 920.43 | 15.87 | 205.60 | 31.42 | 687.75 | 26.86 | 40.64 | 29.52 |
| Tulu Bolo | 1104.13 | 16.82 | 224.13 | 32.91 | 811.63 | 27.08 | 45.54 | 32.36 |
| Welenkomi | 922.49 | 15.34 | 194.30 | 30.98 | 660.40 | 27.09 | 57.49 | 25.79 |
| Enselale | 662.92 | 15.69 | 148.79 | 30.03 | 483.57 | 26.53 | 30.56 | 27.81 |

## Appendix Figure

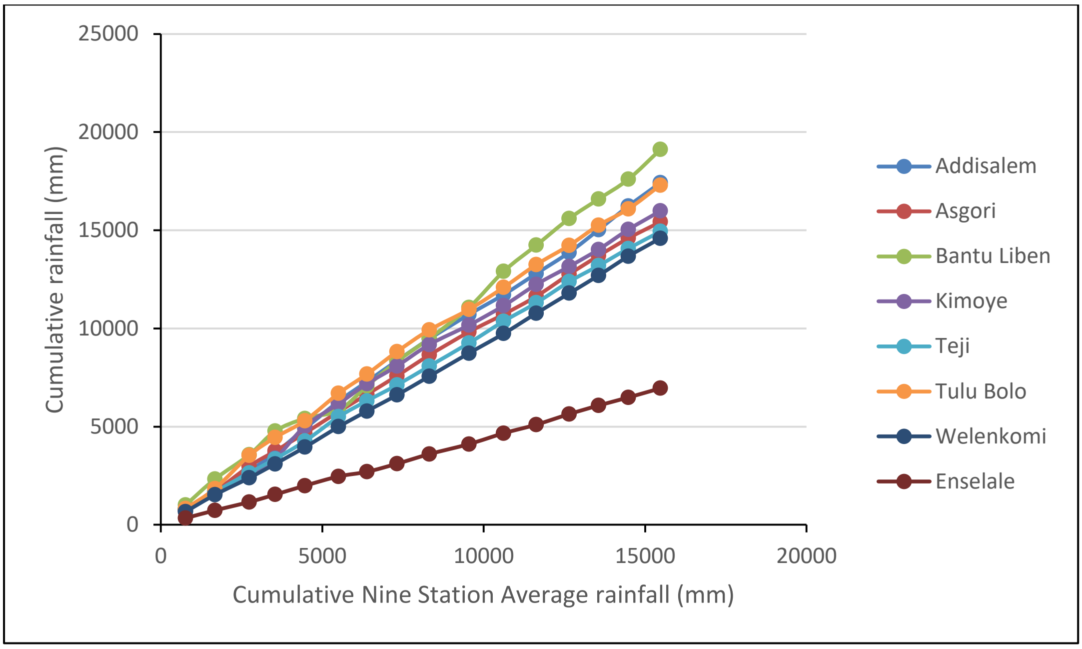


Appendix Figure 1: Double mass curves

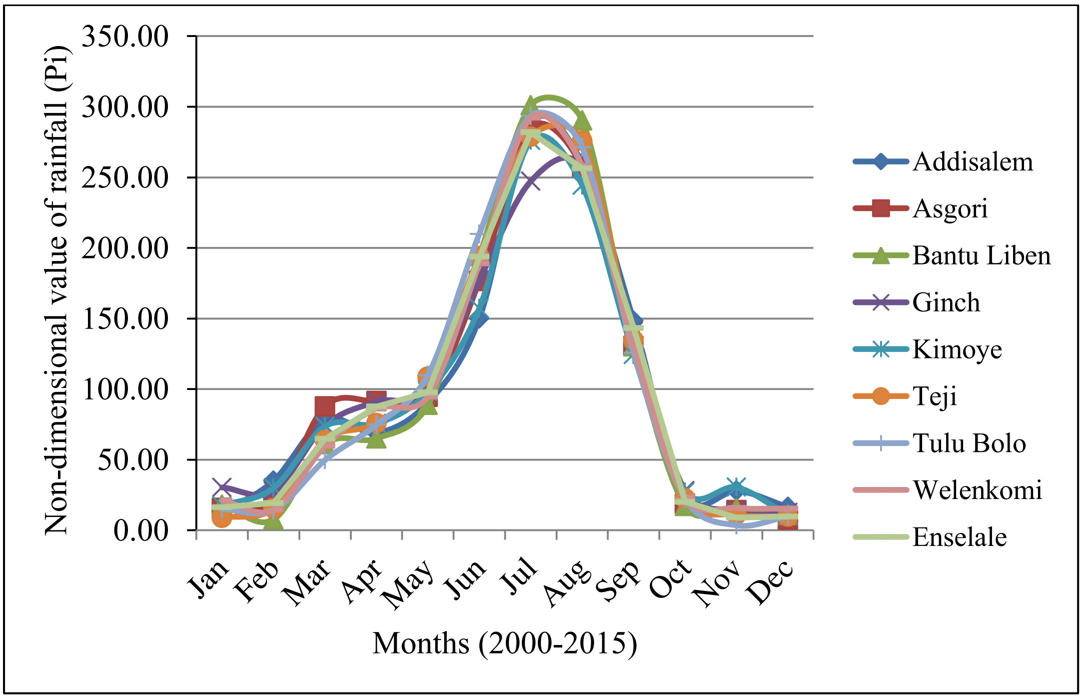


Appendix Figure 2: Non-dimensionalized rainfalls for selected meteorological stations in the Melka Kunture watershed

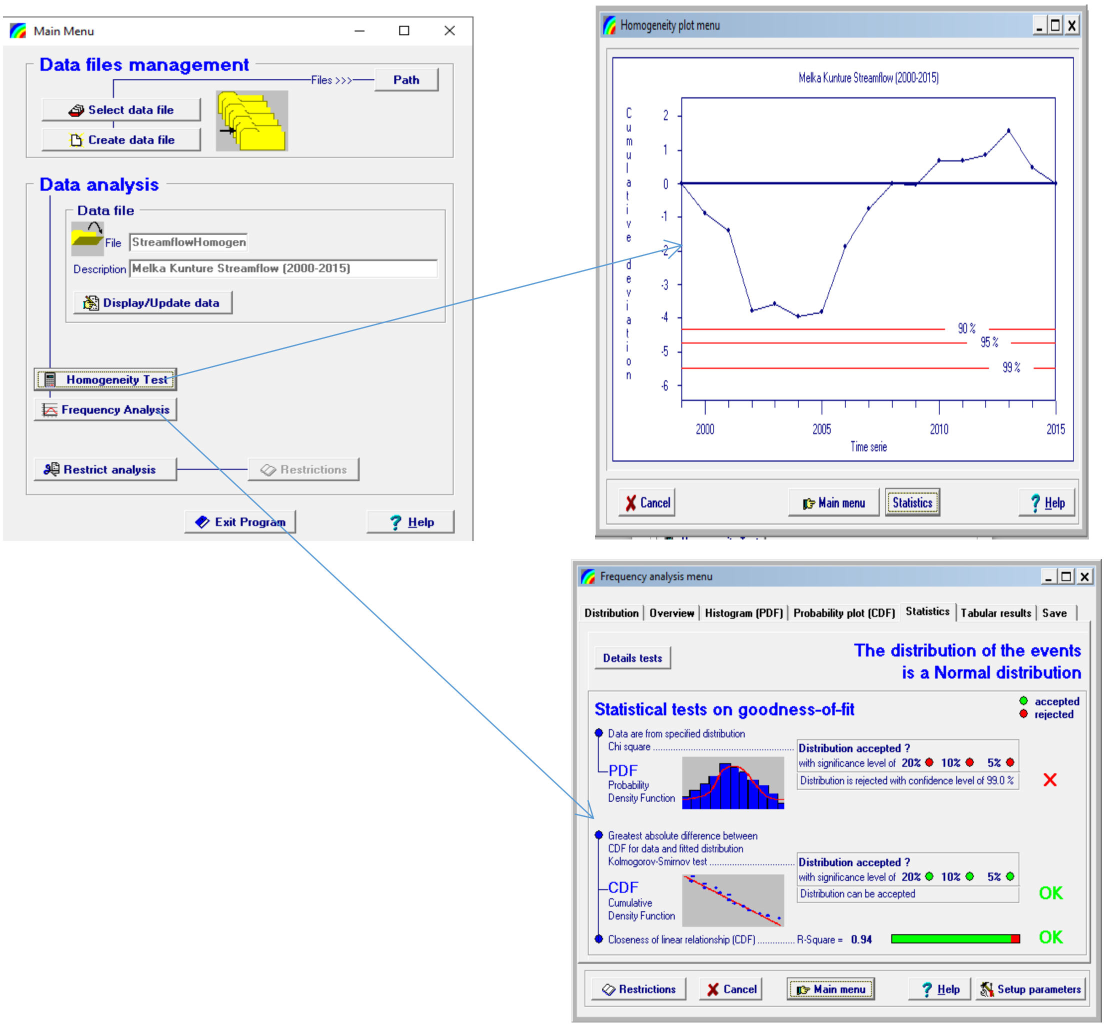


Appendix Figure 3: Homogeneity test of streamflow data (2000-2015) using Rainbow software package